Untersuchung der Energie- und Nährstoffflüsse mikrobieller Gemeinschaften

Dissertation zur Erlangung des Doktorgrades

der Naturwissenschaften (Dr. rer. nat.)

Fakultät Naturwissenschaften

Universität Hohenheim

Institut für Nutztierwissenschaften, Jun.-Prof. Dr. Jana Seifert

Institut für Mikrobiologie, Prof. Dr. Julia Fritz-Steuber

vorgelegt von

Robert Starke

aus *Leipzig*

2016

Dekan:	Prof. Dr. Heinz Breer
1. berichtende Person:	Jun.-Prof. Dr. Jana Seifert
2. berichtende Person:	Prof. Dr. Julia Fritz-Steuber
Eingereicht am:	15.12.2016
Mündliche Prüfung am:	17.03.2017

Die vorliegende Arbeit wurde am 09.02.2017 von der Fakultät Naturwissenschaften der Universität Hohenheim als „Dissertation zur Erlangung des Doktorgrades der Naturwissenschaften“ angenommen.

Inhaltsverzeichnis

Zusammenfassung

Die Aktivität von Organismen in komplexen, mikrobiellen Gemeinschaften wurde in den letzten Jahrzehnten vermehrt durch den Einbau stabiler Isotope in die Biomasse aktiver Spezies untersucht. Der Isotopeneinbau kann in allen Biomolekülen, aber hauptsächlich in DNA, RNA, Proteinen und Phospholipidfettsäuren nachverfolgt werden. Hierbei nimmt die phylogenetische Information, der Genotyp, ausgehend von der DNA über die RNA hin zu den Proteinen ab, wohingegen der Phänotyp maßgeblich durch die Proteine geprägt wird. Folglich liefert die Untersuchung von DNA und RNA präzisere phylogenetische Daten, während Proteine genauere Aussagen über den tatsächlichen Zustand im System erlauben. In dieser Arbeit wurde die Markierung mit stabilen Isotopen (^{13}C und ^{15}N) in Proteinen (Protein-SIP) für zwei grundsätzlich verschiedene mikrobielle Gemeinschaften angewandt: (a) Die Benzolmineralisation einer sedimentären Gemeinschaft, die aus einem anaeroben Grundwasseraquifer angereicht wurde sowie (b) die kurzzeitige und aerobe Assimilation von Pflanzenmaterial im Boden.

*Markierung des Sekundärstoffwechsels einer benzolmineralisierenden und sulfatreduzierenden, mikrobiellen und in Zeitz angereicherten Gemeinschaft mittels $^{13}C_2$-Acetat (**Artikel 3.2**)*

Die seit 2007 untersuchte und aus Zeitz angereicherte, mikrobielle Gemeinschaft wurde mit dem zuvor postulierten Hauptintermediat der syntrophen Benzolmineralisation, Acetat, inkubiert. Das Substrat wurde vollständig ^{13}C-markiert täglich in geringen Mengen zugegeben, um den sekundären Abbau während verschiedener Stadien des Benzolabbaus aufzuschlüsseln. Es wurde demonstriert, dass zusätzlich zur Benzolmineralisation zugegebenes Acetat keinen Einfluss auf das Ausmaß der Sulfidbildung als Endprodukt der Sulfatreduktion hat. Stattdessen wird Acetat in absteigender Reihenfolge von den Campylobacterales, den Syntrophobacterales, den Archaeoglobales, den Clostridiales und den Desulfobacterales assimiliert. Die epsilonproteobakteriellen Campylobacterales zeigten den schnellsten und höchsten Einbau, wodurch zuvorige metagenombasierende Studien bestätigt und den Epsilonproteobakterien dieser Gemeinschaft erstmals eine physiologische Rolle gegeben werden konnte.

*Physiologie des primären Acetatverwerters einer benzolmineralisierenden und sulfatreduzierenden, mikrobiellen und in Zeitz angereicherten Gemeinschaft (**Artikel 3.1**)*

In dieser Studie wurde das Genom des primären Acetatverwerters (Artikel 3.2) aus dem vollständigen Metagenom der benzolmineralisierenden, mikrobiellen Gemeinschaft

rekonstruiert. Die genomische DNA stammte aus einer Hungerkultur des gleichen Aquifers, die zuvor auf *m*-Xylen wuchs und eine Anreicherung des epsilonproteobakteriellen Phylotyps dieser Gemeinschaft aufzeigte. Die Präsenz der Sulfidquinonoxidoreduktase (*sqr*) und der Polysulfidreduktase (*psr*) suggeriert eine Schlüsselrolle im Schwefelzyklus. Das Epsilonproteobakterium ist in der Lage, das aus der Sulfatreduktion des Sekundärstoffwechsels entstandene und toxische Sulfid mittels SQR zu Polysulfid zu oxidieren und anschließend mittels PSR zu reduzieren. Die in der zuvorigen Studie demonstrierte direkte Acetatassimilation wurde durch die Detektion eines Acetattransporters (*actP*) und der Acetyl-CoA Synthetase (*acsA*) zur Acetataktivierung bestätigt.

*Kurzzeitige Assimilation von ^{15}N-markiertem Pflanzenmaterial im Boden (**Artikel 3.3**)*

In dieser Protein-SIP Studie wurde die Assimilation von Pflanzenmaterial im Boden erstmals mittels ^{15}N-markiertem Tabak gezeigt. Gegensätzlich zu der bisher vorherrschenden Annahme, dass Pilze die aus den Pflanzen stammenden, komplexen Verbindungen wie Cellulose und Lignin abbauen und niedermolekulare Verbindungen abgeben, die anschließend von Bakterien metabolisiert werden, wurde gezeigt, dass Bakterien die dominanten Organismen während der kurzzeitigen Assimilation von Pflanzenmaterial sind. Die in den Pflanzen enthaltenen, niedermolekularen Verbindungen werden zunächst von den Bakterien genutzt bis die komplexen Verbindungen angereichert und von den langsam wachsenden Pilzen umgesetzt werden. Die Verwendung von multiOMIK-Techniken resultierte in einem multidimensionalen Schema, dass die Gruppierung und Kategorisierung unterschiedlicher Verhaltensweisen von Mikroorganismen ermöglicht.

Summary

The activity of microorganisms was heavily investigated using the incorporation of stabile isotopes in the last decade. Here, all biomolecules but predominantly DNA, RNA, proteins and phospholipid derived fatty acids are used to trace the label in the biomass of active microbes. Thereby, the phylogenetic information decreases from DNA and RNA to proteins whereas the latter allow to describe the actual phenotype. In this work, protein stable isotope probing (protein-SIP) was applied to two different microbial systems: (a) the anaerobic mineralization of benzene and (b) the assimilation of plant-derived organic matter in soil.

*Labeling of the secondary metabolism of the benzene-mineralizing and sulfate-reducing community using $^{13}C_2$-acetate (**article 3.2**)*

The well-described microbial community enriched from the Zeitz aquifer was fed daily with the postulated and fully ^{13}C-labeled intermediate of syntrophic benzene fermentation, acetate, to unveil detailed secondary utilization processes. Additional acetate amended to the ongoing benzene mineralization showed no influence on sulfide produced by sulfate reduction. Instead, labeled acetate was incorporated by Campylobacterales, Syntrophobacterales, Archaeoglobales, Clostridiales and Desulfobacterales in descending order. The epsilonproteobacterial Campylobacterales featured the fastest and the highest ^{13}C-incorporation to confirm previous metagenome-based studies and to assign a physiological role to this phylotype of the community for the first time.

*Metagenome based labeling of the secondary metabolism of the benzene-mineralizing and sulfate-reducing community (**article 3.1**)*

In this study, the population genome of the primary acetate utilizer (article 3.2) was reconstructed from the metagenome of the benzene mineralizing community obtained by whole-genome shotgun sequencing. Genomic DNA originated from a starvation enrichment culture previously metabolizing *m*-xylen and enriched in the identical epsilonproteobacterial phylotype of this community. The presence of the sulfide quinone oxidoreductase (*sqr*) and the polysulfide reductase (*psr*) suggested a key role in sulfur cycling. Hence, the epsilonproteobacterial phylotype is able to oxidize otherwise toxic sulfide produced by sulfate reduction to polysulfide via SQR and its subsequent reduction to sulfide via PSR. Further, the detection of an acetate transporter (*actP*) and the acetyl-CoA synthetase (*acsA*) for acetate activation approved direct assimilation as shown in the previous study.

*Short-term assimilation of plant-derived organic matter in soil (**article 3.3**)*

In this protein-SIP study, the short-term assimilation of plant-derived organic matter in soil was demonstrated using ^{15}N-labeled tobacco for the first time. In contrast to the postulated model in which fungi degrade plant-derived complex compounds and secrete low molecular weight compounds which are then degraded by bacteria, our study demonstrated the dominance of bacteria over fungi during the short-term assimilation of plant-derived organic matter. Bacteria outcompete fungi for the easy available plant-derived compounds until complex compounds such as cellulose and lignin are enriched and degraded by slow growing fungi. The use of multiOMIC techniques resulted in a multidimensional scheme to easily group and categorize different behaviours of microorganisms.

Abkürzungsverzeichnis

BTEX	Benzol, Toluol, Ethylbenzol und *ortho*-, *meta*- und *para*-Xylol
C	Kohlenstoff
CO_2	Kohlenstoffdioxid
CUE	Kohlenstoffaufnahmeaktivität
DNA	Desoxyribonukleinsäure
DOI	Digitale Objektidentifikation
GW	Grundwasser
H	Wasserstoff
LR	Markierungsverhältnis
MW	Mittelwert
N	Stickstoff
NUE	Nährstoffaufnahmeaktivität
O	Sauerstoff
PB	Proteobakterien
PLFA	Phospholipidfettsäuren
PSD	Polysulfiddisproportionierung
PSR	Polysulfidreduktase
RIA	Relatives Isotopenverhältnis
RNA	Ribonukleinsäure
rTCA	Reduktiver Citratzyklus
S	Schwefel
SA	Standardabweichung
SIP	Markierung mit stabilen Isotopen
SQR	Sulfidquinonoxidoreduktase
ΔE	Standardpotenzial
ΔG	Gibbs-Energie

Abbildungs- und Tabellenverzeichnis

1. Einleitung

Mikroorganismen sind in der Lage, sowohl natürlich vorkommende als auch anthropogen in die Umwelt eingebrachte, xenobiotische Verbindungen vollständig abzubauen. Die stoffumwandelnden Prozesse können unter vielfältigen Rahmenbedingungen stattfinden. Ein Beispiel dafür ist das Zusammenspiel von Boden und Grundwasser. Der im Boden vorkommende Sauerstoff wird von aerob lebenden Mikroorganismen genutzt, um hauptsächlich die einfachen Energie- (C) und Nährstoffquellen (N) zu verstoffwechseln. Energiereiche und damit persistente Verbindungen werden häufig in den Grundwasserleiter translokalisiert und anschließend von anaerob lebenden Mikroorganismen, denen anstelle von Sauerstoff andere terminale Elektronenakzeptoren wie Nitrat und Sulfat zur Verfügung stehen, als Energie- und Nährstoffquelle genutzt (**Abbildung 1**).

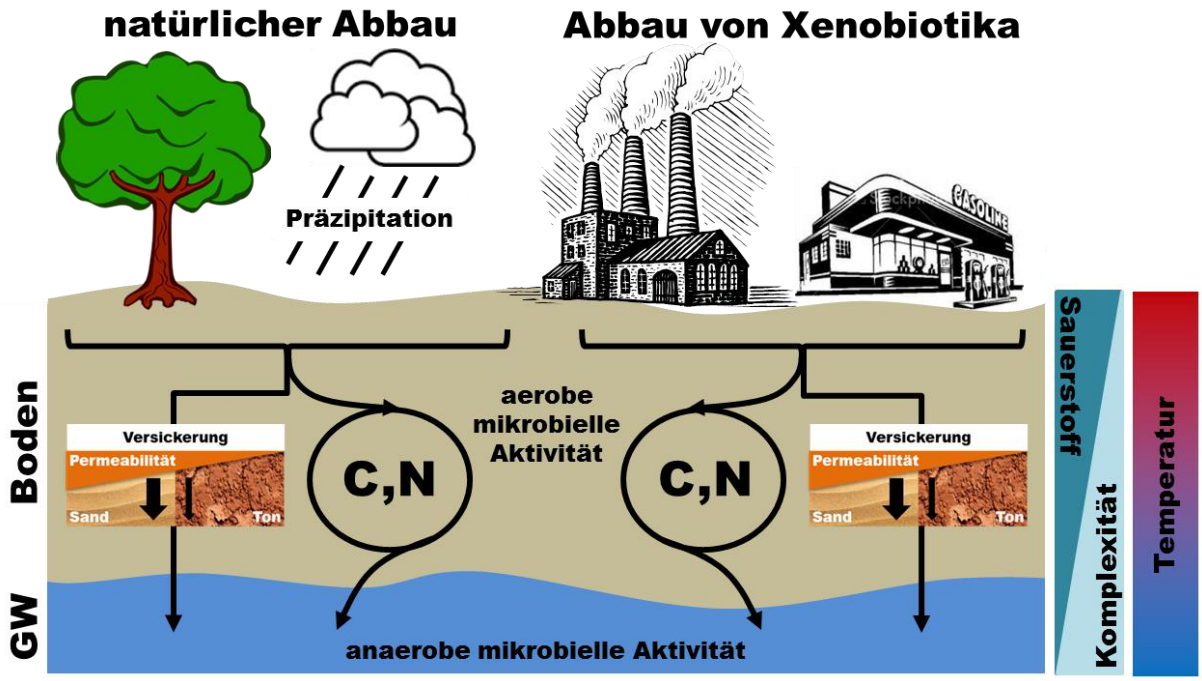

Abbildung 1: Die Kohlenstoff- (C) und Stickstoffkreisläufe (N) ausgehend von natürlichen und xenobiotischen Verbindungen im Boden und im Grundwasser (GW). Die einfachen Energie- und Nährstoffquellen werden von aerob lebenden Mikroorganismen im Boden verwendet, während die energiereichen komplexen Verbindungen von anaerob lebenden Mikroorganismen im Grundwasser genutzt werden.

1.1. Mikrobielle Aktivität

Mikroorganismen stellen die älteste Form von Leben auf der Erde dar und sind damit der Ursprung komplexer Organismen (1-3). Zudem trugen prähistorische Mikroorganismen maßgeblich zur Formation der oxischen Atmosphäre (4) und der geologischen Beschaffenheit der Erde bei (5, 6). Mikroorganismen umfassen den größten Teil der globalen Biomasse und sind damit entscheidend für die genetische Diversität (7). Außerdem sind Mikroorganismen bedeutsam für die atomaren Kreisläufe von Kohlenstoff, Sauerstoff, Stickstoff und Schwefel, aber auch für den Zyklus von Metallen und Halogenen wie Chlor (8, 9). Ihre Fähigkeit, einzigartige, biochemische Reaktionen durchzuführen, wird oftmals auch von höheren Organismen genutzt. Beispielsweise wurden symbiotische Lebensweisen für stickstofffixierende Bakterien in Pflanzenwurzeln (10, 11) und für lignocelluloseabbauende Mikroorganismen im Termitendarm beschrieben (12). Weiterhin können Mikroorganismen nicht nur energiereiche Verbindungen vollständig abbauen, sondern auch komplexe Stoffgemische als Energie- und Nährstoffquelle nutzen. Diese vielfältigen Stoffwechselpotentiale tragen unter anderem zur Sanierung kontaminierter Habitate bei. Im Vergleich zur abiotischen, physikochemischen Sanierung wie der Hochdruckextraktion und der thermischen Bodensanierung weist der biotische, mikrobielle Abbau wesentliche Vorteile wie beispielsweise den vollständigen Abbau der Kontaminationen, die geringen Behandlungskosten, die höhere Sicherheit sowie die geringe Belastung der Umwelt auf (13). Im Gegensatz zum Abbau anthropogen eingebrachter, organischer Energie- und Nährstoffquellen steht der natürliche Abbau. Dabei werden natürlich vorkommende Verbindungen aus beispielsweise Pflanzen, Streu oder Holz von Mikroorganismen vollständig metabolisiert (14). In den vergangenen Jahrzehnten hat sich die mikrobielle Forschung insofern weiterentwickelt, dass nicht mehr nur der Abbau einer Verbindung durch einen einzelnen Mikroorganismus untersucht wird, sondern vielmehr der Abbau von mehreren Verbindungen oder Stoffgemischen durch mikrobielle Gemeinschaften. Tatsächlich sind diese Gemeinschaften die natürliche Organisationsform mikrobiellen Lebens, die durch ihre hohe Diversität in der Lage sind, eine Vielzahl extremer, ökologischer Habitate wie Gletscher (15), submarine, hydrothermale Öffnungen (16), Seebodensedimente (17), Schlammvulkane (18) oder Geysire (19) zu besiedeln. Dabei wird grundsätzlich zwischen einem Stoffwechsel mit Sauerstoff, der aeroben Atmung und einem ohne Sauerstoff, der anaeroben Atmung, unterschieden. Innerhalb der anaeroben Atmung können verschiedene Elektronenakzeptoren wie Nitrat, Sulfat oder Schwefel verwendet werden, wobei das Redoxpotential der anaeroben

Atmung typischerweise geringer als das der aeroben Atmung ist (**Tabelle 1**). Daraus resultierend folgt, dass aerobe Mikroorganismen den Energiegewinn aufgrund des hohen Redoxpotentials des Sauerstoffs in den Aufbau von Biomasse investieren können. Im Gegensatz dazu müssen anaerobe Mikroorganismen die gewonnene Energie hauptsächlich für die Aufrechterhaltung des Stoffwechsels aufbringen und sind damit generell durch eine geringe Biomasseproduktion gekennzeichnet. Daher stellen anaerobe Mikroorganismen aufgrund ihrer geringen Umweltbelastung vor allem bei der biologischen Sanierung kontaminierter Gebiete eine zukunftsweisende Alternative zur abiotischen Sanierung dar, während meistens aerob lebende Mikroorganismen für den natürlichen Abbau verantwortlich sind.

Tabelle 1: Atmungstypen mit Redoxpotential nach Ottow (20). Der bei der anaeroben Atmung verwendete Sauerstoff bringt durch das hohe Redoxpotential einen höheren Energiegewinn als bei der anaeroben Atmung.

Atmungstyp	Elektronenakzeptor	Reaktionsprodukt(e)	$E^{0'}$ (V)
Aerobe Atmung	Sauerstoff	Wasser + CO_2	+ 0,82
Denitrifikation	Nitrat	Nitrit	+ 0,75
Manganreduktion	Mangan(IV)	Mangan(II)	+ 0,41
Eisenatmung	Eisen(III)	Eisen(II)	+ 0,15
Fumaratatmung	Fumarat	Succinat	+ 0,03
Desulfurikation	Sulfat	Sulfid	- 0,22
Methanogenese	CO_2	Methan	- 0,25
Schwefelreduktion	Schwefel	Sulfid	- 0,27
Acetogenese	CO_2	Acetat	- 0,30

In der vorliegenden Dissertation wurden eine gut verstandene mikrobielle Grundwassergemeinschaft sowie eine Bodengemeinschaft getrennt voneinander untersucht. Im Folgenden werden beide Habitate beschrieben.

1.1.1. Habitat 1: Anaerober Benzolabbau einer sedimentären mikrobiellen Grundwassergemeinschaft

Die Kontamination mit Petroleumkohlenwasserstoffen wie den BTEX-Verbindungen zu denen Benzol, Toluol, Ethylbenzol sowie *ortho*-, *meta*- und *para*-Xylol zählen, wird hauptsächlich durch versehentliches Verschütten und undichte Lagertanks verursacht (21). Die Sanierung von Benzolkontaminationen ist aufgrund der Persistenz in der Umwelt und der Toxizität bedeutsam

(22, 23). In kontaminierten, unterirdischen Habitaten wird der Sauerstoff durch die Aktivität aerober Mikroorganismen und chemischer Oxidationsprozesse rasch verbraucht, wodurch sich eine anaerobe Zone bildet. Der Großteil stark hydrophober Kohlenwasserstoffe wird in dieser Zone von anaerob lebenden Mikroorganismen abgebaut (24, 25), wobei Benzol die renitenteste der BTEX-Verbindungen ist. Der anaerobe Abbau von Benzol wurde seit den 1990er Jahren untersucht (26-28) und postuliert, dass die initiale, oxidative Aktivierung über Carboxylierung, Hydroxylierung oder Methylierung zu Benzoat, Phenol oder Toluol als erstes Intermediat im Abbau führt (29, 30). Die in dieser Arbeit behandelte, benzolmineralisierende und sulfatreduzierende, mikrobielle Gemeinschaft wurde in einem BTEX-kontaminierten, sulfidischen Grundwasserleiter angereichert und intensiv untersucht (31-35). Vorherige Studien mittels der Analyse der terminalen Restriktionsfragementlängen-polymorphismen (TRFLP), der Sequenzierung von 16S rRNA Genen sowie DNA-SIP mit $^{13}C_6$-markiertem Benzol offenbarten die benzolabbauende Aktivität von einen Phylotyp, der zur Cryptanaerobacter/Pelotomaculum-Gruppe innerhalb der Clostridiales gehört (32, 33). Der entsprechende Protein-SIP Versuch mit vollständig ^{13}C-markiertem Benzol sowie mit ^{13}C-markiertem Carbonat bestätigte, dass ein Pelotomaculum-ähnlicher Organismus Kohlenstoff aus Benzol und CO_2 assimiliert (35). Mit Hilfe dieser Studien wurde die mikrobielle Gemeinschaft bezüglich ihrer ^{13}C-Einbaucharakteristiken in drei Gruppen geteilt: (I) Clostridiales fermentieren Benzol und fixieren Kohlenstoff aus CO_2 während (II) Deltaproteobakterien sich von den Fermentationsprodukten, CO_2-Fixierung und Sulfatreduktion ernähren sowie (III) die vermeintlichen Aasfresser toter Biomasse oder Metaboliten, die zur Bacteroidetes/Chlorobi-Gruppe gehören. Basierend auf thermodynamischen Berechnungen wurden Acetat und Wasserstoff als Schlüsselmetabolite der Benzolfermentation beschrieben, was eine syntrophe Beziehung mit den Sulfatreduzierern suggeriert (33). Tatsächlich wurde kürzlich demonstriert, dass die Zugabe von Acetat und Wasserstoff in hohen Konzentrationen die Benzolfermentation reversibel inhibiert (34). Außerdem zeigten DNA-SIP Experimente den Einbau von $^{13}C_6$-markiertem Benzol von einem Mitglied der Epsilonproteobakterien, das entfernt verwandt mit dem Genus *Sulfurovum* ist, aber nicht in den entsprechenden Protein-SIP Versuchen gefunden wurde (32, 35) (**Abbildung 2**).

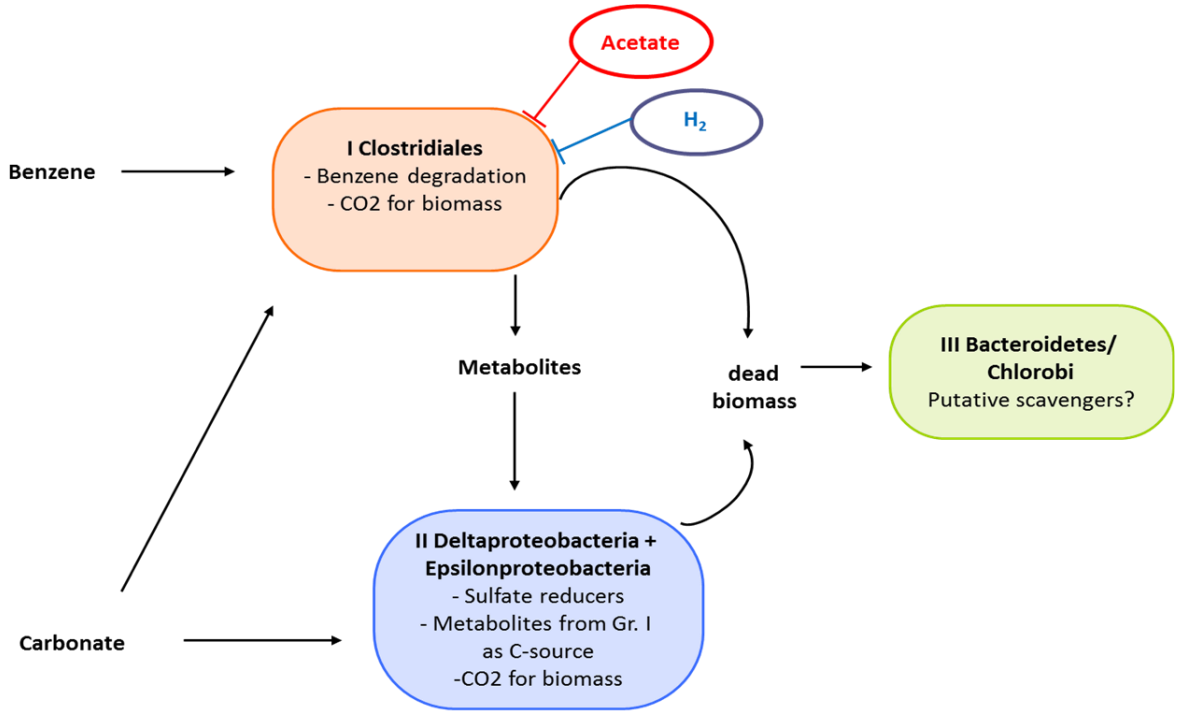

Abbildung 2: Das Modell der Stoffflüsse der benzolmineralisierenden und sulfatreduzierenden, mikrobiellen und in Zeitz angereicherten Gemeinschaft nach Taubert, 2012 (35). Benzol wird von den Clostridiales zu Metaboliten fermentiert, welche dann von Delta- und Epsilonproteobakterien unter sulfatreduzierenden Bedingungen oxidiert werden. Die tote Biomass wird letztlich von Bacteroidetes und Chlorobi metabolisiert.

Daher war die ökophysiologische Rolle dieses epsilonproteobakteriellen Phylotyps in der mikrobiellen Gemeinschaft bisher unklar. Aktuelle Studien zeigten, dass chemolithoautotrophe Epsilonproteobakterien, die verwandt mit dem Genus *Sulfurovum* sind, vorherrschend in sulfidischen Umgebungen wie hydrothermalen Tiefseeöffnungen (36-38) oder sulfidischen Höhlen und Quellen sind (39-41). Trotzallem wurde auch mixotrophes Wachstum diskutiert, da Epsilonproteobakterien durch Acetatzugabe in einem sulfidischen Grundwasserleitersediment stimuliert wurden (42). Daher wird vermutet, dass die Epsilonproteobakterien in der hier untersuchten, mikrobiellen Gemeinschaft sich von Produkten der Benzolfermentation und der Sulfatreduktion ernähren. Ferner wurde das Netzwerk der sekundären Kohlenstoffverwertung aus Acetat noch nicht aufgeklärt.

1.1.2. Habitat 2: Pflanzenabbau durch Bodenmikroorganismen

Boden ist ein lebender natürlicher Rohstoff, der die Fruchtbarkeit und die Nachhaltigkeit der Erde durch die Aktivität einer großen Diversität an Mikroorganismen bestimmt (43). Die hohe Komplexität mikrobiellen Lebens im Boden, wobei in 1 cm^3 10^7 bis 10^{10} prokaryotische Zellen und 350 bis 8000 verschiedene, genomische Spezies vorhanden sein können, resultiert aus den Interaktionen mit den vier Sphären des Lebens – der Atmosphäre, der Biosphäre, der Hydrosphäre und der Lithosphäre (43). Dabei hängt die Viabilität der Bodenmikroorganismen stark von verfügbaren Energie- und Nährstoffquellen ab. Unter den Nährstoffen zählt Stickstoff zu den bedeutsamsten, welcher hauptsächlich von Pflanzen in den Boden eingebracht wird (44). Der pflanzliche Stickstoff ist vor allem in Proteinen enthalten, die 2-5% des Trockengewichts ausmachen, da die Konzentrationen von frei verfügbaren Aminosäuren normalerweise 100-fach geringer ist (45). Andererseits können diese Aminosäuren direkt über mehrere Membrantransportsysteme aufgenommen werden (46), während Proteine vor der Aufnahme zunächst von extrazellulären Proteasen depolymerisiert werden müssen, was den geschwindigkeitsbestimmenden Schritt im Abbau organischer Materie aus Pflanzen darstellt (47-49). Die daraus resultierenden, einfachen, organischen Stickstoffverbindungen können durch Mikroorganismen zügig als Energie- und Nährstoffquelle genutzt werden (50). Der Zyklus von anorganischem Stickstoff, wie beispielsweise Nitrifikation und Denitrifikation, wurde detailliert erforscht und beschrieben (51, 52), wohingegen der Zyklus von organischem Stickstoff im Boden noch nicht komplett verstanden ist (47). Im Gegensatz dazu wurde der Abbau und die Assimiliation von organischem Kohlenstoff durch Bodenmikroorganismen bereits mehrfach gezeigt (53-55). Dabei wurde die Dominanz der Pilze im Abbau und der Assimilation von polymerem, organischem Kohlenstoff aus Pflanzen demonstriert (56). Weiterhin wurden sowohl synergistisches als auch antagonistisches Verhalten zwischen Pilzen und Bakterien beschrieben (57-61). Bisher wurde angenommen, dass Bakterien die niedermolekularen Verbindungen wie Proteine und Zucker, die beim Abbau von Pflanzenpolymeren wie Cellulose oder Lignin durch Pilze entstehen, während der biochemischen Pflanzendekomposition metabolisieren (**Abbildung 3**).

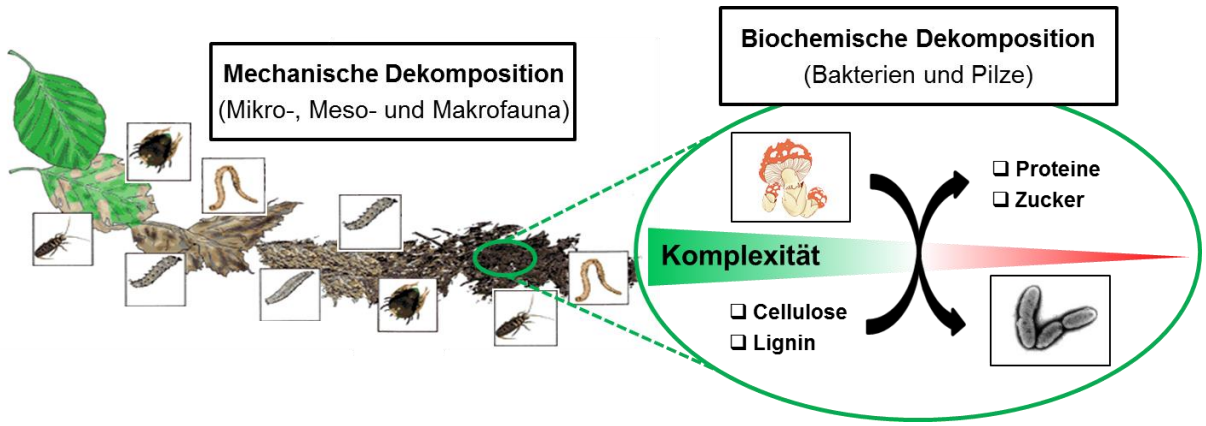

Abbildung 3: Der Pflanzenabbau unterteilt in mechanische und biochemische Prozesse nach Schmidt, 1989. Im mechanischen Abbau wird die Pflanze von der Mikro-, Meso- und Makrofauna zerkleinert während im biochemischen Abbau die freigesetzten Chemikalien metabolisiert werden. Dabei werden die komplexen Stoffe wie Cellulose und Lignin von den Pilzen abgebaut und die entstehenden, einfachen Verbindungen wie Proteine und Zucker von den Bakterien genutzt.

Dieses Verhalten wurde als „*cheating*“ bezeichnet, da Bakterien ohne eigenen Aufwand Wachstumsvorteile auf Kosten der Pilze erlangen (62). Trotz allem ist bisher unklar, wie anorganischer und organischer Stickstoff aus Pflanzen in die mikrobielle Bodengemeinschaft eingespeist wird und welche Mikroorganismen daran beteiligt sind (63, 64).

1.2. OMIK-Techniken

Die bioanalytische Methodik beschäftigt sich mit vier zentralen Bausteinen: der Genomik, der Transkriptomik, der Proteomik und der Metabolomik. Während die DNA die phylogenetische Information beschreibt, wird der Phänotyp von einem Organismus maßgeblich durch die RNA, die Proteine und die Metabolite definiert. Es wurde beschrieben, dass die genetische Information der DNA über die Transkription zur mRNA hin zur Translation zu den Proteinen, die abschließend Verbindungen umsetzen und damit für Stoffwechselaktivität sorgen, weitergetragen wird (65) (**Abbildung 4**). Folglich wurde angenommen, dass die genetische und funktionale Abundanz von DNA, mRNA und Proteinen vergleichbar ist. Jedoch wurde bisher in vielen Studien gezeigt, dass nur eine sehr schlechte, beziehungsweise keine direkte Korrelation besteht (66-68). Es ist ratsam, eine Kombination von OMIK-Techniken bestehend aus Genomik, Transkriptomik, Proteomik und Metabolomik zu nutzen, um ein umfassendes Verständnis für ein mikrobielles System aufzustellen.

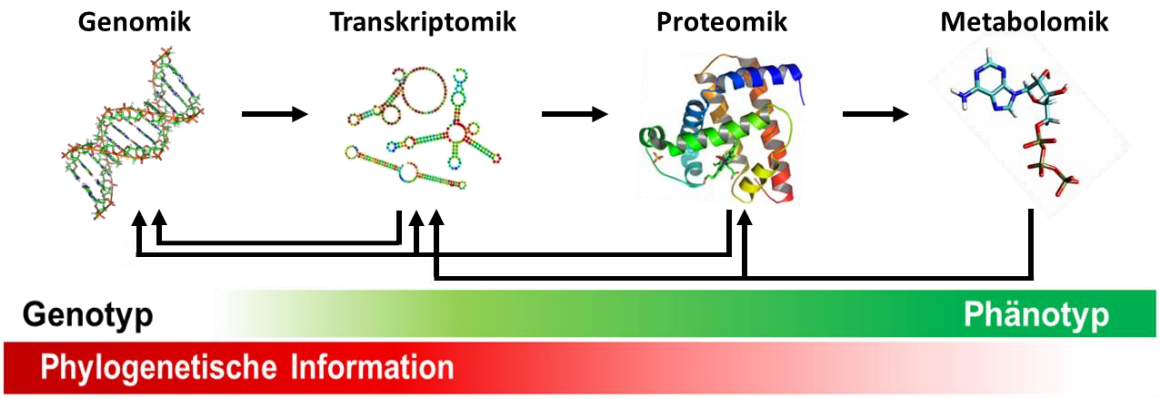

Abbildung 4: Die vier zentralen Bausteine der bioanalytischen Methodik. In der DNA liegt die phylogenetische Information während die RNA, die Proteine und die Metabolite den Phänotyp von einem Organismus beschreiben.

Jedoch bieten diese OMIK-Techniken noch keine Aussage über die Funktionalität einzelner Organismen in einer mikrobiellen Gemeinschaft. Erst die Verbindung von molekularbiologischen Methoden, beispielsweise mit stabilen Isotopen, ermöglicht die Verknüpfung der Identität mit der Funktion in der Umwelt (69). Die Markierung mit stabilen Isotopen wurde bereits für Phospholipidfettsäuren (PLFA) (70), Nukleinsäuren (RNA und DNA) (71), Aminosäuren (72) und Proteinen (73) durchgeführt. Üblicherweise dienen ^{13}C- oder ^{15}N-markierte Verbindungen oder komplexe Gemische als Marker für biologische Aktivität, die den Mikroorganismen entweder direkt im geschlossenen System oder auf Trägermaterialien wie Aktivkohle zur Verfügung gestellt werden (74). Hierbei bietet der PLFA-SIP trotz einer hohen Sensitivität für Einbau (<0.01%) nur eine schlechte phylogenetische Auflösung und es ist keine funktionale Analyse möglich (69). Im Gegensatz dazu versprechen Nukleinsäure-SIPs eine hohe phylogenetische Auflösung und potentielle, funktionale Informationen, wenn mehrere Primer genutzt werden (75), wobei eine Einbaurate von mindestens 40% vorhanden sein muss (76). Weiterhin beweist und quantifiziert das Aminosäure-SIP Verfahren lediglich den zugrundeliegenden Abbau und ermöglicht damit keine Aussage über die Struktur und die Funktion in der mikrobiellen Gemeinschaft (72). Dagegen zeichnet sich die Verwendung von Proteinen einerseits durch die hohe Sensitivität, wodurch auch geringe Einbauaktivitäten detektiert werden können (77, 78), und andererseits durch die Verknüpfung funktionaler und phylogenetischer Analyse der mikrobiellen Gemeinschaft aus (79).

1.2.1. Stabile Isotope

Bei der funktionalen Metaproteomik werden die verfügbaren Energie- und Nährstoffquellen mit stabilen Isotope markiert und von aktiven Mikroorganismen in die Biomasse eingebaut. Dabei sind die in den Aminosäuren vorkommenden Elemente Kohlenstoff (C), Wasserstoff (H), Stickstoff (N), Sauerstoff (O) und Schwefel (S) bedeutsam. Aus der durchschnittlichen Häufigkeit der einzelnen Aminosäuren in Proteinen (80) ergeben sich die relativen Häufigkeiten der Atome in den jeweiligen Proteinen. Der bisher am häufigsten untersuchte Kohlenstoff tritt durchschnittlich zu 31,56% in Proteinen auf, während Stickstoff nur 8,79% ausmacht (**Abbildung 5**).

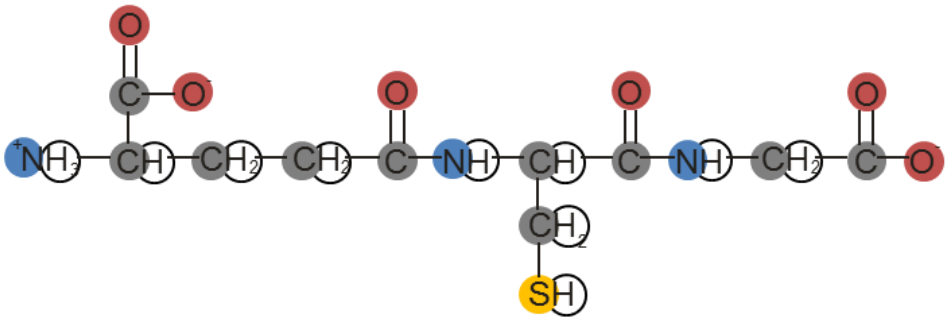

	Element	Heavy stable isotopes	# of atoms per "average" amino acids	Substrate for classic SIP-experiments	Potential application for micropollutant-SIP	General activity marker
●	Carbon	13C	4.93	***	**	**
○	Hydrogen	2H	7.75	*	*	***
●	Nitrogen	15N	1.35	***	*	**
●	Oxygen	18O	1.47	*	*	**
●	Sulfur	34/36S	0.04	*	*	*

Abbildung 5: Die Isotopenabundanz verschiedener Atome im Durchschnittsmodell eines Proteins nach Jehmlich, 2016 (81). Die atomare Zusammensetzung des Tripeptids Glu-Cys-Gln wird gezeigt. In der Tabelle ist die Abundanz der verschiedenen Atome in einer durchschnittlichen Aminosäure. Die Anwendbarkeit der Atome für klassische SIP-Experimente, für Mikroschadstoff-SIPs und für generelle Aktivität sind als hoch (***), mittel (**) und niedrig (*) eingestuft.

Elemente werden durch die Anzahl an Protonen und Neutronen im Atomkern sowie der Anzahl an Elektronen in der Atomhülle beschrieben (82). Dabei setzt sich die Atommasse aus der Protonen- und der Neutronenanzahl zusammen. Ein Element kann durch die unterschiedliche Neutronenanzahl im Atomkern eine unterschiedliche Atommasse haben. Die daraus

resultierenden Atome werden Nuklide genannt. Nuklide mit gleicher Protonenanzahl aber unterschiedlicher Atommasse werden Isotope genannt. Es wurden bisher ungefähr 270 stabile Isotope und 2.000 Radionuklide identifiziert (83). Radionuklide sind nicht stabil und durch eine geringe Halbwertszeit gekennzeichnet, wohingegen stabile Isotope sehr große Halbwertszeiten aufweisen und dadurch keinen sichtbaren Zerfall zeigen. ^{13}C ist das bisher am häufigsten verwendete stabile Isotop in Aminosäure-SIPs (72), PLFA-SIPs (84), Nukleinsäure-SIPs (85) und Protein-SIPs (35, 86, 87), um den Abbau von einzelnen Chemikalien, aber auch von kompleten Stoffgemischen wie dem Pflanzenabbau im Boden durch mikrobielle Gemeinschaften zu untersuchen.Bisher wurden nur wenige SIP-Versuche mit anderen stabilen Isotopen veröffentlicht. Dies kommt dadurch, dass viele Kohlenwasserstoffe ohne Heteroatome, wie beispielsweise Benzol oder Naphthalin, als Modellverbindungen genutzt werden. Bei der Untersuchung des Abbaus komplexer Stoffgemische werden andere Isotope wie ^{15}N und ^{18}O zunehmend berücksichtigt. Derartig wurden Nukleinsäure-SIPs mit ^{15}N-markierten Pflanzen (63, 64) und $H_2{}^{18}O$ (88) durchgeführt, um die aktiven Schlüsselorganismen und die jeweiligen atomaren Flüsse in den mikrobiellen Gemeinschaften zu identifizieren. Das umfassende Verständnis von atomaren Zyklen ist von Bedeutung, denn in allen terrestrischen Organismen zählen Kohlenstoff, Wasserstoff, Sauerstoff und Stickstoff zum Hauptbestandteil der Biomasse, die beispielsweise im Menschen 96,3% des Gewichts ausmachen und einen ähnlich hohen Anteil in allen anderen terrestrischen Organismen haben (89). Dabei bestehen diese Organismen mit knapp 90% aller Atome beziehungsweise 75% des Gewichts zum größten Teil aus Wasser. Der Kreislauf des Kohlenstoffs steht stellvertretend für den Energiekreislauf, während Stickstoff den Nährstofffluss beschreibt (50). In einer Studie von Mooshammer und Kollegen wurde gezeigt, dass sich der Kohlenstoff- und Stickstoffkreislauf beziehungsweise der Energie- und Nährstofffluss in Mikroorganismen konträr verhalten. Bei der Limitation von Kohlenstoff ist Stickstoff im Überfluss vorhanden und kann demnach sowohl mineralisiert als auch zum Aufbau von Biomasse assimiliert werden. Bei Stickstofflimitation herrscht Kohlenstoffüberfluss, wodurch der gesamte aufgenommene Stickstoff assimiliert wird, um Verluste zu vermeiden. Dieser Zyklus sollte vice versa für Kohlenstoff interpretiert werden können. Abgesehen davon wurde erst kürzlich die Markierung von Aminosäuren mit ^{34}S publiziert, die aufgrund der geringen Abundanz von Schwefel in Proteinen (0,29%) jedoch nur eine geringe Auflösung des Einbaus ermöglicht (90). Andererseits könnte die Verwendung von ^{2}H (D) und ^{18}O über die Zugabe von H_2O eine gewinnbringende Lösung darstellen, um eine systemunabhängige, mikrobielle Aktivität zu ermitteln. Dabei ist jedoch zu beachten, dass trotz

hoher Abundanz von H- (49,68%) und O-Atomen (9,68%) in Proteinen kein Abbau von H_2O im eigentlichen Sinne erfolgt. Demnach ist keine Sortierung der Einbaumuster bezüglich der Abbauwege möglich, aber es könnte der flexible Einbau in die Biomasse aktiver Spezies gezeigt werden. Dabei unterscheiden sich der Stoffwechsel von Wasserstoff und Sauerstoff aus Wasser grundsätzlich. Sauerstoff wird ausgehend vom Citratzyklus über Oxalacetat und über α-Ketoglutarat in alle Aminosäuren eingebaut, während der abiotische Austausch von Deuterium mit azidischen Wasserstoffen bereits beschrieben ist (91). Fraglich ist, ob der Einbau durch Enzyme bei Sauerstoff und der abiotische HD-Austausch mit der Aktivität von Mikroorganismen korreliert und welches Isotop eine genauere Auflösung bietet. Bekannt ist, dass die Kosten für $H_2{}^{18}O$ durch die aufwändigere Herstellung um ein Vielfaches größer sind als bei D_2O. Besonders für Experimente im großen Maßstab könnte das den limitierenden Faktor darstellen. Bereits etabliert wurde der Einbau von D_2O für die Bestimmung der mikrobiellen Aktivität mittels RAMAN-Spektroskopie (92), die in Kombination mit Protein-SIP eine funktional und phylogenetisch detaillierte Identifizierung mikrobieller Gemeinschaften ermöglichen könnte.

1.2.2. Funktionale Metaproteomik (Protein-SIP)

Die Proteomik wurde als Studie der exprimierten Proteine in einer Zelle, einem Gewebe oder einem Organismus zu einem bestimmten Zeitpunkt definiert (93). Die Forschung untersucht dabei nicht nur die Abundanz, sondern auch die möglichen Modifikationen wie Acetylierung, Phosphorylierung, und die Interaktionen von Proteinen, um ihre Rolle und die zugrundeliegenden Funktionen in zellulären Prozessen zu verstehen (94-97). Von Metaproteomik wird gesprochen, wenn eine Umweltprobe mit *n* Spezies ($n > 1$) untersucht wird. Derartig wurde die Identifikation von Proteinen in Bodenmikroorganismen zuvor als Bodenmetaproteomik beschrieben (98). Die Proteinabundanz in proteomischen Experimenten erlaubt detaillierte Aussagen über den Phänotyp von einem Organismus, kann diese aber nicht direkt mit Aktivität verbinden. Die von Jehmlich und Kollegen eingeführte funktionale Metaproteomik, der sogenannten stabilen Isotopenmarkierung von Proteinen (engl.: *protein stable isotope probing*, Protein-SIP), stellt eine etablierte Methode dar, um eine direkte Verbindung zur metabolischen Aktivität von einem Organismus in einer mikrobiellen Gemeinschaft zu knüpfen (86, 99, 100). Im Vergleich zu Nukleinsäure-SIPs, die einen Einbau von mindestens 25-30 Atom% erfordern (100), können im Protein-SIP mit weitaus genauerer Auflösung bis zu 0.1 Atom% detektiert werden, um metabolische Aktivität zu identifizieren

(77). Trotz der hohen Sensitivität bei der Einbaudetektion ist die funktionale Metaproteomik durch eine niedrigere Auflösung der taxonomischen Affiliation als in den entsprechenden Nukleinsäure-SIPs gekennzeichnet (79, 101). Im Detail wird die genaue taxonomische Zuordnung von Proteinen aufgrund von Homologien erschwert, wodurch eine valide Aussage über die Phylogenie von Mikroorganismen in Gemeinschaften nur auf der Stufe von Ordnungen und Familien getroffen werden kann. Dies trifft vor allem auf Proteine der Homöostase wie beispielsweise dem Chaperonin GroEL oder der DNA-Polymerase III, die in allen prokaryotischen Zellen abundant sind, zu. Andererseits ermöglicht die Identifizierung von spezifischen Proteinen wie der Benzoyl-CoA Reduktase, die eine Schlüsselfunktion im anaeroben Abbau von aromatischen Verbindungen trägt (102), eine genauere taxonomische Affiliation als die Stufe von Ordnung und Familie, weil die Benzoyl-CoA Reduktase nur von einem Teil der *Rhodocyclales* (Ordnung) beziehungsweise *Rhodocyclaceae* (Familie), namentlich beispielsweise *Thauera aromatica* K172 (103), exprimiert wird. Dagegen sind Nukleinsäure-SIPs in der Lage bis auf die Stufe des Genus zu identifizieren. Zusätzlich wird der Einbau beim Protein-SIP hochaufgelöst und differenziert dargestellt, wohingegen bei den restlichen SIP-Ansätzen lediglich zwischen leichter Phase ohne Einbau und schwerer Phase mit Einbau unterschieden werden kann. Der Einbau stabiler Isotope in Proteine wird durch die relative Isotopenabundanz (RIA) und dem Markierungsverhältnis (engl.: *labeling ratio*, LR) beschrieben (**Abbildung 6**).

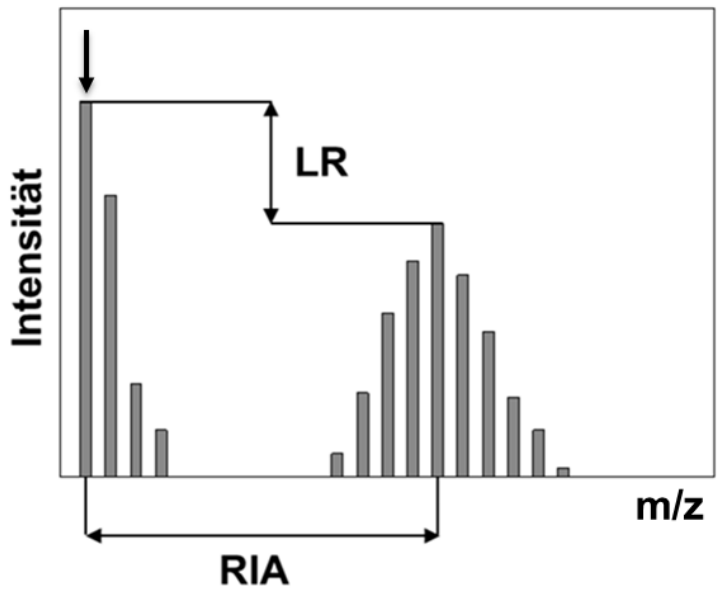

Abbildung 6: Schematische Darstellung eines Spektrums, wobei *m* für Masse und *z* für Ladung steht, mit den spezifischen Protein-SIP Werten, relative Isotopenabundanz (RIA) und Markierungsverhältnis (LR) ausgehend von der monoisotopischen Spitze (Pfeil).

Aus dem mit Flüssigkeitschromatographie gekoppelten massenspektrometrischen (MS) Messung resultierenden Spektrum ist die natürliche Abundanz von Kohlenstoff anhand der monoisotopischen ^{12}C-Spitze bestimmbar (**Abbildung 5, Pfeil**). Es handelt sich dabei nicht nur um eine Spitze, sondern um eine Verteilung, da die natürliche Abundanz vom leichten Isotop ^{12}C 98,9% und vom schweren Isotop ^{13}C 1,1% beträgt, und damit ungefähr jedes hundertste Kohlenstoffatom von Natur aus schwer ist. Das entscheidende Merkmal der Isotopenmarkierung von Proteinen in einem Spektrum ist die Verteilung der schweren Isotopologe in der Gesamtmenge eines Proteins. Dabei ist die zugrundeliegende Wahrscheinlichkeitsdichte eine Normalverteilung, wodurch das resultierende Einbaumuster typischerweise eine Gaußverteilung aufweist. Der RIA-Wert ist dabei die Abundanz von schweren Isotopen eines Proteins und wird durch den Abstand zwischen monoisotopischer ^{12}C-Spitze und dem Höchstpunkt der ^{13}C-Gaußverteilung beschrieben. Andererseits beschreibt der LR-Wert die Synthese von markierten Proteinen und ergibt sich aus der Höhe der ^{13}C-Gaußverteilung im Verhältnis zur monoisotopischen ^{12}C-Spitze (100). Diese charakteristischen Werte werden mittlerweile mit dem Programm *MetaProSIP* automatisiert berechnet (104). Aufgrund der ermittelten Einbaumuster kann die primäre, sekundäre und tertiäre Verwertung bezüglich einer Energie- oder Nährstoffquelle separiert werden, wodurch der atomare Fluss in einer mikrobiellen Gemeinschaft aufgezeigt werden kann.

Zusammenfassend sollte in Zukunft die parallele Verwendung von verschiedenen Isotopen angestrebt werden, um nicht nur die Aktivität bezüglich eines Atoms, aber vielmehr multiatomare Aktivitätsmuster zu generieren. Außerdem wird die Verbindung verschiedener OMIK-Techniken immer häufiger genutzt, um umfassendere Aussagen über die phylogenetischen und phänotypischen Informationen von Organismen in mikrobiellen Gemeinschaften zu treffen (105-108). Dabei erlaubt die differentielle Isolierung von Nukleinsäuren und Proteinen aus einer Probe multidimensionale SIP-Ansätze, die die phylogenetische Genauigkeit der Nukleinsäure-SIPs mit der hohen funktionalen Auflösung des Protein-SIPs verbindet.

2. Zielsetzungen

Das Ziel der vorliegenden Dissertation war es, die Energie- und Nährstoffflüsse von zwei mikrobiellen Gemeinschaften mittels funktionaler Metaproteomik zu untersuchen. Dabei wurden zwei unterschiedliche, ökologische Modelle verwendet: Einerseits die Energieflüsse (Kohlenstoff) im anaeroben Abbau von Benzol durch eine angereicherte, mikrobielle Grundwassergemeinschaft und zum anderen die Nährstoffflüsse (Stickstoff) während des Pflanzenabbaus durch Bodenmikroorganismen.

Genauer wurden folgende Fragen untersucht:

2.1. Welche Organismen sind an der sekundären Kohlenstoffverwertung von Acetat resultierend aus der Benzolfermentation in einer benzolmineralisierenden und sulfatreduzierenden, mikrobiellen Gemeinschaft beteiligt? (**Artikel 3.2**)

2.2. Welche Physiologie des dominanten Acetatverwerters der benzolmineralisierenden und sulfatreduzierenden, mikrobiellen Gemeinschaft kann basierend auf der Anreicherung von diesem Organismus mit anschließender Metagenomanalyse abgeleitet werden? (**Artikel 3.1**)

2.3. Welche Bodenmikroorganismen sind für die schnelle Assimilation von Stickstoff aus ^{15}N-markiertem Pflanzenmaterial verantwortlich? (**Artikel 3.3**)

3. Veröffentlichungen

3.1. Metagenome-Based Metabolic Reconstruction Reveals the Ecophysiological Function of Epsilonproteobacteria in a Hydrocarbon-Contaminated Sulfidic Aquifer.

Keller, A.H., Schleinitz, K.M., **Starke, R.**, Bertilsson, S., Vogt, C., und Kleinsteuber, S. (2015)

Front Microbiol. **6**: 1396.

DOI: 10.3389/fmicb.2015.01396

In dieser Arbeit wurde das aus einer Hungerkultur angereicherte Metagenom des epsilonproteobakteriellen Phylotyps hinsichtlich des Kohlenstoff- und Energiemetabolismus, der Schwefel- und Stickstoffassimilation sowie der Transportsysteme untersucht. Die eigenen Anteile umfassten die Genomannotation und die Datenanalyse sowie die Überarbeitung des von A. H. Keller angefertigten Manuskripts, der von A. H. Keller angefertigten Abbildungen (Abbildungen 1.1 und 2.1) und der von A. H. Keller angefertigten Tabellen (Tabellen 1.1, 2.1 und 4.1).

3.2. Pulsed $^{13}C_2$-Acetate Protein-SIP Unveils Epsilonproteobacteria as Dominant Acetate Utilizers in a Sulfate-Reducing Microbial Community Mineralizing Benzene.

Starke, R., Keller, A., Jehmlich, N., Vogt, C., Richnow, H.H., Kleinsteuber, S., von Bergen, M., und Seifert, J. (2016)

Microb Ecol. **71**(4): 901-911.

DOI: 10.1007/s00248-016-0731-y

In dieser Arbeit wurde der sekundäre Metabolismus, resuliertend aus der Benzolfermentation, anhand eines gepulsten Protein-SIPs vom komplett ^{13}C-markierten Intermediat Acetat aufgedeckt. Die eigenen Anteile umfassten die Planung und die Durchführung des Experiments, die Proteinextraktion und die massenspektrometrischen Analysen, die Datenanalyse sowie die Erstellung des Manuskripts, der Abbildungen (Abbildungen 1.2, 2.2, 3.2, 4.2 und 5.2) und der Tabellen (Tabellen 1.2 und 2.2).

3.3. Bacteria dominate the short-term assimilation of plant-derived N in soil.

Starke, R., Kermer, R., Ullmann-Zeunert, L., Baldwin, I.T., Seifert, J., Bastida, F., von Bergen, M., und Jehmlich, N. (2016)

Soil Biology & Biochemistry **96**: 30-38.

DOI*:* 10.1016/j.soilbio.2016.01.009

In dieser Arbeit wurde die Aktivität von Bodenmikroorganismen im kurzzeitigen Pflanzenabbau anhand eines Protein-SIPs von komplett ^{15}N-markiertem Tabak beschrieben. Die eigenen Anteile umfassten die Datenanalyse, die Erstellung des Manuskripts, der Abbildungen (Abbildungen 1.3, 2.3, 3.3, 4.3 und 5.3) und der Tabellen (Tabellen 1.3 und 2.3).

3.1. Keller et al., Frontiers in Microbiology (2015)

Metagenome-Based Metabolic Reconstruction Reveals the Ecophysiological Function of *Epsilonproteobacteria* in a Hydrocarbon-Contaminated Sulfidic Aquifer

Andreas H. Keller[1,2], Kathleen M. Schleinitz[2], Robert Starke[3], Stefan Bertilsson[4], Carsten Vogt[1] and Sabine Kleinsteuber[2*]

[1]Department of Isotope Biogeochemistry, Helmholtz Centre for Environmental Research - UFZ, Leipzig, Germany,

[2]Department of Environmental Microbiology, Helmholtz Centre for Environmental Research - UFZ, Leipzig, Germany

[3]Department of Proteomics, Helmholtz Centre for Environmental Research - UFZ, Leipzig, Germany

[4]Department of Ecology and Genetics, Limnology and Science for Life Laboratory, Uppsala University, Uppsala, Sweden

[*]Corresponding author: Sabine Kleinsteuber, sabine.kleinsteuber@ufz.de

Received: 01 October 2015

Accepted: 23 November 2015

December 2015, Volume 6, Issue 1396, pp 1-14

DOI: 10.3389/fmicb.2015.01396

Keywords: Campylobacterales, sulfur cycling, rTCA cycle, acetate assimilation, anaerobic hydrocarbon degradation, nitrogen fixation, niche adaptation, intermediary ecosystem metabolism

Abstract

The population genome of an uncultured bacterium assigned to the *Campylobacterales* (*Epsilonproteobacteria*) was reconstructed from a metagenome dataset obtained by whole-genome shotgun pyrosequencing. Genomic DNA was extracted from a sulfate-reducing, *m*-xylene-mineralizing enrichment culture isolated from groundwater of a benzene-contaminated sulfidic aquifer. The identical epsilonproteobacterial phylotype has previously been detected in toluene- or benzene-mineralizing, sulfate-reducing consortia enriched from the same site. Previous stable isotope probing experiments with $^{13}C_6$-labeled benzene suggested that this phylotype assimilates benzene-derived carbon in a syntrophic benzene-mineralizing consortium that uses sulfate as terminal electron acceptor. However, the type of energy metabolism and the ecophysiological function of this epsilonproteobacterium within aromatic hydrocarbon-degrading consortia and in the sulfidic aquifer are poorly understood.

Annotation of the epsilonproteobacterial population genome suggests that the bacterium plays a key role in sulfur cycling as indicated by the presence of a *sqr* gene encoding a sulfide quinone oxidoreductase and *psr* genes encoding a polysulfide reductase. It may gain energy by using sulfide or hydrogen/formate as electron donors. Polysulfide, fumarate, as well as oxygen are potential electron acceptors. Auto- or mixotrophic carbon metabolism seems plausible since a complete reductive citric acid cycle was detected. Thus the bacterium can thrive in pristine groundwater as well as in hydrocarbon-contaminated aquifers. In hydrocarbon-contaminated sulfidic habitats, the epsilonproteobacterium may generate energy by coupling the oxidation of hydrogen or formate and highly abundant sulfide with the reduction of fumarate and/or polysulfide, accompanied by efficient assimilation of acetate produced during fermentation or incomplete oxidation of hydrocarbons. The highly efficient assimilation of acetate was recently demonstrated by a pulsed $^{13}C_2$-acetate protein stable isotope probing experiment. The capability of nitrogen fixation as indicated by the presence of *nif* genes may provide a selective advantage in nitrogen-depleted habitats. Based on this metabolic reconstruction, we propose acetate capture and sulfur cycling as key functions of *Epsilonproteobacteria* within the intermediary ecosystem metabolism of hydrocarbon-rich sulfidic sediments.

Introduction

Representatives of the *Epsilonproteobacteria* inhabit a broad spectrum of environments like mammalian digestive systems (109, 110), brackish Engberg et water (111), hydrothermal sediments (112), or subsurface systems (113-116). Previously obtained isolates have been described as chemolithoautotrophs (117, 118) fixing carbon via the reductive tricarboxylic acid (rTCA) cycle (119). Notably, they are recognized as key players in sulfidic habitats (120) capable of oxidizing sulfide, sulfur or thiosulfate, or using elemental sulfur/polysulfide as terminal electron acceptors. Furthermore, oxygen, nitrate and fumarate can be electron acceptors (120, 121). Besides reduced inorganic sulfur compounds, hydrogen or organic substances such as malate and formate were shown to be electron donors (120). The broad spectrum of habitats where *Epsilonproteobacteria* can be found is underlined by their capability to grow under aerobic, microaerobic or anoxic conditions. A model organism representing the metabolic versatility of this proteobacterial class is *Wolinella succinogenes*. It couples anaerobic fumarate or nitrate respiration with hydrogen, sulfide or formate oxidation (122, 123) but can also grow under limited oxic conditions (110). During the last decade, research focused on *Epsilonproteobacteria* thriving in marine systems such as hydrothermal vents (124-127) or pelagic oxic-anoxic interfaces (128) as well as in terrestrial sulfidic caves and springs (129-133), or mud volcanos (134) where they are thought to be mainly involved in the oxidation or reduction of sulfur compounds.

Recently, *Epsilonproteobacteria* were also found to be abundant in anoxic hydrocarbon-rich habitats like oil reservoirs (115), phenol-degrading methanogenic sludge (135), petroleum-contaminated soil (136), and hydrocarbon-degrading sulfate-reducing enrichment cultures (137-142). The metabolism of *Epsilonproteobacteria* in anoxic hydrocarbon-contaminated subsurface systems and especially in sulfate-reducing consortia is poorly understood as they are neither known to perform dissimilatory sulfate reduction nor to degrade aromatic or aliphatic hydrocarbons. However, they seem to be stimulated by acetate amendment in anaerobic sediments (114) or even assimilate acetate as shown by DNA stable isotope probing (SIP) with $^{13}C_2$-labeled acetate (143).

In this study, we investigated a member of the epsilonproteobacterial order *Campylobacterales* originating from a sulfidic, hydrocarbon-contaminated aquifer at an industrial site near Zeitz, Germany (144-146). It was originally enriched under sulfate-reducing conditions in a syntrophic, benzene-mineralizing consortium and was shown to be distantly related to the genus

Sulfurovum (139, 147). An identical phylotype (in the following named as Zeitz epsilonproteobacterium) was consistently detected in various toluene-degrading (138, 140, 141) and *m*-xylene-degrading (137) sulfate-reducing enrichment cultures from the same site and remained abundant after prolonged incubation. The closest relatives of this phylotype based on 16S rRNA gene sequences were found in pristine sulfidic springs and caves (131, 132). A DNA-SIP experiment with $^{13}C_6$-benzene revealed significant labeling of the Zeitz epsilonproteobacterium, besides the putative initial benzene degrader, a clostridial phylotype assigned to the genus *Pelotomaculum (147).*

However, the respective protein-SIP experiment did not confirm labeling of the Zeitz epsilonproteobacterium whereas benzene assimilation by the initial degrader *Pelotomaculum* sp. was verified (35). Likewise, protein-SIP with methyl-labeled *m*-xylene (1,3-dimethyl-$^{13}C_2$-benzene) did not lead to a labeling of epsilonproteobacterial peptides within the *m*-xylene-degrading enrichment culture (137, 148). Thus, the Zeitz epsilonproteobacterium seems to be not primarily involved in hydrocarbon degradation, despite being consistently present in the respective consortia in varying relative abundances. We hypothesize that it uses metabolites from hydrocarbon degradation under sulfate-reducing conditions, but the type of energy metabolism and its specific ecophysiological role in the consortia have remained unknown so far. To shed light on the ecological niche and metabolic function of *Epsilonproteobacteria* in hydrocarbon-rich sulfidic environments, we aimed at a metabolic reconstruction of the Zeitz epsilonproteobacterium based on genome-centric metagenomics.

Materials and methods

DNA isolation and whole genome amplification

Cells originated from a batch culture used as a control in a growth experiment with an *m*-xylene-degrading, sulfate-reducing batch culture (137, 148, 149). The medium in the control culture did not contain any organic carbon source. During the experiment, phylogenetic composition was determined by terminal restriction fragment length polymorphism (T-RFLP) analysis using the restriction enzymes *Bst*UI and *Rsa*I according to methods described previously (150). It revealed an exceptionally high proportion of the epsilonproteobacterial terminal restriction fragment (T-RF) in the control culture. Cells from 20 mL of this control culture were harvested by centrifugation. DNA was extracted using the NucleoSpin Tissue Kit (Macherey-Nagel) according to the manufacturer´s support protocol for bacteria. Multiple displacement amplification (MDA) of the extracted DNA was performed with the illustra GenomiPhi V2 Amplification Kit (GE Healthcare Life Sciences). Five parallel MDA reactions were carried out according to the manufacturer´s instructions, using a reaction time of 2 h. Phylogenetic composition of each MDA product was determined by T-RFLP analysis as stated above. The relative abundance of the epsilonproteobacterial T-RF was estimated to be 85.5 – 87.6% (*Bst*UI) and 92.9 – 94.7% (*Rsa*I), respectively. The reaction products were purified using the Amicon Ultra-0.5 Centrifugal Filter Device (Millipore). DNA quantity and quality was checked photometrically using a NanoDrop ND-1000 UV/Vis spectral photometer (PeqLab, Germany) and by agarose gel electrophoresis. The products of the five MDA reactions were then pooled and used for whole genome sequencing.

Whole genome shotgun sequencing and sequence analysis

Amplified DNA was sequenced in two separate runs with 200 cycles on the Roche 454 FLX platform using Titanium chemistry. The average read length of the first run (310 Mbp) was 391 bp. The second run (235 Mbp) was a mate-pair library with 3 kbp inserts and had an average read length of 389 bp. All sequencing was performed at the SciLifeLab SNP/SEQ sequencing facility at Uppsala University. Contigs from both runs were assembled with Newbler using a minimal overlap of 40 bp and 90% identity.

Phylogenetic binning of the contigs ≥1 kb was performed with PhylopythiaS (http://binning.bioinf.mpi-inf.mpg.de/; (151)) using the sample-specific model type. Additionally, contigs containing rRNA genes were identified by RNAmmer 1.2

(http://www.cbs.dtu.dk/services/RNAmmer/; (152)). The detected rRNA genes were phylogenetically assigned using the RDP Classifier (153). All contigs assigned to the *Epsilonproteobacteria* were reordered with the Mauve Aligner (154) using the genome of *Sulfurovum* sp. NBC37-1 (125) as scaffold (acc. no. NC_009663).

Genome annotation and pathway analysis

Reordered contigs were uploaded to the Micro Scope platform (v. 2.5.4, May 2014; (155)) and automatically annotated. Automatic annotation was manually edited using the microbial annotation system Magnifying Genome (MaGe) (156) that includes PsortB, SwissProt, TrEMBL and COGnitor. Metabolic pathways were predicted using the integrated pathway tools of MaGe that are based on the KEGG and MicroCyc databases. Genome completeness was estimated based on the MaGe Minimal Gene Set comprising 205 essential genes (157) and using the set of 139 conserved single copy genes (CSCG) which occur only once in at least 90% of all bacterial genomes (158). The annotated contigs have been submitted to the European Nucleotide Archive (ENA) under the study accession no. PRJEB11632 (www.ebi.ac.uk/ena/data/view/PRJEB11632).

Results

Genome overview and phylogenetic assignment

Table 1.1: Number of coding DNA sequences (CDS) assigned to cluster of orthologous groups (COG).

Process	Class ID	Description	CDS
Cellular processes and signaling	D	Cell cycle control, cell division, chromosome partitioning	28
	M	Cell wall/membrane/envelope biogenesis	118
	N	Cell motility	23
	O	Posttranslational modification, protein turnover, chaperones	88
	T	Signal transduction mechanisms	51
	U	Intracellular trafficking, secretion, and vesicular transport	52
	V	Defense mechanisms	18
Information storage and processing	J	Translation, ribosomal structure and biogenesis	144
	K	Transcription	68
	L	Replication, recombination and repair	91
Metabolism	C	Energy production and conversion	129
	E	Amino acid transport and metabolism	131
	F	Nucleotide transport and metabolism	52
	G	Carbohydrate transport and metabolism	54
	H	Coenzyme transport and metabolism	82
	I	Lipid transport and metabolism	37
	P	Inorganic ion transport and metabolism	88
	Q	Secondary metabolites biosynthesis, transport and catabolism	21
Poorly characterized	R	General function prediction only	221
	S	Function unknown	121

Overall, the reconstructed population genome has a sequence length of around 1.6 Mb with a GC content of about 33%. Within 105 contigs, 1832 genomic objects with an average sequence length of about 850 bp were identified, comprising 30 tRNA genes, two not further specified

RNA genes, and 1797 protein coding sequences (CDS). A 16S rRNA gene was detected showing 94% similarity to that of *Sulfurovum* sp. NCBI-37 and a 23S rRNA gene with 93% similarity to the same next relative. Additionally, a 5S rRNA gene was detected on the contig harboring the 23S rRNA gene. 1384 of the CDS belonged to at least one cluster of orthologous groups (COG). **Table 1.1** summarizes the COG assignment. The genome completeness based on the Minimal Gene Set is 93% as 15 of the 205 genes are missing. Based on the CSCG set, the completeness is 97% (four genes of the 139 CSCG are missing).

An overview of general genome characteristics is given in **Table 2.1**. The phylogenetic assignment of the population genome was analyzed based on Maximum Likelihood trees calculated from 16S rRNA gene sequences (only from cultured species) and DNA gyrase subunit A (encoded by *gyrA*) sequences of representative members of the class *Epsilonproteobacteria* (**Supplementary Figure 1.1**). Both trees show that the Zeitz epsilonproteobacterium forms a clade with members of the genus *Sulfurovum*. Based on the *gyrA* phylogeny, the next relative is *Sulfurovum* sp. AS07-7 which represents a *Sulfurovum*-like population genome retrieved from Acquasanta Terme (130).

Table 2.1: General features of the reconstructed population genome.

Feature	
Genome length	1,625,596 bp
GC content	33%
Genome completeness	93-97%
No. of contigs	105
Average CDS length	850 bp
Protein coding density	89%
Genomic objects	1832
No. of CDS	1797
tRNA genes	30
rRNA genes	3
Other RNA genes	2

Carbon metabolism

The genome contains all genes necessary for a complete rTCA cycle, indicating that the Zeitz epsilonproteobacterium can fix CO_2 to build up biomass (**Figure 1.1**).

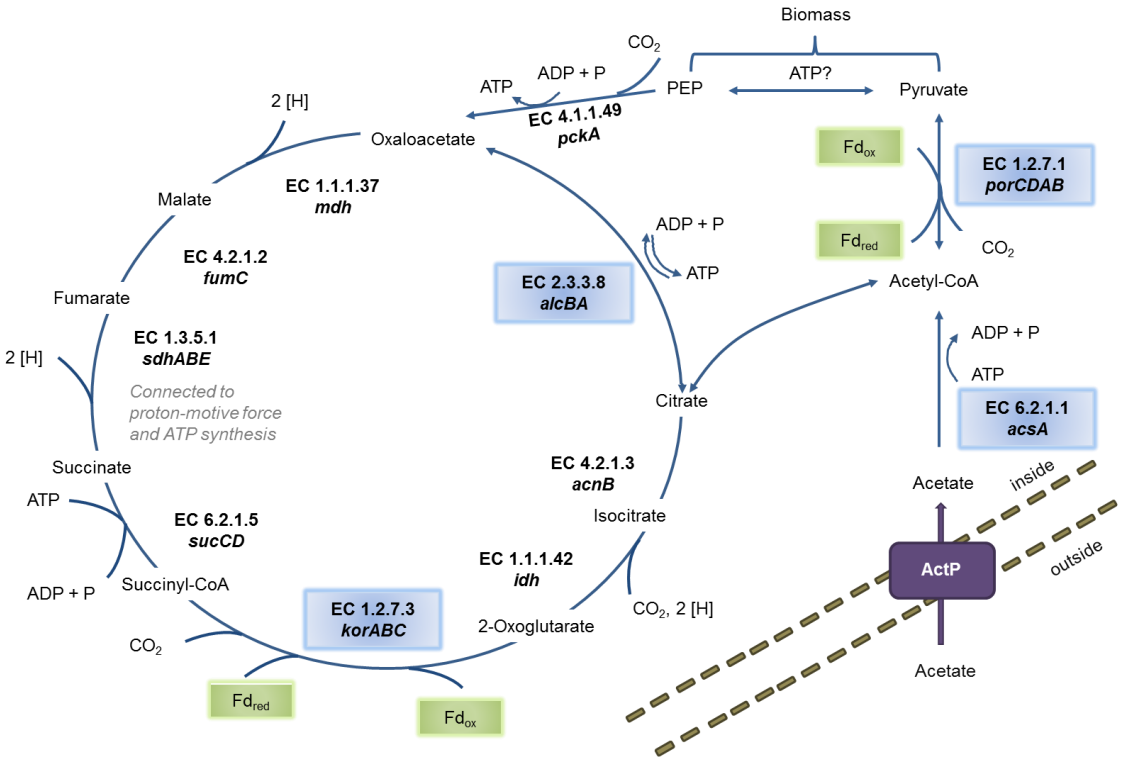

Figure 1.1: Predicted pathways of biomass buildup from CO_2 or from acetate. The reconstructed population genome encodes two different mechanisms of carbon assimilation: Either by importing acetate from the surrounding environment and activation via the acetyl-CoA synthetase AcsA (EC 6.2.1.1) or by CO_2 fixation via the reductive citric acid (rTCA) cycle. Involved enzymes are: ATP-citrate lyase (EC 2.3.3.8), malate dehydrogenase (EC 1.3.3.7), fumarate hydratase (EC 4.1.2.1), fumarate reductase (EC 1.3.5.1), succinyl-CoA synthetase (EC 6.2.1.5), 2-oxoglutarate ferredoxin oxidoreductase (EC 1.2.7.3), NADP-dependent isocitrate dehydrogenase (EC 1.1.1.42) and citrate lyase (EC 4.2.1.3). The corresponding genes are denoted below the EC numbers. The two oxygen-sensitive ferredoxin-dependent CO_2-fixation reactions are labeled in green boxes. Unique enzymes either part of the rTCA or involved in acetate processing are labelled in blue boxes. Activated acetyl-CoA is further processed to pyruvate and phosphoenolpyruvate (PEP) for the regeneration of rTCA intermediates or for biomass buildup. The enzymes pyruvate ferredoxin oxidoreductase (EC 1.2.7.1) and phosphoenolpyruvate carboxykinase (EC 4.1.1.49) are involved in this step. No enzyme catalyzing the reaction of pyruvate to PEP was detected in the population genome.

All genes encoding the three key enzymes of the rTCA cycle were detected: *alcBA* encoding the ATP citrate lyase (EC 2.3.3.8), *korABC* encoding the 2-oxoglutarate ferredoxin oxidoreductase (EC 1.2.7.3), and *porCDAB* encoding the pyruvate ferredoxin oxidoreductase (EC 1.2.7.1). In this process, two CO_2 molecules are fixed to synthesize one molecule of acetyl-

CoA. A second source for acetyl-CoA is potentially the direct uptake of acetate and further processing to acetyl-CoA. The genes encoding the appropriate and unique enzyme acetyl-CoA synthetase AcsA (EC 6.2.1.1) and the acetate permease ActP were found in the genome. In a subsequent reaction, acetyl-CoA is converted to pyruvate by addition of a further CO_2 molecule via the third key enzyme of the rTCA cycle, pyruvate ferredoxin oxidoreductase. A gene for the next step catalyzing the conversion of pyruvate to phosphoenolpyruvate (PEP) was not found. The gene *pckA* encoding a phosphoenolpyruvate carboxykinase (EC 4.1.1.49) was detected. PEP or pyruvate either regenerate the intermediates of the rTCA cycle or can be used for gluconeogenesis. Enzymes involved in the rTCA cycle participate also in other cell processes, such as the fumarate reductase/succinate dehydrogenase (EC 1.3.5.1) which can also function in fumarate respiration. In the genome, two fumarate reductases/succinate dehydrogenases are encoded on two different contigs (see next section).

Energy metabolism

An overview on the predicted pathways involved in energy metabolism and the corresponding electron donors and acceptors is shown in **Figure 2.1.** Genome analysis showed that hydrogen may function as electron donor. Two Ni-Fe containing hydrogenases are encoded in the genome, namely the uptake hydrogenase HupSL (EC 1.12.99.6) and the quinone-reactive hydrogenase HydABC (EC 1.12.5.1), both associated with the periplasmic membrane (159, 160). The former is expressed under nitrogen-fixing conditions when hydrogen is generated and converted to minimize energy loss during fixation catalysis. Electrons released in this process are transferred to the ubiquinone pool. The oxidation of hydrogen via HydABC is coupled to the reduction of NAD^+ and ferredoxin, establishing a proton gradient for ATP generation (161). In addition, the gene *sqr* encoding a sulfide quinone oxidoreductase (EC 1.8.5.4) was found. This membrane-bound enzyme catalyzes the initial step in dissimilatory sulfide oxidation, the conversion of hydrogen sulfide to polysulfides (162, 163). Genes for the complete oxidation of reduced sulfur species to sulfate via the Sox system were not detected. Furthermore, formate could serve to provide electrons. The gene *fdhA* encoding one of the three subunits of formate dehydrogenase (FDH) was identified (164). FDH oxidizes formate to carbon dioxide coupled with the reduction of NAD^+ to NADH.

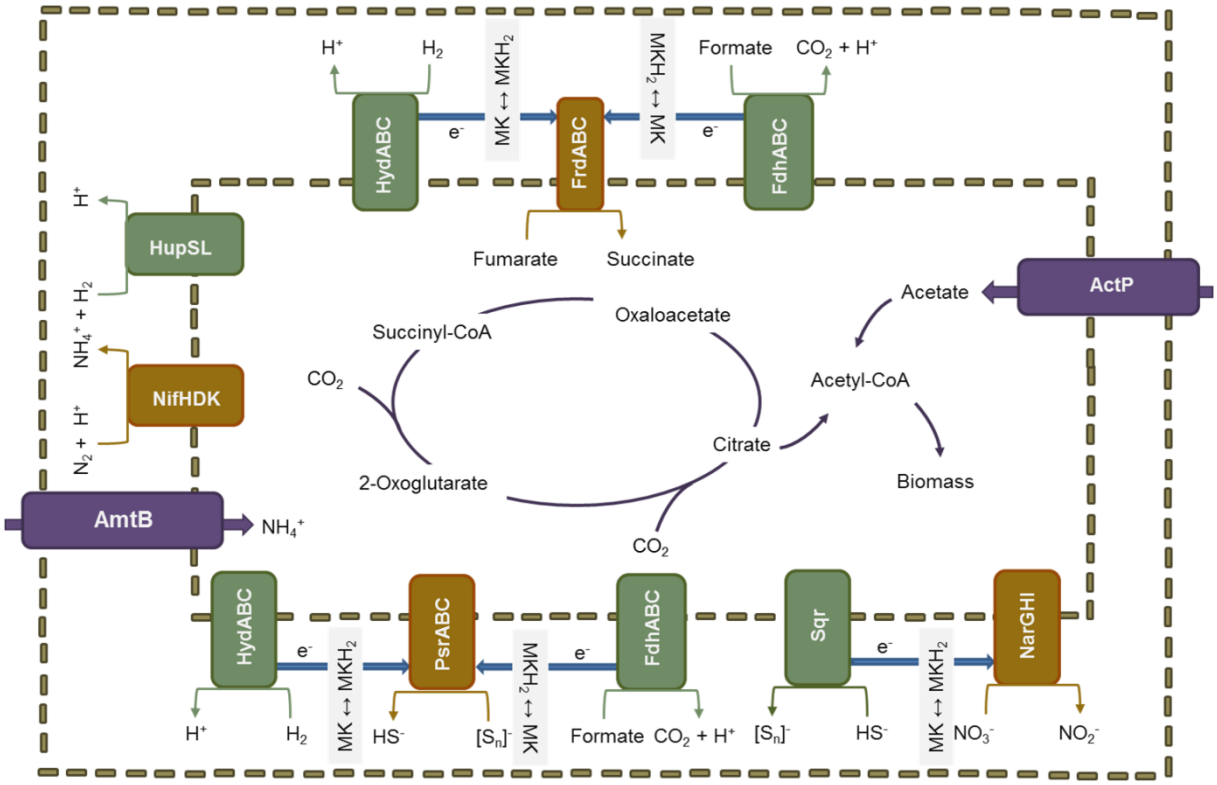

Figure 2.1: Schematic overview about the predicted metabolic pathways. The capability to fix nitrogen as alternative to ammonium uptake and to fix CO_2 as alternative to acetate assimilation as well as the versatility regarding electron donors and acceptors might provide a selective advantage of the Zeitz epsilonproteobacterium in groundwater systems. Electron donors and acceptors are shown as redox couples as described in the literature. It is supposed that specifically the high affinity to acetate generated as intermediate of hydrocarbon degradation and a higher tolerance to sulfide accumulating due to sulfate reduction by *Deltaproteobacteria* define its ecological niche in the Zeitz aquifer.

The Zeitz epsilonproteobacterium is a facultative anaerobe but has a strictly respiratory type of energy metabolism. The genome contains all genes necessary for oxidative phosphorylation with oxygen, including genes for an NADH-quinone oxidoreductase (EC 1.6.5.11), a succinate dehydrogenase/fumarate reductase (EC 1.3.5.1), a ubiquinol-cytochrome c reductase (EC 1.10.2.2), a cytochrome c oxidase cbb3-type (EC 1.9.3.1), an F-type ATPase (EC 3.6.3.14), and both ATPase-supporting enzymes polyphosphate kinase (*ppk*; EC 2.7.4.1) and inorganic pyrophosphatase (*ppa*; EC 3.6.1.1). In organisms exposed to oxygen, a mechanism to cope with oxygen-generated radicals would be expected. The *sodB* gene encoding a superoxide dismutase subunit (EC 1.15.1.1) was annotated, but the gene for the second subunit *sodA* is missing. A second oxygen protection mechanism is based on alkyl hydroperoxide reductase (EC 1.11.1.15). The respective gene *ahpC* was annotated. Under anoxic conditions, nitrate,

polysulfide or fumarate can serve as terminal electron acceptor for oxidative phosphorylation. For the reduction of nitrate to nitrite, *narG* and *narH* encoding a membrane-bound nitrate reductase were found (165). The gene *narI* is putatively encoded in the CDS downstream of *narH*. No gene *narK* for the nitrate/nitrite transporter was found. Three genes are necessary for polysulfide reduction: *psrA* encoding the catalytic subunit PsrA, *psrB* encoding the electron-transferring subunit PsrB, and *psrC* encoding the membrane anchor PsrC (166). Complete *psrB* and *psrC* were found, but only a fragment of *psrA* was identified. In *Epsilonproteobacteria*, the fumarate reductase involved in fumarate respiration consists of three subunits FrdABC. FrdA is the catalytic subunit, FrdB contains iron-sulfur clusters, and FrdC the cytochrome transferring the electrons to carriers and anchoring the enzyme in the membrane (123). As mentioned above, two copies of succinate dehydrogenase/fumarate reductase are encoded in the genome of the Zeitz epsilonproteobacterium. One copy comprises only the genes for FrdA and FrdB, whereas the other copy contains the genes for all three subunits.

Sulfur and nitrogen assimilation

No sulfate uptake system was detected, except for *yvdB* encoding a subunit of a sulfate transporter-like protein. Furthermore, the genome harbors the *sat* gene for sulfate adenylyltransferase (EC 2.7.7.4) which is responsible for the activation of sulfate to adenylyl sulfate (APS). Alternatively, sulfide rather than sulfate could be assimilated. Both enzymes necessary for sulfur assimilation from sulfide, serine O-acetyltransferase (EC 2.3.1.30) and cysteine synthase A (EC 2.5.1.47), are encoded in the population genome.

Genes encoding nitrogen fixation and ammonium uptake were identified. A dinitrogenase responsible for nitrogen fixation is encoded by *nifHDK* (EC 1.18.6.1). The MoFe-protein NifDK is the site for nitrogen reduction and the Fe-protein NifH transfers electrons (167). As a result of this catalytic process, ammonia is synthesized and fed into metabolic pathways. For an active dinitrogenase complex, further *nif* genes are required. Distributed over the genome, eighteen genes were assigned as related to nitrogen fixation (**Table 3.1**). The *nifEN* gene products act as scaffolding agents for cofactors, NifWZ is related to catalytic stability, and NifVB, NifQ as well as NifT are involved in the biosynthesis of dinitrogenase subunits (168). Regulators of gene expression are encoded by *nifA*, *nifX*, *nifU (169-171)*. Furthermore, *amtB* encoding an ammonia importer was detected. Ammonia, imported or produced via nitrogen fixation, is subsequently funneled into the amino acid metabolism via glutamine synthetase (EC

6.3.1.2) and glutamate synthase (EC 1.4.1.13), or glutamate dehydrogenase (EC 1.4.1.4). All of the respective genes are present in the genome.

Table 3.1: Genes involved in nitrogen assimilation.

Gene	Function	Reference
nifT	Maturation	Simon et al. (1996)
nifH	Fe dinitrogenase reductase	Steenhoudt and Vanderleyden (2000)
nifD	FeMo dinitrogenase	Steenhoudt and Vanderleyden (2000)
nifK	FeMo dinitrogenase	Steenhoudt and Vanderleyden (2000)
nifE	Scaffold for FeMo-cofactor	Raymond et al. (2004)
nifN	Scaffold for FeMo-cofactor	Raymond et al. (2004)
nifB	Biosynthesis of FeMo-cofactor	Temme et al. (2012)
glnB	N-signal transmitter protein PII	Steenhoudt and Vanderleyden (2000)
nifU	Biosynthesis FeMo-cofactor	Böhme (1998)
nifX	Negative regulator	Gosink et al. (1990)
nifA	Transcriptional activator	Steenhoudt and Vanderleyden (2000)
nifW	Catalytic stability	Böhme (1998)
nifZ	Catalytic stability	Böhme (1998)
nifQ	Biosynthesis of FeMo-cofactor	Temme et al. (2012)
nifV	FeMo-cofactor	Böhme (1998)

Transport systems

Over 30 genes were assigned as related to ABC transporters. The specificity in annotation of these genes varied making it difficult to assign a (clear) function to all encoded transporters specifically. Those with definite assignment comprise the molybdenum transporter encoded by *modABCDE*, the energy-consuming TonB transport system consisting of *tonB*, *exbB* and *exbD*, the specific phosphate transporter Pst encoded by *pstSCAB* and the corresponding regulators *phoU* and *phoB*. Furthermore, uptake complexes for potassium (*ktrAB*), ferrous iron (*feoAB* with the corresponding regulator gene *fur)*, and zinc (*znuBCA*) were detected. The export of large organic molecules from the cell may be accomplished using the type II secretion system together with the translocation pathways Tat and Sec-SRP. Almost all genes for both translocation pathways are present in the genome. The *secM* gene of the Sec SRP pathway and

some subunits of the membrane crossing type II transporter are missing. Additionally, *ffh* encoding a signal recognition particle and targeting proteins for relocation was identified.

Discussion

Genome size and completeness

The typical genome sizes of *Epsilonproteobacteria* from comparable habitats range from 2.1 to 3.0 Mb (117, 121, 128, 172, 173). The G+C content of epsilonproteobacterial genomes varies between 32 and 48% (124, 172). With 33% G+C content and a size of 1.6 Mb, the Zeitz epsilonproteobacterial population genome seems to be within the lower range within this group. However, the reconstructed population genome is incomplete as shown by the completeness estimation based on the Minimal Gene Set and the CSCG set. Moreover, only 30 tRNA genes were detected compared to up to 47 tRNA genes in *Sulfurimonas gotlandica* str. GD1 (128) and just one copy of 16S rRNA and 23S+5S rRNA genes was identified, whereas typically around three copies of rRNA operons are found in epsilonproteobacterial genomes (117). Consequently, the present annotation likely does not cover the complete metabolic capabilities, resulting potentially in pathway gaps and missing essential metabolic functions. Thus, the annotation results need to be interpreted with caution, at least regarding the absence of metabolic functions. Nevertheless, the present annotated genes provide important insights into the metabolic versatility of the Zeitz epsilonproteobacterium as discussed below.

Metabolic versatility in carbon source and energy supply

Epsilonproteobacteria are known to possess the capability of carbon fixation establishing them as important primary producers in oligotrophic environments and underscoring their ability to adapt to carbon-limited habitats (119, 127, 128). Overall, six pathways for autotrophic carbon fixation have been described: the Calvin-Benson reductive pentose phosphate cycle, the rTCA cycle, the reductive acetyl coenzyme A (Wood-Ljungdahl) pathway, the 3-hydroxypropionate bi-cycle, the 3-hydroxypropionate/4-hydroxybutyrate cycle, and the dicarboxylate/4-hydroxybutyrate cycle (174). The rTCA cycle has been described only for a few bacterial groups such as green sulfur bacteria and *Deltaproteobacteria*, but it seems to be widely distributed among *Epsilonproteobacteria* (117, 119, 120, 173). Correspondingly, the Zeitz epsilonproteobacterium genome encodes a complete rTCA cycle, including the genes for the key enzymes ATP citrate lyase, pyruvate ferredoxin oxidoreductase and 2-oxoglutarate ferredoxin oxidoreductase (175). The fumarate reductase/succinate dehydrogenase is also part of the rTCA cycle and two copies of this enzyme are present in the genome with three and two subunits, respectively. A similar observation was reported by Sievert et al. (2008) (117). They

suggested the two-subunit fumarate reductase/succinate dehydrogenase to be cytoplasmic and involved in the rTCA cycle.

As an alternative to an inorganic carbon source, the potential for direct acetate assimilation is given which requires the expression of *actP* acting as acetate import system and the acetyl-CoA synthetase gene *acsA* responsible for acetate activation (176, 177). Considering the presence of a complete rTCA cycle and the alternative of direct acetate import and assimilation, the organism is equipped for a mixotrophic lifestyle, which was proposed for other *Epsilonproteobacteria* as well (120). Recently, a time-resolved protein-SIP experiment with $^{13}C_2$ acetate, daily spiked at a concentration of 10 µM to the benzene-degrading consortium, revealed that the Zeitz epsilonproteobacterium exhibited the fastest and highest incorporation of labeled carbon from acetate compared to other acetate utilizers, indicating its role as a primary and highly efficient acetate scavenger within the syntrophic consortium (178). Mixotrophy which can be inferred from the genome and the capability of highly efficient acetate capture as demonstrated by Starke et al. (178) are metabolic traits which can confer selective advantages in groundwater habitats and in particular in hydrocarbon-contaminated aquifers, where acetate is formed as metabolite of syntrophic hydrocarbon degradation or is leaked out in small concentrations from the anaerobic degradation of organic compounds (179).

Different combinations of organic and inorganic electron donors and acceptors have been described for *Epsilonproteobacteria* (120, 122). An overview of the potential electron donors and acceptors according to the genome annotation is given in **Table 4.1**. Since the Zeitz epsilonproteobacterium was enriched from a sulfidic environment and under sulfate-reducing conditions, the most obvious electron donor would be sulfide. The oxidation of reduced S-species to sulfate via the Sox system has frequently been observed in marine *Epsilonproteobacteria* (117, 125, 128). However, genes for the Sox system were not found in the present (incomplete) genome.

Table 4.1: Potential electron acceptors and donors and their redox potentials.

Electron acceptor	**ΔE**	**Reference**
$NO_3^- \rightarrow NO_2^-$	+ 433 mV	Thauer et al. (1977)
$[S_n]^{2-} \rightarrow HS^-$	+ 260 mV	Dietrich and Klimmek (2002)
Fumarate → Succinate	+ 30 mV	Kröger et al. (1992)

Electron donor	**ΔE**	**Reference**
$H_2 \rightarrow H^+$	- 414 mV	Dietrich and Klimmek (2002)
Formate → CO_2	- 432 mV	Thauer et al. (1977)
$HS^- \rightarrow [S]$	-275 mV	Dietrich and Klimmek (2002)

Sulfide oxidation to polysulfide using sulfide quinone oxidoreductase (SQR) was suggested for the betaproteobacterium *Thiobacillus denitrificans* which additionally contains also parts of the Sox pathway and may oxidize sulfide simultaneously by SQR and Sox under nitrate-reducing conditions (180, 181). This oxidation could be coupled via menaquinone with the polysulfide reductase PsrABC which has the capability to reduce polysulfides. The respective *psr* operon was found in the genomes of other *Epsilonproteobacteria* as well, and Psr activity was detected (128, 182). Such coupling generates only limited energy, but might serve for other purposes like an internal sulfur cycle. Alternatively, polysulfide reduction may be linked to hydrogen or formate oxidation with menaquinone again acting as electron carrier (182-184). However, only the subunit gene *fdhA* of the formate dehydrogenase was explicitly annotated whereas all genes for the respective hydrogenase (*hydABC*) were found. Hydrogen and formate oxidation might be also coupled to fumarate reduction, a respiration type which is well investigated for *Epsilonproteobacteria* such as *Wolinella* (185). Electrons released via hydrogen/formate oxidation to build up the proton gradient are transferred via menaquinone to fumarate reductase. Fumarate reduction in terms of energy metabolism is a membrane-bound process (185). Hence, the second copy of a fumarate reductase/succinate dehydrogenase annotated in the genome with three subunits could be the appropriate enzyme for this reaction. Sources for fumarate could be degraded carbohydrates or proteins whereby it is unclear if the degradation is an inner cell process or fumarate is taken up from the surrounding medium (185). Specific dicarboxylate

transporters (DcuAB) for fumarate uptake (186) were not identified in the present genome, but nonspecifically annotated transporter genes could encode an appropriate uptake system (172). Theoretically, if rTCA cycle and acetate assimilation work in parallel, fumarate could be internally generated by diverting PEP into the rTCA cycle (see **Figure 1.1**). However, the respiration of internally produced fumarate with hydrogen/formate or sulfide as electron donor would probably not generate net ATP allowing growth. The conversion of acetate to fumarate costs at least 1 mol ATP per mol acetate (**Figure 1.1**), whereas fumarate reduction with hydrogen/formate or sulfide probably produces less than 1 mol ATP per fumarate (123).

Similar to enzymes of the rTCA cycle, the hydrogenase HydABC is a ferredoxin-dependent enzyme coupling hydrogen oxidation with the reduction of NAD^+ and ferredoxin (187). Thus, this enzyme is oxygen-sensitive showing that the Zeitz epsilonproteobacterium is adapted to anoxic or microoxic conditions. However, the genetic capability to utilize low levels of oxygen exists as all genes necessary for aerobic respiration are present in the genome. This circumstance was also described for *Candidatus* Sulfuricurvum sp. in a previous study (173). Another study proved growth of *Sulfuricurvum kujiense* under microaerobic conditions (188). Similar results were obtained with *Sulfurovum* sp. NBC37-1 which is the next cultured relative of the Zeitz epsilonproteobacterium and was found to grow with various combinations of electron donors and acceptors, e.g. hydrogen and oxygen (182).

Another common electron acceptor for *Epsilonproteobacteria* is nitrate (111, 124, 125). The genome studied here encodes the nitrate reductase NarGHI. Growth tests in the studies of Handley et al. (2014) and Yamamoto et al. (2010) showed positive results for various combinations including coupling with hydrogen or sulfide as electron donor (173, 182). Although no nitrate importer gene was detected in the present genome, nitrate reduction could be a viable option since the redox potential of nitrate to nitrite is relatively positive compared to other anaerobic terminal electron acceptor processes (see **Table 4.1**). Regarding the ecological niche in contaminated groundwater, nitrate can be relevant and *Epsilonproteobacteria* are known to be involved in nitrate-dependent reoxidation of reduced sulfur compounds (189). However, the capability of nitrate respiration does not explain the ecophysiology of the Zeitz epsilonproteobacterium in our enrichment cultures as the growth media did not contain any nitrate.

Pathways for sulfur and nitrogen assimilation

Besides its role as an electron donor, sulfide plays a role as a nutrient in bacterial cells. Based on the metagenome data, the Zeitz epsilonproteobacterium cannot assimilate sulfate; genes for an appropriate sulfate import system are missing as well as genes involved in the sulfate activation pathway except of the *sat* gene which encodes ATP sulfurylase catalyzing the formation of adenosine 5'-phosphosulfate (190). Although it cannot be rules out that the enzymes for assimilatory sulfate reduction are encoded in the missing parts of the genome, the direct assimilation of sulfide by the cysteine synthase saves energy and is thus plausible in sulfidic environments. Notably, other *Epsilonproteobacteria* have been described to be capable of assimilating sulfate (172). It is conspicuous that the Zeitz epsilonproteobacterium harbors a *sat* gene but possibly no other genes for assimilatory sulfate reduction. One could speculate that this capability was lost during adaptation to sulfidic environments with a shift towards a specialization in sulfide as energy and sulfur source.

For nitrogen assimilation, ammonium can be directly used due to the presence of *amtB.* AmtB is a membrane uptake protein importing ammonium into the cell at low concentrations (191, 192). In analogy to the use of sulfide as sulfur source, the direct use of ammonia as nitrogen source might be an adaptation to an anaerobic lifestyle as the energy-consuming reduction of oxidized N species is avoided. Notably, dinitrogen fixation is not common in *Epsilonproteobacteria* and was so far only described for *Wolinella succinogenes* (172) and *Arcobacter nitrofigilis* (193). *N*itrogen fixation provides a selective advantage in nitrogen-limited habitats even though this process is very energy-demanding. The nitrogen fixation is linked to hydrogen formation. Hence, recovery of energy via hydrogen oxidation minimizes the loss of energy during the nitrogen fixation process. The subunits for the appropriate hydrogenase (HupSL) are encoded in the genome. Combining N-fixation with hydrogen oxidation to save energy has been described for cyanobacteria (194, 195) but also mentioned for other *Proteobacteria* such as *Allochromatium* (196) and *Rhodospirillum* (197).

Oxygen-sensitive enzymes and oxygen tolerance

Enzymes specific for the rTCA cycle are dependent on the interaction with ferredoxin, an extremely oxygen-sensitive electron carrier (198). Both oxidoreductases (2-oxoglutarate ferredoxin oxidoreductase and pyruvate ferredoxin oxidoreductase) are ferredoxin-dependent enzymes and thus highly sensitive to oxygen (175). Other ferredoxin-dependent enzymes are

directly inhibited in the presence of oxygen such as the nitrogen-fixing nitrogenase (199). Simultaneously, the genome encodes the complete oxidative phosphorylation pathway to generate energy via oxygen reduction. Taking both circumstances into account, the Zeitz epsilonproteobacterium could potentially tolerate oxygen and grow under microoxic conditions as described for other representatives of this class (117, 121, 173, 200). To handle excess oxygen which may form radicals within the cell and interfere with fundamental pathways such as carbon fixation, two mechanisms for radical scavenging are likely. Indeed, only *sodB* encoding the superoxide dismutase subunit converting superoxide radicals into hydrogen peroxide and water (201) was found in the genome. The *sodA* gene is missing as well as the gene for the subsequent catalase, a circumstance which was previously described for *Epsilonproteobacteria* (200). This limitation might be overcome by the alkyl hydroperoxide reductase AhpC, which alternatively scavenges hydrogen peroxides (202, 203).

Transport systems

Several uptake transporters and exporting pathways are encoded in the genome and are crucial for the organism. The molybdenum transporter ModABC is essential for nitrogen-fixing organisms since the nitrogenase depends on molybdenum (204, 205). Furthermore, the specific phosphate transporter PstSCAB for environments with low phosphate concentrations was detected (206). For its induction, regulators are needed which both were found adjacent to the *pst* operon. Thereby, the function of PhoU is not completely understood, but it is likely involved in an interaction of the two-component signal system PhoRB (207, 208) and transporter subunit PstB (209). Other nutrient uptake systems such as a potassium transporter with the subunit genes *ktrB* and *krtC* (210) or the zinc transporter ZnuBCA (211) are also encoded. The genome analysis suggests that the Zeitz epsilonproteobacterium might have different strategies to gather iron from the environment. Ferric iron is insoluble under pH neutral conditions and Gram-negative bacteria use the energy-consuming TonB transporter to import ferric iron by binding the ion to chelating siderophores (212). The gene *tonB* encodes the protein to transduce energy derived from a proton motive force for the energy-consuming translocation, and *exbB* and *exbD* encode proteins responsible for restoring the conformational structure of TonB. Since the Zeitz epsilonproteobacterium originates from an anaerobic environment, the major form of iron is ferrous iron. Under these conditions, the encoded ferrous iron uptake complex FeoAB acts as supply system for iron (213, 214).

Besides import pathways, the export of proteins or toxic metabolites from the cytoplasm to the extracellular space is of similar importance. The function of protein secretion is likely carried out by the type II secretion system which is common among Gram-negative bacteria (215). The genes for several subunits of the type II secretion apparatus are missing but the presence of genes for Sec- and Tat-dependent translocation can be seen as a clear hint for its use. Both the Sec and Tat systems for the translocation across the inner membrane interact with the type II secretion pathway to transport proteins from the periplasm out of the cell (216).

Ecological niche of the Zeitz epsilonproteobacterium

The Zeitz epsilonproteobacterium shares some metabolic features with other members of this class, such as the capabilities to fix CO_2 via the rTCA cycle (118), to utilize hydrogen as energy source (118, 217), to use sulfur compounds as electron acceptors and donors (173, 189, 217), and to tolerate oxygen on microoxic levels (125, 188). A feature not described for other *Epsilonproteobacteria* is the genomic capability to gather carbon via both, acetate assimilation and carbon dioxide fixation, which means in consequence a potentially mixotrophic lifestyle. Acetate assimilation is a rare feature for *Epsilonproteobacteria* (117, 218). Also the capability to fix dinitrogen is rarely described for representatives of this group (172, 193). Nevertheless, there are still gaps in the annotated genome potentially hiding many genomic properties which cannot be considered so far.

The Zeitz epsilonproteobacterium originates from a sulfidic benzene-contaminated aquifer and was enriched as member of a syntrophic community. The key player, a *Pelotomaculum* sp. initially attacks benzene and shares carbon and electrons from benzene degradation with other community members belonging to several *Deltaproteobacteria* and the epsilonproteobacterium. The whole degradation is coupled to sulfate reduction as terminal electron acceptor process (139, 147). It was unclear why the Zeitz epsilonproteobacterium persisted in this enriched consortium or even increased in its abundance, considering that *Epsilonproteobacteria* are not known to use sulfate as electron acceptor, and the involved *Deltaproteobacteria* are potentially capable to consume and mineralize all intermediates from syntrophic benzene degradation such as acetate, hydrogen or formate. In DNA-SIP experiments with $^{13}C_6$-labeled benzene, the epsilonproteobacterium was shown to incorporate ^{13}C over time. It was supposed that acetate as a putative intermediate of syntrophic benzene degradation may serve as carbon source for the epsilonproteobacterium (147). This hypothesis was not supported by the respective protein-

SIP experiment with $^{13}C_6$-labeled benzene (35), probably due to the low abundance of *Epsilonproteobacteria* in those cultures and the low coverage of epsilonproteobacterial genes in the metagenome dataset applied for peptide identification. However, the recently performed protein-SIP experiment spiking fully $^{13}C_2$-labeled acetate in addition to the ongoing mineralization of unlabeled benzene (178) as well as the presence of genes for an acetate importer and for acetate activation confirm the hypothesis that the Zeitz epsilonproteobacterium is a key acetate scavenger within the consortium.

The capability to use various electron donors such as hydrogen, formate and sulfide, and various electron acceptors such as oxygen, nitrate, polysulfide and fumarate provides the metabolic versatility to colonize different groundwater environments. Although nitrate and oxygen may be present in upper groundwater levels at the fringe of the contamination plume of the Zeitz aquifer, they were neither relevant in central and lower parts of the plume where the samples for enrichment cultures were taken from, nor present in the sulfate-reducing enrichment cultures. The Zeitz site has been contaminated with hydrocarbons since 70 years or longer (145). Hence, strictly anoxic, sulfidic conditions may have persisted for decades. Thus, fumarate and polysulfide are assumed to be relevant electron acceptors, whereas hydrogen, formate, and sulfide are the likely electron donors. Except for the redox couple polysulfide – sulfide, each combination is theoretically feasible (see **Table 4.1**). Hydrogen or formate is formed during syntrophic benzene degradation and sulfide is generated during growth of the sulfate-reducing *Deltaproteobacteria* (139). It can be assumed that the hydrogenotrophic *Deltaproteobacteria* outcompete the epsilonproteobacterium for hydrogen as electron donor due to a proposed higher affinity to hydrogen (179, 219). However, at higher sulfide levels which are toxic to other bacteria, the epsilonproteobacterium might get a selective advantage due to a higher sulfide tolerance, rendering hydrogen oxidation feasible. For instance, benzene degradation by a sulfate-reducing consortium was inhibited at sulfide concentrations above 1.5 mM (35) whereas *Epsilonproteobacteria* oxidizing sulfide with nitrate as electron acceptor have been described to tolerate sulfide levels of 2 mM (220) or even 3 mM (221). This is in accordance with the observation that the Zeitz epsilonproteobacterium increases in abundance in aromatics-degrading batch cultures which contain high sulfide levels (137). Besides hydrogen or formate, sulfide is a common electron donor for *Epsilonproteobacteria* (120). The generation of polysulfide might be a result of sulfide oxidation, potentially leading to the formation of elemental sulfur which reacts spontaneously to polysulfide (222). Elemental sulfur/polysulfide could serve in reverse as electron acceptor. Alternatively, electrons are transferred to fumarate

as part of the rTCA cycle. Potential sources of fumarate could be an internal process of a combined rTCA cycle and acetate assimilation, or fumarate released by other bacteria in the community.

The capability to assimilate nitrogen by direct import of ammonium via AmtB is characteristic for the adaptation to groundwater systems in which ammonium is the major nitrogen source. Ammonium was also provided as nitrogen source in the enrichment cultures. The capability to fix dinitrogen might be a selective advantage in habitats generally depleted in nutrients, such as aquifers impacted by massive hydrocarbon input and biodegradation.

Summarizing the genomic features of the Zeitz epsilonproteobacterium, this organism is well adapted to pristine and hydrocarbon-contaminated sulfidic aquifers considering the mixotrophic lifestyle, the type of energy metabolism, and the mechanisms of nitrogen and sulfur assimilation. It can potentially adapt to changing environmental conditions (microoxic, altered redox conditions or carbon and nitrogen sources). The most striking features defining its ecophysiological role in the hydrocarbon-degrading, sulfate reducing consortia are the high affinity to acetate and the high tolerance to sulfide which can simultaneously be used for assimilatory and dissimilatory purposes. Thus, the Zeitz epsilonproteobacterium may occupy a specific ecological niche in the intermediary ecosystem metabolism of hydrocarbon-contaminated sulfidic subsurface habitats by metabolizing the key intermediate acetate and recycling sulfide which cannot be consumed by other community members. The latter might be the reason for the co-occurrence or even mutualistic relationship with sulfate-reducing *Deltaproteobacteria*. However, the hypothesized role needs to be proven in cultivation experiments. The annotated population genome provides clues on the possible enrichment strategies for isolating the Zeitz epsilonproteobacterium which will be applied in future experiments.

Acknowledgements

We thank Ute Lohse for skilled technical assistance and Tesfaye Wubet for support with contig assembly. We also acknowledge the LABGeM team and the National Infrastructure France Genomique for providing the MicroScope annotation service and the reviewers for their valuable comments improving the manuscript.

3.2. Starke et al., Microbial Ecology (2016)

Pulsed $^{13}C_2$-Acetate Protein-SIP Unveils *Epsilonproteobacteria* as Dominant Acetate Utilizers in a Sulfate-Reducing Microbial Community Mineralizing Benzene

Robert Starke[1,2] & Andreas Keller[3,4] & Nico Jehmlich[2] & Carsten Vogt[3] & Hans H. Richnow[3] & Sabine Kleinsteuber[4] & Martin von Bergen[2,5] & Jana Seifert[1*]

[1]Institute for Animal Science, University of Hohenheim, Emil-Wolff-Str. 6-10, 70599 Stuttgart, Germany

[2]Department of Proteomics, Helmholtz-Centre for Environmental Research (UFZ), Permoserstr. 15, 04318 Leipzig, Germany

[3]Department of Isotope Biogeochemistry, Helmholtz-Centre for Environmental Research (UFZ), Permoserstr. 15,04318 Leipzig, Germany

[4]Department of Environmental Microbiology, Helmholtz-Centre for Environmental Research (UFZ), Permoserstr. 15, 04318 Leipzig, Germany

[5]Department of Metabolomics, Helmholtz-Centre for Environmental Research (UFZ), Permoserstr. 15, 04318 Leipzig, Germany

[*]Corresponding author: Jana Seifert, jseifert@uni-hohenheim.de

Received: 12 October 2015

Accepted: 18 January 2016

May 2016, Volume 71, Issue 4, pp 901-911

DOI: 10.1007/s00248-016-0731-y

Keywords Anaerobic benzene degradation, Metaproteomics, Carbon flow

Abstract

In a benzene-degrading and sulfate-reducing syntrophic consortium a clostridium affiliated to the genus *Pelotomaculum* was previously described to ferment benzene while various sulfate-reducing *Deltaproteobacteria* and a member of the *Epsilonproteobacteria* were supposed to utilize acetate and hydrogen as key metabolites derived from benzene fermentation. However, the acetate utilization network within this community was not yet unveiled.

In this study, we performed a pulsed $^{13}C_2$-acetate protein stable isotope probing (protein-SIP) approach continuously spiking low amounts of acetate (10 µM per day) in addition to the ongoing mineralization of unlabeled benzene. Metaproteomics revealed high abundances of *Clostridiales* followed by *Syntrophobacterales*, *Desulfobacterales*, *Desulfuromonadales*, *Desulfovibrionales*, *Archaeoglobales* and *Campylobacterales*. Pulsed acetate protein-SIP results indicated that members of the *Campylobacterales*, the *Syntrophobacterales*, the *Archaeoglobales*, the *Clostridiales* and the *Desulfobacterales* were linked to acetate utilization in descending abundance. The *Campylobacterales* revealed the fastest and highest ^{13}C-incorporation. Previous experiments suggested that the activity of the *Campylobacterales* was not essential for anaerobic benzene degradation in the investigated community. However, these organisms were consistently detected in various hydrocarbon-degrading and sulfate-reducing consortia enriched from the same aquifer. Here, we demonstrate that this member of the *Campylobacterales* is the dominant acetate utilizer in the benzene-degrading microbial consortium.

Introduction

The contamination of field sites by gasoline derived hydrocarbons such as BTEX (benzene, toluene, ethylbenzene and *o*-, *m*- and *p*-xylene) is pervasive due to accidental spillages or leaking storage tanks (21). The remediation of benzene contaminations is of particular interest because of its persistence in the environment and its toxicity (22, 23). In contaminated subsurface habitats, oxygen is rapidly depleted due to the activity of aerobic microorganisms and chemical oxidation processes leading to the development of anoxic zones in contaminated field sites. The majority of hydrocarbons can be degraded by anaerobic microorganisms within this anoxic zone (24, 25) while benzene is the most recalcitrant BTEX compound. The anaerobic degradation of benzene has been investigated since the 1990s (26, 28) and was suggested to initially proceed via hydroxylation to phenol (223), carboxylation to benzoate (224) or methylation to toluene (29, 30).

The benzene-degrading and sulfate-reducing microbial community investigated here originated from a BTEX-contaminated sulfidic aquifer and has been intensively studied (31-35, 146). Previous studies involving terminal restriction fragment length polymorphism analysis and sequencing of 16S rRNA genes as well as DNA-SIP using $^{13}C_6$-benzene revealed a phylotype belonging to the *Cryptanaerobacter*/ *Pelotomaculum* group within the *Clostridiales* being associated with benzene degradation (32, 33). Further, protein-SIP experiments with $^{13}C_6$-benzene and ^{13}C-carbonate approved the *Pelotomaculum*-like organism to assimilate carbon from benzene and CO_2 (35). Apart from that, the microbial community was divided into three functional groups according to the distinct ^{13}C incorporation characteristics - (a) the above-mentioned benzene fermenters belonging to the *Clostridiales*, (b) *Deltaproteobacteria* thriving on fermentation products, CO_2 fixation and sulfate reduction and (c) putative scavengers of dead biomass or metabolites belonging to the *Bacteroidetes*/*Chlorobi* group (35). Based on thermodynamic calculations, acetate and hydrogen were discussed to be key metabolites derived from benzene fermentation suggesting a syntrophic relationship with sulfate reducers (33). Indeed, it was previously demonstrated that the addition of acetate or hydrogen inhibits benzene fermentation in a reversible manner, confirming the syntrophy hypothesis (34).

However, 16S rRNA gene sequencing also revealed a member of the *Epsilonproteobacteria* (distantly related to the genus *Sulfurovum*) as most abundant phylotype in the community (33). In compliance, $^{13}C_6$-benzene DNA-SIP demonstrated significant labeling of this phylotype (32) indicating an important role in benzene mineralization. Surprisingly, *Epsilonproteobacteria*

were not detected in the respective protein-SIP experiment (35). Thus, the ecophysiological role of this organism in syntrophic benzene mineralization is not yet clear, neither regarding the energy source nor the terminal electron acceptor (TEA). Recent studies revealed that chemolithoautotrophic *Epsilonproteobacteria* related to the genus *Sulfurovum* were predominant in sulfidic environments such as deep-sea hydrothermal vents (36-38) or sulfidic caves and springs (39-41) performing unique reactions such as sulfur respiration or sulfide oxidation (225-227). Also mixotrophic growth was discussed as *Epsilonproteobacteria* were stimulated by acetate amendment in a sulfidic aquifer sediment (42) but they are not known as sulfate reducers. Thus, the *Epsilonproteobacteria* in the present community are suspected to feed on metabolites from benzene fermentation and sulfate reduction.

In this study, $^{13}C_2$-acetate was continuously amended (10 µM per day) in addition to the present concentration of unlabeled acetate derived from the degradation of unlabeled benzene to unveil acetate utilization processes in the microbial community. Microcosms were sacrificed at four different time points in benzene degradation to obtain a time-resolved image of acetate metabolization.

Materials and Methods

Setting up of the microcosms for the pulsed protein-SIP approach

Sample material was derived from an on-site reactor at a contaminated industrial site near Zeitz, Saxony-Anhalt, Germany. The main contaminant is benzene being present in two connected aquifers. The aquifers are anoxic with sulfate as the main TEA (145). The on-site reactor consists of four serially connected columns containing gravel granules (grain size 2-3 mm). The columns (190 cm in length and 27.3 cm in diameter) are made of stainless steel and have been continuously percolated with groundwater from the lower aquifer at a flow rate of 0.5 L h^{-1} since 2006. Benzene degradation under sulfate-reducing conditions has been observed in all columns since 2007. For the setting up of microcosms, gravel granules from the first column were transferred into sterile 1 L glass bottles which were filled immediately with anoxic groundwater and closed with butyl stoppers and screw caps. The groundwater was exchanged inside an anaerobic glove box (gas atmosphere: 95% nitrogen and 5% hydrogen; Coy Laboratory Products Inc., Grass Lake, MI USA) with anoxic mineral salt medium containing 20 mM sulfate as TEA (146). For the pulsed labeled acetate protein-SIP experiment, sodium $^{13}C_2$-acetate with an isotope purity of 99 atom% was obtained from Sigma-Aldrich (St. Louis, MO, USA). Nine bottles were prepared including four microcosms with unlabeled benzene amended with ^{13}C-acetate, four growth controls with only unlabeled benzene, and one sterile control where the biomaterial was autoclaved twice at 120°C with an interval of one day. After exchange of the medium, 700 µM of unlabeled benzene was added through the butyl stopper using a glass syringe (Hamilton, Reno, NV, USA). To maintain steady labeled acetate concentrations, $^{13}C_2$-acetate was dissolved in anoxic mineral salt medium and a final concentration of 10 µM was added using a glass syringe to the four microcosms with amendment every day. The microcosms were kept in the dark at room temperature during cultivation.

Growth monitoring and protein extraction

Benzene and sulfide concentrations were measured as previously described to monitor microbial growth (35, 146) (**Supporting Information**). The bottles were sacrificed at 25%, 50%, 100% and 200% (after a second amendment of 700 µM) of complete benzene degradation. The resulting sampling times were at days 4, 6, 31 and 74 of cultivation. Protein extraction from

the sediment was carried out using a modified phenol extraction protocol as previously described (228) with minor modifications (35) (**Supporting Information**).

Sample preparation for mass spectrometry

Complete samples were used for one-dimensional (1D) gel electrophoresis without prior determination of protein amounts. Air-dried protein pellets were suspended in 30 µL 1x Laemmli buffer (229), dissolved via ultrasonication and incubated under shaking at 500 rpm and 60°C for 10 min. Samples were centrifuged at 12,000 x g (Sorvall RC 6 plus, Thermo Electron Corporation, Waltham, MA, USA) to remove precipitates before loading on sodium dodecyl sulfate gels (4% stacking gel and 12% separating gel). Electrophoresis was performed at 10 mA per gel. Polypeptides were stained by colloidal Coomassie Brilliant Blue G-250 (Roth, Kassel, Germany). Entire lanes were cut into gel pieces for each sample and an in-gel tryptic digestion was performed (73). Excised gel bands were washed thrice with 200 µL 10 mM ammonium bicarbonate in acetonitrile (40%, v/v) for 10 min. Gel slices were dried with 200 µL acetonitrile for 5 min. After removal of acetonitrile, the gel slices were reduced and alkylated by subsequent incubation with 30 µL 10 mM dithiothreitol in 10 mM ammonium bicarbonate and 30 µL 100 mM iodoacetamide in 10 mM ammonium bicarbonate. Gel slices were incubated with both solutions for 30 min each. Afterwards, the solution was removed and the slices were dried in a vacuum centrifuge. Further, the slices were incubated with acetonitrile as described above. After removal of the solution, the slices were equilibrated with 200 µL 10 mM ammonium bicarbonate for 10 min and subsequently incubated with acetonitrile as described above. Gel slices were incubated with 30 µL 5 mM ammonium bicarbonate containing 0.01 µg μL^{-1} trypsin (Promega) over night at 37°C. After proteolytic cleavage, trypsin solution was collected and the peptides from gel bands were extracted twice with 30 µL acetonitrile/formic acid (50%/5%, v/v). Solutions were combined and dried in a vacuum centrifuge as described above. Samples were resuspended in 0.1% formic acid as well as desalted and purified by ZipTip® treatment (EMD Millipore, Billerica, MA, USA).

MS analysis by nanoUPLC-Orbitrap Fusion-MS/MS

Peptides were analyzed by UPLC-Orbitrap Fusion-MS/MS. The peptides were eluted using a linear gradient of 120 min with 4-55% solvent B (80% acetonitrile, 0.08% formic acid). Continuous scanning of eluted peptide ions was carried out between 400 and 1,500 *m/z* at a resolution of 120,000 and a maximum injection time of 100 ms, automatically switching to

MS/MS HCD mode using a normalized collision energy of 30%. Raw data obtained was processed for database searches with the Thermo Proteome Discoverer (v1.4.0.288; Thermo Fisher Scientific, Waltham, MA, USA). Searches were performed using the Sequest HT algorithm with the following parameters: tryptic cleavage with maximal two missed cleavages, a peptide tolerance threshold of ±10 ppm and an MS/MS tolerance threshold of ±0.1 Da, and carbamidomethylation at cysteines as static and oxidation of methionines as variable modifications. Searches were performed against a combined metagenome dataset from the benzene-degrading community analyzed in the previous protein-SIP experiment with labeled benzene and carbonate (35) and from an *m*-xylene-degrading sulfate-reducing culture enriched from the same contaminated aquifer and containing the same epsilonproteobacterial phylotype (230). From the latter metagenome, the contigs binned as *Epsilonproteobacteria* were included in the analysis [44] as *Epsilonproteobacteria* were underrepresented in the metagenome dataset generated from the benzene-degrading community (**Support Information Figure S1.2**). Contigs were considered as identified with at least one unique peptide with high confidence (false discovery rate (FDR) < 0.01). FDR was determined by decoy database searches. For the identification of ^{13}C-labeled peptides, the respective unlabeled peptides were measured as well comparing chromatographic retention time and MS/MS fragmentation patterns as described previously (73).

Metaproteome analyses

Contigs encoding identified peptides were annotated and analyzed regarding protein function and taxonomy. In case of the metagenome dataset from the benzene-degrading community, affiliation was performed by blast (National Library of Medicine, Bethesda, MD, USA) using the NCBI non-redundant database (version 22 April 2014) as previously described (35). For the metagenome dataset from the *m*-xylene-degrading community enriched in *Epsilonproteobacteria*, automated annotations of coding sequences (CDS) by the microbial genome annotation and analysis platform MicroScope (231) were checked and manually re-annotated if necessary using tools and databases implemented in the microbial annotation system Magnifying Genome (MaGe) (232) including PsortB, SwissProt, TrEMBL and COGnitor. Metabolic pathways were predicted and identified by analyzing the re-annotated genome with integrated pathway tools of MaGe based on the KEGG and MicroCyc databases [44]. For the metaproteome analysis, explored protein functions comprised general metabolic functions such as CO_2 fixation, aromatic compound degradation, dissimilatory sulfate reduction

and energy metabolism. To gain a first estimation of the taxonomic distribution, contigs were affiliated to their respective phylum and plotted regarding relative abundance in time. For protein-SIP analyses, the MetaProSIP tool of OpenMS was used (104, 233, 234). At first, raw data was converted into *.mzML files using MSConvert of ProteoWizard (235). Subsequently, the latter *.mzML files were converted to smaller *.mzML and *.featureXML files using a precursor mass tolerance of ± 10 ppm and a fragment mass tolerance of ±0.02 Da as well as carbamidomethylation at cysteines as static and oxidation at methionines as variable modifications. The generated files were then used for the MetaProSIP searches with an m/z tolerance of ±10 ppm as well as an intensity threshold of 1000 and a correlation threshold of 70%. As database, the above-mentioned combined metagenome including random contaminants for false discovery rate determination was used.

Cultivation with elemental sulfur

In order to test the capability of the consortium to use elemental sulfur as possible TEA, the medium was changed in microcosms set up as explained above while replacing 20 mM of sodium sulfate with 20 mM of double-ground elemental sulfur (>99% purity, VEB Laborchemie, Apolda, Germany). Five bottles were prepared including one microcosm with elemental sulfur as TEA, three growth controls with sulfate, and one sterile control where the biomaterial was autoclaved twice at 120°C with an interval of one day. The incubations started when 700 µM of unlabeled benzene was applied to each microcosm. The microcosms were kept in the dark at room temperature during cultivation. Growth was monitored by benzene and sulfide concentration as mentioned above.

Results

Benzene degradation kinetics

Microcosms were fed with 10 µM of $^{13}C_2$-acetate daily. The benzene degradation rate of the non-amended culture (8.7 µM d^{-1}) was slightly lower than the degradation rates of the acetate amended microcosms of 10.0-15.4 µM d^{-1} (**Figure 1.2A**). Sulfide peaked at 1.2-1.4 mM but did not change compared to the non-amended culture even though 740 µM of acetate have been added over 74 days (**Figure 1.2B**).

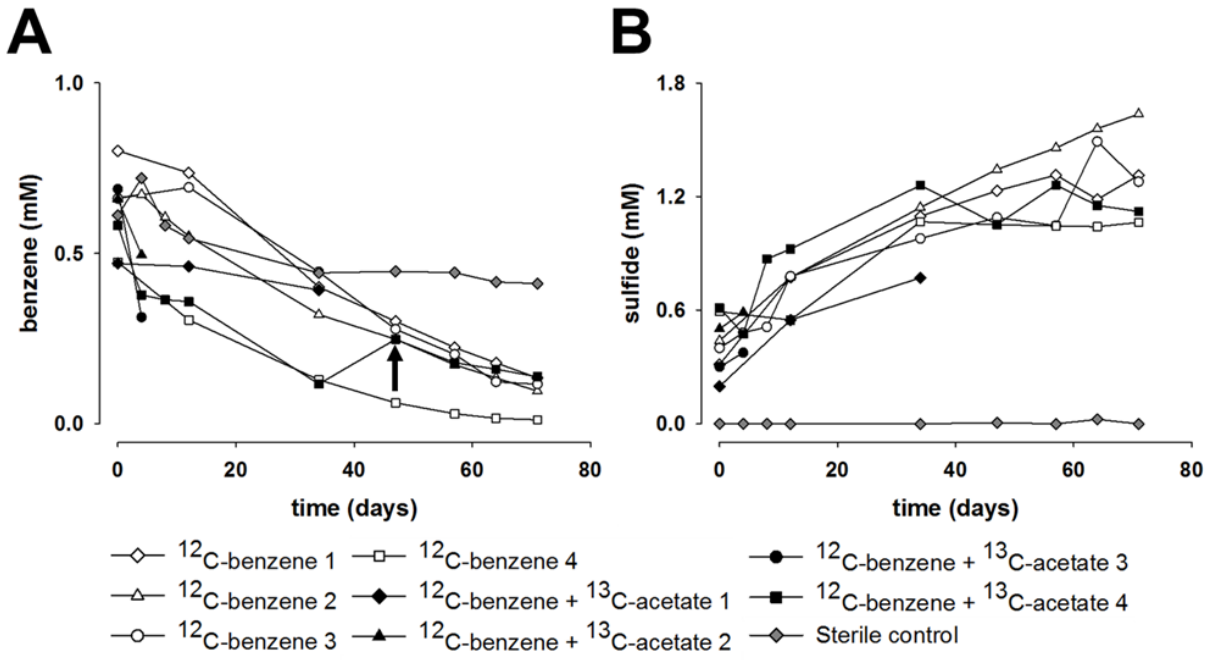

Figure 1.2: Benzene (A) and sulfide concentrations (B) during pulsed 13C2-acetate protein-SIP. Data of four biological replicates amended with labeled acetate (black circle, triangle, square and diamond), four growth controls with only benzene (white circle, triangle, square and diamond) as well as a sterile control (grey diamond) are shown. The arrow indicates the addition of unlabeled benzene to the 13C2-acetate replicate 4.

The stoichiometry of benzene mineralization was determined in accordance to the hypothesized syntrophy model of benzene fermentation to acetate and hydrogen while the products are further oxidized to carbon dioxide and water, respectively, (**Equations 1-3**) with respect to mineralized benzene, added acetate and produced sulfide. Measured sulfide production in comparison to the consumption of benzene was 45±11% (n=3 biological replicates) when acetate was amended and 47±16% (n=14 biological replicates) for the unamended cultures (**Table 1.2**).

$$[\mathbf{1}]\ \text{benzene} + 6H_2O \rightarrow 3\text{acetate} + 3H^+ + 3H_2$$

$$[\mathbf{2}]\ 3H_2 + 0.75SO_4^{2-} + 1.125H^+ \rightarrow 3H_2O + 0.375HS^- + 0.375H_2S$$

$$[\mathbf{3}]\ 3\text{acetate} + 3SO_4^{2-} + 1.5H^+ \rightarrow 3HCO_3^- + 1.5HS^- + 1.5H_2S$$

Table 1.2: Stoichiometric calculations using a simplified syntrophy model as reference (**Equation 1-3**). The values for oxidized benzene, added acetate and produced sulfide originated from the experiment. The expected productions of both acetate and hydrogen were calculated in accordance to the proposed syntrophy model. The expected sulfate reduction was determined by summarizing acetate from the expected acetate production (ratio 1:1) and the added acetate as well as hydrogen from the expected hydrogen production (ratio 4:1). Abbreviations were used for average (AVG) and standard deviation (SD).

	#	benzene oxidized (mM)	expected acetate & hydrogen produced (mM)	acetate added (mM)	expected sulfate reduced (mM)	sulfide produced (mM)	sulfide vs. sulfate	AVG	SD
model	1	1.00	3.00	0.00	3.75	3.75	1.00		
acetate-amended	1	0.24	0.72	0.26	1.16	0.39	0.34		
	2	0.11	0.33	0.24	0.65	0.31	0.48		
	3	0.08	0.24	0.14	0.44	0.25	0.57	0.46	0.12
non-amended	1	0.32	0.97	0.00	1.21	0.79	0.65		
	2	0.58	1.73	0.00	2.17	1.17	0.54		
	3	0.30	0.90	0.00	1.12	0.61	0.55		
	4	0.35	1.04	0.00	1.30	0.94	0.73		
	5	0.38	1.13	0.00	1.41	0.68	0.48		
	6	0.32	0.97	0.00	1.21	0.68	0.56		
	7	0.47	1.40	0.00	1.75	0.61	0.35		
	8	0.47	1.42	0.00	1.78	0.55	0.31		
	9	0.29	0.88	0.00	1.10	0.80	0.73		
	10	0.48	1.43	0.00	1.78	0.78	0.44		
	11	0.45	1.36	0.00	1.70	0.60	0.35		
	12	0.48	1.44	0.00	1.81	0.47	0.26		
	13	0.47	1.41	0.00	1.76	0.65	0.37		
	14	1.26	3.77	0.00	4.71	1.41	0.30	0.47	0.16

The rates of benzene mineralization rates for unmanended cultures (13.5±2.4 mM, n=14 biological replicates) and ^{13}C-acetate amended cultures (12.8±3.2 mM, n=3 biological replicates) as well as the sulfide production rates for unamended (15.6±4.1 mM, n=14 biological replicates) and acetate amended cultures (16.7±5.1 mM, n=3 biological replicates were calculated (**Support Information Table S1.2**). In the sterile control, benzene initially decreased from 0.56 mM after 4 days to 0.42 mM after 7 days but remained constant afterwards (**Figure 1.2A**) whereas no sulfide was formed over the time period of 213 days (**Figure 1.2B**).

^{13}C-incorporation of labeled acetate

For a first estimation of the ^{13}C-incorporation, the relative isotope abundances (RIA) of all peptides were assigned to the corresponding time point in cultivation (**Figure 2.2A**). Herein, incorporation started immediately in the first days of $^{13}C_2$-acetate amendment. After 74 days, the mean RIA values strongly increased compared to the previous time point. In addition, observed abundances comprised a wide range indicating different types of incorporation patterns. Further, the time-resolved utilization of labeled acetate was evaluated for the dominant phylotypes revealing diverse patterns of incorporation (**Figure 2.2B**).

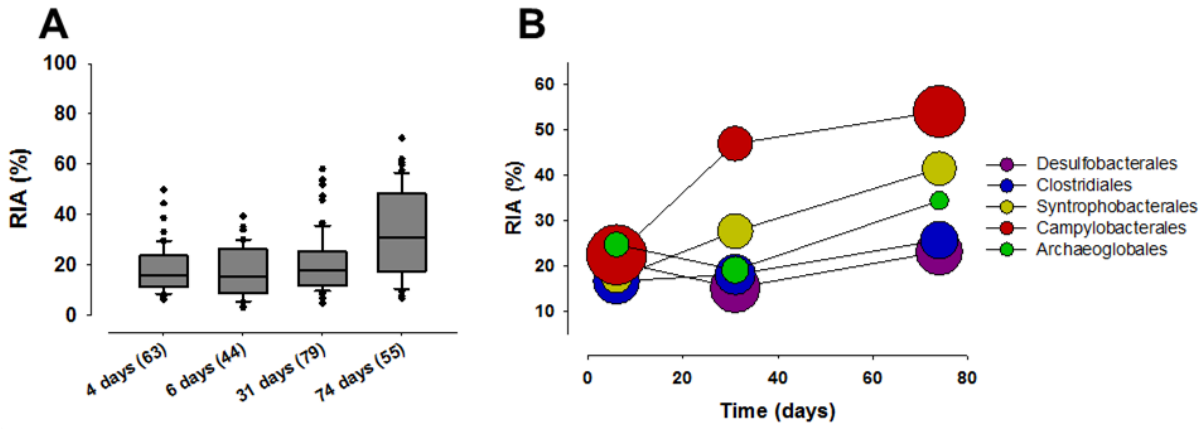

Figure 2.2: Mean relative isotope abundances (RIA) of all identified peptides with incorporation patterns (**A**) and with the affiliation to the dominant acetate consumers (**B**). The size of the circle indicates the labeling ratio.

The *Campylobacterales* showed a direct and by far, the fastest acetate incorporation. The ^{13}C-incorporation derived from labeled acetate by the *Archaeoglobales* and the *Syntrophobacterales* was significantly higher than the one determined for the *Clostridiales* and the *Desulfobacterales* after 74 days. The labeling ratio was steady for *Clostridiales* (~0.5), *Syntrophobacterales* (~0.5) and *Desulfobacterales* (~0.7). For the *Archaeoglobales*, it remained constant until day 31 (~0.4) and finally decreased to 0.3. For the *Campylobacterales*, it started at a ratio of 0.8 after 6 days, decreased to 0.5 after 31 days and finally increased to 0.7 after 74 days again.

Metaproteome analysis

The protein groups identified with high confidence were each affiliated to a distinct phylum in the metagenome. *Firmicutes* and *Proteobacteria* were the most abundant phyla within the protein groups of the consortium (**Figure 3.2A**). Nevertheless, *Euryarchaeota*, *Bacteroidetes*, *Chlorobi* and *Chloroflexi* were identified among the most frequent phyla as well. On the level

of microbial orders, the *Clostridiales* comprised up to 45% abundance followed by the *Syntrophobacterales* (up to 10%), the *Desulfobacterales* (up to 6%), the *Desulfuromonadales* (up to 6%), the *Desulfovibrionales* (up to 5%), the *Archaeoglobales* (up to 3%) and the *Campylobacterales* (up to 4%). (**Figure 3.2B)**.

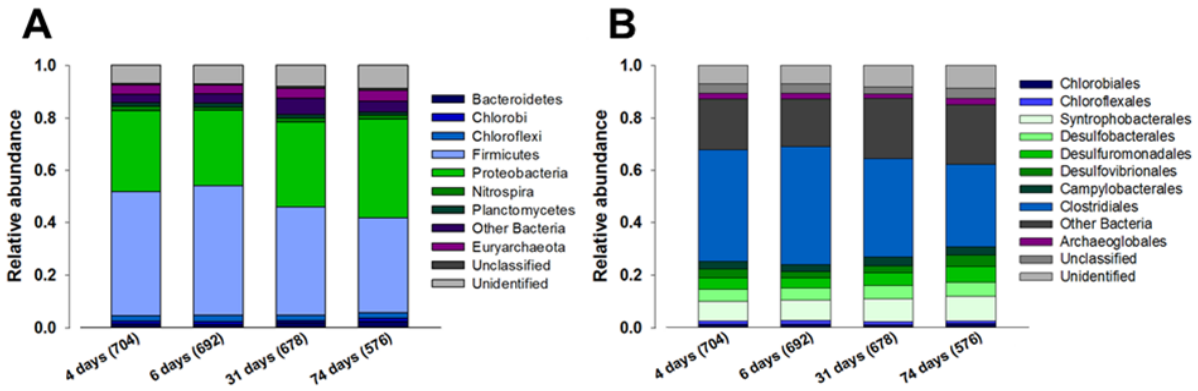

Figure 3.2: Time-resolved distribution of the identified protein groups assigned to phyla (**A**) and orders (**B**). Unidentified microorganisms were not assigned to any taxonomic information whereas for unclassified ones, at least the domain was known.

The relative abundances of the key players during prolonged incubation with additional acetate were explicitly calculated revealing an increase in abundances of *Syntrophobacterales*, *Campylobacterales*, *Archaeoglobales* and *Desulfobacterales* while the abundance of *Clostridiales* decreased (**Supporting Information Table 2.2**). Enzymes identified in the metaproteome were further considered for functional evaluation (**Table 2.2**). Enzymes related to the C1 metabolism and CO_2 assimilation, particularly the Wood-Ljungdahl pathway, were affiliated to *Clostridiales* and *Desulfobacterales*. Enzymes related to aromatic compound degradation were assigned to *Clostridiales* and *Desulfuromonadales*. Regarding the sulfur cycle, enzymes of the dissimilatory sulfate reduction were identified for *Clostridiales* and *Syntrophobacterales*. In general, enzymes related to maintenance such as ATP synthesis, chaperonines, regulation and transcription were dominantly assigned to *Clostridiales* but also to *Syntrophobacterales*, *Campylobacterales*, *Archaeoglobales* and *Desulfobacterales*.

Table 2.2: Important metabolic pathways of the benzene-degrading consortium identified by metaproteome analysis including CO_2 assimilation (Wood-Ljungdahl pathway), aromatic compound degradation as well as enzymes involved in dissimilatory sulfate reduction and energy metabolism. The numbers of unique protein hits are indicated.

	Clostridiales	Syntrophobacterales	Campylobacterales	Archaeoglobales	Desulfobacterales	Desulfuromonadales	Desulfovibrionales	Other microbes
Aromatic compound degradation (9)	3					1		5
ATP synthesis (16)	4	5	5					2
Binding (65)	26	8	2	2	2	2	5	18
Biomolecule synthesis, other metabolic processes (45)	24	5	2		2		1	11
Cellular processes and signaling (26)	12	3	6				1	4
C1 metabolism, CO2 fixation (12)	6				4			2
Dissimlatory sulfate reduction (20)	7	2						11
Energy metabolism (44)	11	9	5	3	2	3	2	9
Regulation (21)	6	3	2			3	2	5
Transcription (25)	13	3	1	1	3	2	1	1
Conserved hypothetical protein (164)	70	8	22	2	5	6	3	48
Unique hypothetical protein (230)	23	5	2	2	11	13	3	171

Elemental sulfur as potential TEA

In comparison to the sterile control, results indicated that benzene degradation in the sulfur amended microcosm tremendously slowed down as only 170 µM of applied benzene was transformed over 213 days of incubation (**Figure 4.2A**). In contrast, microcosms amended with sulfate completely degraded three feedings of 700 µM benzene. The respective benzene degradation rates were 13.5±3.0 µM d^{-1} (n=3 biological x 3 technical replicates) with sulfate as TEA and 1.7±0.9 µM d^{-1} (n=3 technical replicates) using sulfur whereas 0.8±0.6 µM d^{-1} (n=3 technical replicates) were measured for the sterile control. Compared to the sulfide production when sulfate was used as TEA, sulfide concentration increased faster to at maximum 1.4 mM after 39 days when sulfur was applied (**Figure 42.B**). In case of the sulfate-reducing microcosms, sulfide was produced up to 0.8±0.2 mM (n=3 technical replicates) after 46 days, 0.9±0.1 mM (n=3 technical replicates) after 109 days and 1.0±0.2 mM (n=3 technical replicates) after 180 days. However, after the above-mentioned maximum, sulfide concentration decreased once benzene vanished from the media in the sulfate-containing microcosms (**days 50, 109 and 180, Figure 4.2B**).

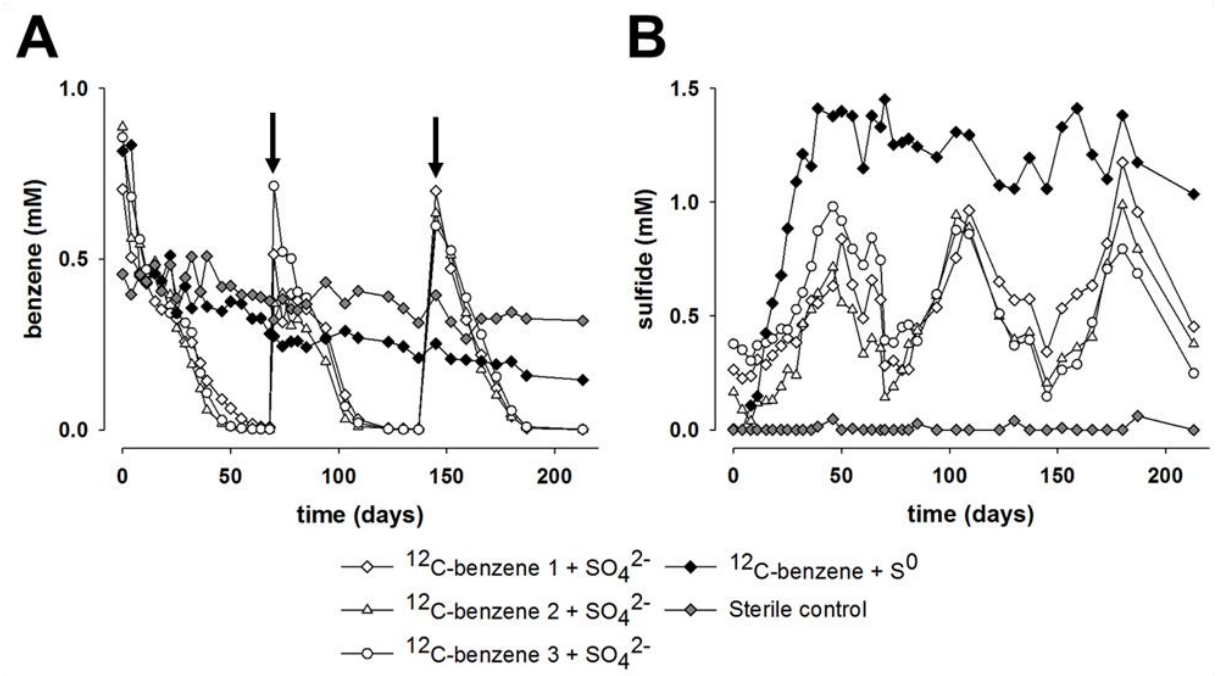

Figure 4.2: Benzene (**A**) and sulfide concentrations (**B**) during replacement of sulfate with sulfur as possible TEA. Data of three biological controls with sulfate (white circle, triangle and diamond), a microcosm with sulfur (black diamond) as well as a sterile control (grey diamond) are shown. The arrow indicates the addition of unlabeled benzene to the sulfate-reducing microcosms.

However, sulfide production started again after the amendment of benzene (**days 0, 70 and 145, Figure 4.2B**). In sulfidic media, elemental sulfur will spontaneously and abiotically react with sulfide forming polysulfides which has to be integrated in polysulfide-transforming reactions (**Equation 4**).

$$[\mathbf{4}]\ \mathrm{nS^0 + HS^- \rightarrow S^{2-}_{n+1} + H^+}$$

Formed polysulfide could either be used by polysulfide respiration (PSR) (**Equation 5 and 6**) or polysulfide disproportionation (PSD) (**Equation 7**) to sulfide and sulfate while the latter is channeled in the dissimilatory sulfate reduction (DSR) (**Equation 2 and 3**).

$$[\mathbf{5}]\ \mathrm{H_2 + S^{2-}_n \rightarrow HS^- + S^{2-}_{n-1} + H^+}$$

$$[\mathbf{6}]\ \mathrm{acetate + S^{2-}_n + 4H_2O \rightarrow 2HCO_3^- + HS^- + S^{2-}_{n-1} + 2H^+ + H_2}$$

$$[\mathbf{7}]\ \mathrm{S^{2-}_n + 4H_2O \rightarrow SO_4^{2-} + 3HS^- + S^{2-}_{n-4} + 5H^+}$$

Discussion

The pulsed $^{13}C_2$-acetate protein-SIP experiment was designed to neither affect benzene degradation nor change microbial composition. Hence, 10 µM of $^{13}C_2$-acetate was amended daily in addition to the previously determined 17±2 µM of unlabeled acetate originating from benzene degradation (34). The initial decrease of benzene in the sterile control was likely due to adsorption to the butyl stopper and thus, an abiotic effect which was confirmed by the lack of sulfate-reducing activity. The benzene degradation rates measured were in the range of previously published rates of 2.4-14.1 µM d^{-1} (146). As indicated by these rates, the activity of the benzene degraders was not influenced by additional acetate but surprisingly, acetate amendment was not directly linked to sulfate reduction as sulfide production rates were comparable to that of the non-amended culture. Hence, acetate was assimilated rather than oxidized which would have been coupled to sulfate reduction and by that, led to a faster and higher sulfide production. Accordingly, observed sulfide production compared to the consumption of benzene was similar for acetate-amended (46±12%) and non-amended cultures (47±16%) but both were lower than anticipated. This discrepancy was reported in previous experiments as well (34, 146, 236) and suggests further sulfide transformation processes such as precipitation or oxidation.

Metaproteome analysis regarding microbial phyla and orders revealed that the microbial community did not shift with prolonged acetate amendment. This is in accordance to the previous protein-SIP experiments with labeled benzene or carbonate (35).The identified protein groups in this study were mainly assigned to *Clostridiales*, *Syntrophobacterales*, *Desulfobacterales*, *Desulfuromonadales*, *Desulfovibrionales*, *Archaeoglobales* and *Campylobacterales* in descending abundance. Otherwise, protein groups assigned to *Bacteroidetes*, *Chlorobi* and *Chloroflexi* showed a minor but increasing abundance in the metaproteome over the experimental time. Though, the abundance of proteins assigned to *Archaeoglobales* and *Syntrophobacterales* which are assumed to be involved in dominant acetate utilization was increasing while the abundance of *Clostridiales* as benzene fermenter was decreasing with prolonged amendment of additional acetate indicating an adaptation of the community to the continuous supply of acetate. Dominant acetate utilization exhibited RIA values of up to 54% in proteins of *Campylobacterales*, *Archaeoglobales* and *Syntrophobacterales* whereas the acetate-utilizing activity assigned to *Clostridiales* and *Desulfobacterales* was significantly lower at a maximum of 26%.

Members of the *Syntrophobacterales* were previously discussed to be affiliated to dissimilatory sulfate reduction and utilization of acetate as a metabolite of benzene fermentation (33, 35). RIA values of up to 41% displayed the assimilation of acetate but did not reach the extent of incorporation observed for the *Campylobacterales* presumably due to additional assimilation of CO_2 and thus, the dilution of the maximal ^{13}C-incorporation. The *Archaeoglobales* were found to utilize acetate but metaproteome information on the potential TEA used was missing. *Archaeoglobus* species are typically related to sulfate reduction (237). Thus, RIA values of up to 35% were in the range of dominant acetate utilization alike the *Deltaproteobacteria* as the label was presumabely diluted by CO_2 assimilation. In contrast, the *Campylobacterales* featured the fastest and highest ^{13}C-incorporation derived from labeled acetate reaching RIA values of up to 54%. The metaproteome lacked information about the specific physiology of this organism. However, the epsilonproteobacterial population genome of a community enriched from the same field site but degrading *m*-xylene under sulfate-reducing conditions revealed genes for a sulfide:quinone oxidoreductase (*sqr*) and a polysulfide reductase (*psr*) [44]. The *m*-xylene-degrading community was used for metagenome sequencing as it was already enriched in the same epsilonproteobacterial phylotype and consisted of only one more member of the *Deltaproteobacteria* (230). Sulfur respiration catalyzed by the polysulfide reductase using polysulfide instead of elemental sulfur to oxidize e.g. hydrogen is well understood as it was intensively studied in the epsilonproteobacterial species *Wolinella succinogenes* (183). Apart from that, the sulfide:quinone oxidoreductase as a single-subunit flavoprotein oxidizing sulfide to polysulfide while reducing quinone to quinol was previously described (238). Further, sulfur respiration and sulfide oxidation have been reported for *Sulfurovum sp.* NBC37-1 which was isolated from a deep-sea hydrothermal vent (225-227) and is the next cultured relative of the epsilonproteobacterial phylotype in our consortium. However, when sulfate was replaced by elemental sulfur, benzene degradation collapsed to 1.7±0.9 µM d^{-1}. In comparison to the benzene depletion of 0.8±0.6 µM d^{-1} in the sterile control which was due to abiotic processes such as adsorption to the butyl stopper, the actual amounts of produced acetate and hydrogen in the sulfur-containing microcosm were minimal. Otherwise, 1.4 mM sulfide was rapidly formed demonstrating ongoing sulfur transformation processes. Extracellular sulfur (as polysulfide) could be channelled into PSR (**Equations 5 and 6**) and PSD (**Equation 7**). If PSR was the only occurring sulfur transformation process, complete oxidation of hydrogen and acetate resulting in 1.4 mM sulfide would require at least 230 µM benzene to be fermented in the same time (39 days). If PSD was the only occurring process, sulfur disproportionation would lead to sulfide

and sulfate in a ratio of 3:1 corresponding to at maximum 350 µM sulfate from 1.4 mM sulfide which can be calculated back to at most 100 µM fermented benzene when produced acetate and hydrogen are equally transformed. In fact, when abiotic benzene depletion is considered, only 170 µM benzene was fermented over 213 days. Therefore, we conclude that extracellular elemental sulfur (as polysulfide) is dominantly used by PSD to form sulfate and sulfide rather than PSR. In addition, the rapid sulfide production will likely inhibit DSR of produced sulfate which leads to the accumulation of acetate and hydrogen causing the collapse of benzene fermentation. Interestingly, sulfide concentrations repeatedly decreased in all sulfate-reducing microcosms after benzene was completely consumed (n=3 biological x 3 technical replicates). Under anoxic conditions, sulfide could be precipitated as iron(II)-sulfide or captured by sulfide oxidizing processes. However, only 1.5 mg L^{-1} of $FeCl_2$ x $4H_2O$ was supplied by the media which corresponds to 1.9 µM. Even when sulfide was precipitated as iron(II)-sulfide, this cannot explain the tremendous decrease in sulfide of 0.6±0.1 mM (n=3 biological x 3 technical replicates) but it is unclear if this decrease in sulfide is completely of biotic nature or due to other ongoing abiotic processes. Comprising, the *Campylobacterales* in this community might recycle otherwise toxic sulfide by its oxidation to polysulfide via sulfide:quinone oxidoreductase and subsequent PSR via polysulfide reductase while the sulfur species must be kept intracellular as extracellular polysulfides are rapidly consumed by PSD. In addition, PSR coupled to hydrogen oxidation as described for *Wolinella succinogenes* is presumably not occurring in our community as the members of the *Deltaproteobacteria* will likely outcompete the epsilonproteobacterial phylotype for hydrogen.

Confirming previous studies on this consortium, enzymes involved in aromatic compound degradation were affiliated to *Clostridiales* comprising the previously described initial benzene degrader identified as *Cryptanaerobacter*/*Pelotomaculum* (32, 33). Carbon fixation via the Wood-Ljungdahl pathway (239) was demonstrated for *Clostridiales* and *Desulfobacterales*. After 74 days of incorporation, both *Clostridiales* and *Desulfobacterales* featured RIA values of up to 26% which was significantly lower than the assimilation of the dominant acetate utilizers. This finding demonstrates that the *Clostridiales* did not only secret acetate from benzene fermentation but also assimilated extracellular acetate. The low acetate assimilation assigned to the *Clostridiales* and the *Desulfobacterales* suggests less efficient transport or assimilation mechanisms for acetate and/or other sources for biomass production such as CO_2.

Finally, the putative scavengers belonging to *Bacteroidetes*, *Chlorobi* and *Chloroflexi* were only found in the metaproteome analysis but lacking ^{13}C-incorporation during the pulsed acetate protein-SIP approach. Confirming the previously hypothesized community model (35), the latter phyla were supposed to thrive on dead biomass and metabolites derived from other community members and thus, the carbon sources available after 74 days of $^{13}C_2$-acetate amendment might not have been labeled sufficiently to enable a detectable incorporation.

By uniting the results of metaproteomics and the pulsed $^{13}C_2$-acetate protein-SIP as well as earlier studies, the previously hypothesized model of the syntrophic community mineralizing benzene enriched from the aquifer in Zeitz was improved (**Figure 5.2**). Here, *Clostridiales* ferment benzene to acetate and hydrogen. Acetate is utilized by *Archaeoglobales*, *Campylobacterales*, *Syntrophobacterales*, *Clostridiales* and *Desulfobacterales*. CO_2 is assimilated by *Clostridiales* and *Desulfobacterales* via the Wood-Ljungdahl pathway. Finally, dead biomass and metabolites are scavenged by *Bacteroidetes*, *Chlorobi* and *Chloroflexi*. In summary, we were able to trace the carbon flow derived from labeled acetate in a benzene-degrading and sulfate-reducing microbial community by functional metaproteome analysis using a pulsed $^{13}C_2$-acetate protein-SIP approach. Incorporation of amended $^{13}C_2$-acetate revealed both the capability of the syntrophic consortium to utilize additional acetate while still degrading benzene and its role as key metabolite. The epsilonproteobacterial *Campylobacterales* featured the fastest and highest acetate incorporation. Confirming previous studies, the *Epsilonproteobacteria* were not essential for benzene degradation but proven to be the key acetate utilizers within the benzene-degrading microbial consortium. With the respective enzymes affiliated to sulfide oxidation and polysulfide respiration encoded in its genome, the epsilonproteobacterial phylotype could perform the oxidation of otherwise toxic sulfide forming polysulfide and its subsequent reduction. However, it is unclear to which processes sulfide oxidation and polysulfide reduction are coupled. Nevertheless, our study provides clues on suitable isolation strategies for these *Epsilonproteobacteria* with the aim to unveil their specific physiology.

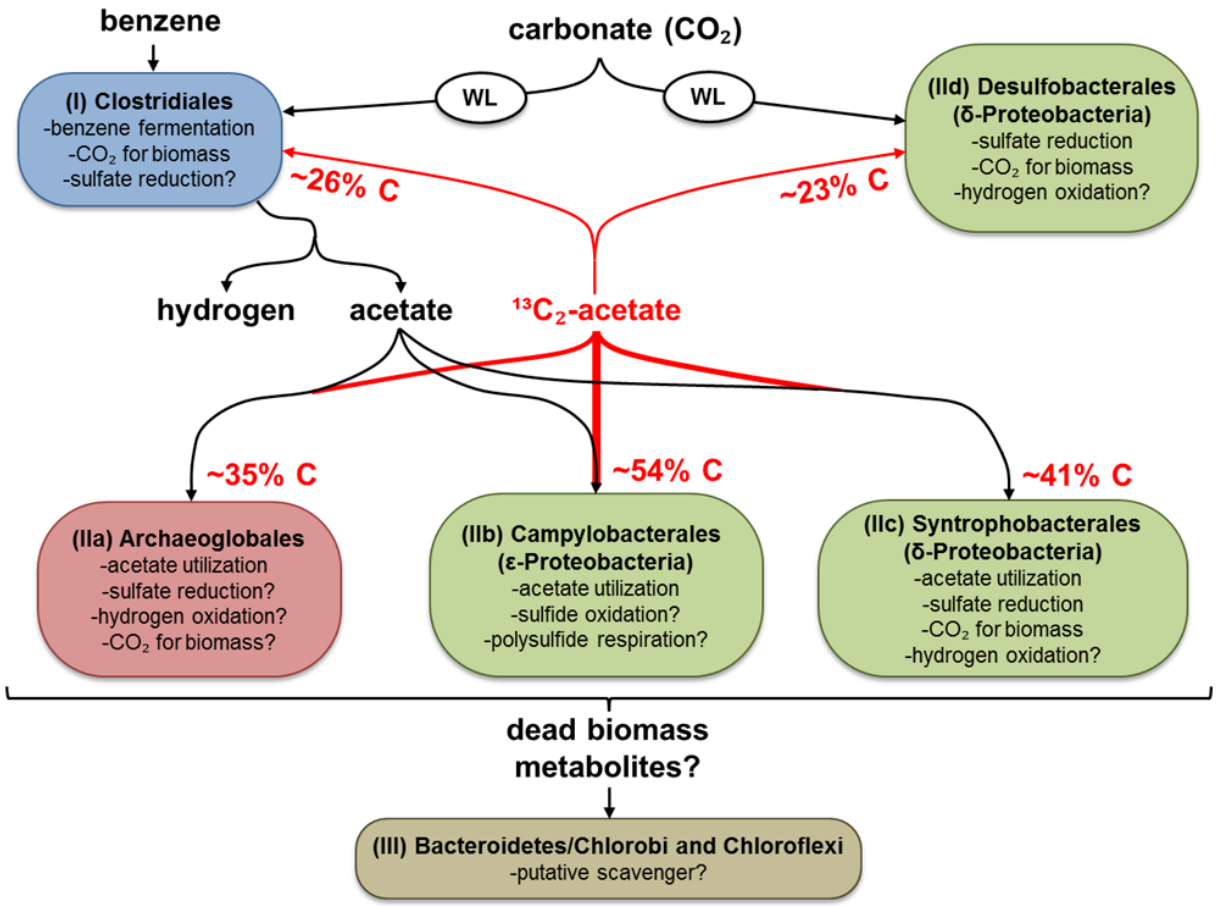

Figure 5.2: Hypothetical overview of the carbon flow and functional interactions within the benzene-degrading, sulfate-reducing community. Carbon sources and carbon flux of the identified groups of organisms separated by their different incorporation behaviour regarding $^{13}C_2$-acetate are indicated. Acetate utilization (red line) is zoned from CO_2 utilization (dotted red line). WL stands for Wood-Ljungdahl pathway and the percentages for the maximum carbon incorporation derived from labeled acetate.

Acknowledgements

We acknowledge the financial support by the German Research Foundation, Priority Program 1319. We are grateful to Michaela Wunderlich and Sibylle Mothes from the UFZ Department Analytical Chemistry for acetate analysis as well as Jörg Ahlheim and Werner Kletzander from the UFZ Department Groundwater Remediation for assistance in sampling of biological material from the columns. Benjamin Scheer is acknowledged for the support in using the Orbitrap in the ProVIS laboratory. The authors are grateful for using the analytical facilities of the Centre for Chemical Microscopy (ProVIS) at the Helmholtz-Centre for Environmental Research which is supported by the European Regional Development Funds (EFRE – Europe funds Saxony) and the Helmholtz-Association. We thank LABGeM and the National Infrastructure France Génomique for enabling the use of the annotation platform MicroScope.

Supporting Information

Growth monitoring

Benzene and sulfide concentrations were monitored during incubation. To determine benzene concentrations, 0.5 mL of the supernatant was dissolved in 9.5 mL ddH_2O pH 2.5 and measured with an automated headspace gas chromatography with a Varian 3800 gas chromatograph (Varian, Palo Alto, USA), a CP SIL 5 CB capillary column (25 m x 0.12 mm x 0.12 µm; Varian, Darmstadt, Germany) and a flame ionization detector. Samples were preheated to 70°C for 30 min. For separation, a gradient of 2 min at 70°C, 10°C min^{-1} up to 90°C and 60°C min^{-1} up to 220°C with a flow rate of 1 mL min^{-1} was used. Benzene eluted at a retention time of 1.8 min. Sulfide was measured with a modified version of the protocol by Cline (236). Liquid samples of up to 100 µL were transferred in test tubes filled with 1 mL saturated zinc acetate dehydrate solution capturing sulfide. After adding 4 mL dH_2O and 400 µL *N*,*N*-dimethyl-1,4-phenylendiamine, the solution was incubated in the dark for 20 min. Subsequently, the absorption at 670 nm was measured and sulfide concentration was determined by the use of a calibration curve.

Protein extraction

For the extraction, 1 L sediment was used. The sediment was incubated with medium in an ultrasonic bath for 10 min under occasional stirring to detach cells. The supernatant was collected and the procedure was repeated twice with ddH_2O. To gather the biomass, the collected liquids were centrifuged at 4°C and 12,000 x g for 10 min (Sorvall RC 6 plus, Thermo Electron Corporation, Waltham, MA, USA). The pellet was resuspended in 20 mM Tris/HCl pH 7.5 and treated with an ultrasonic probe on ice for 4 x 5 min at 50% power (25 W) and 50% duty cycle (UP50H, Hielscher Ultrasonics GmbH, Teltow, Germany). After centrifugation at 12,000 x g at 4°C for 10 min, the supernatant was removed and the pellet was resuspended in 20 mM Tris/HCl pH 7.5. For phenol extraction, an equal volume of phenol solution (10 g mL^{-1} in ddH_2O) was added and incubated under shaking at 500 rpm and room temperature for 1 h. The mixture was centrifuged at 12,000 x g as described above for phase separation. The lower phase was mixed with fivefold volume of ice cold 100 mM ammonium acetate in methanol. Precipitation was performed over night at -20°C followed by centrifugation at 12,000 x g as described above. The supernatant was removed and the pellet was washed with the following solutions: once with 100 mM ammonium acetate, twice with 80% acetone and once with 70%

ethanol. For each washing step, the pellet was resuspended using ultrasonication, incubated for 15 min at -20°C and finally centrifuged at 12,000 x g as described above. Afterwards, the pellet was dried on air.

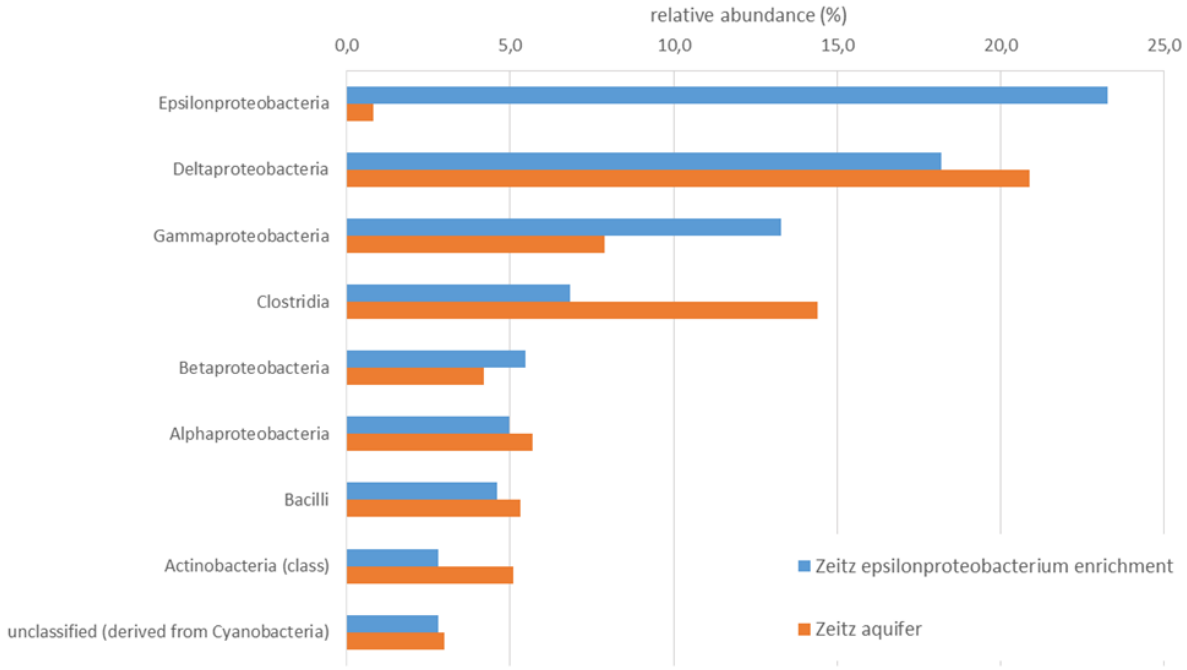

Figure S1.2: Phylogenetic distribution of the two metagenomes used for the metaproteome analyses according to MG-RAST. In the benzene-degrading consortium (Zeitz aquifer) only a minor fraction was affiliated to *Epsilonproteobacteria* whereas in the *m*-xylene-degrading enrichment culture (Zeitz epsilonproteobacterium enrichment), *Epsilonproteobacteria* made up about 24% of the metagenome.

Table S1.2: Growth values used for the evaluation of benzene degradation kinetics comparing acetate-amended and non-amended cultures. Sorption of benzene to the butyl stopper is indicated in red and was not considered as degradation.

Non-amended (mM)							
#	**d**	**benzene**	**sulfide**	**benzene degraded**	**rate**	**sulfide produced**	**rate**
1	12	0.99	0.77				
	34	0.75	1.14				
	47	0.58					
	57	0.50	1.46				
	64	0.42	1.56	0.32	10.74	0.79	15.11
2	58	1.23	0.15				
	87	0.80	0.31				
	99	0.74	0.77				
	121	0.40	1.10				
	134	0.30					
	144	0.22	1.31	0.58	10.13	1.17	13.56
3	246	0.51	0.23				
	250	0.46	0.24				
	253	0.43	0.31				
	257	0.38	0.29				
	260	0.35	0.33				
	264	0.36	0.37				
	267	0.33	0.40				
	271	0.26	0.38				
	274	0.26	0.46				
	278	0.20	0.57				
	281	0.14	0.56				
	288	0.09	0.63				
	292	0.06	0.84	0.30	10.71	0.61	13.33
4	58	0.79	0.13				
	87	0.47	0.59				
	99	0.30	0.55				
	121	0.13	1.07	0.35	10.16	0.94	14.96
5	250	0.54	0.04				
	253	0.46	0.12				
	257	0.49	0.13				
	260	0.42	0.13				
	264	0.40	0.19				
	267	0.30	0.26				
	271	0.25	0.24				
	274	0.19	0.47				
	278	0.12	0.53				
	281	0.06	0.60				
	288	0.02	0.72	0.38	15.65	0.68	17.82
6	312	0.51	0.28				
	316	0.32	0.30				
	320	0.40	0.26				
	323	0.38	0.27				
	327	0.35	0.45				
	336	0.30	0.54				
	345	0.10	0.76				
	351	0.03	0.96	0.32	13.44	0.68	17.47

7	387	0.70	0.34				
	394	0.47	0.53				
	401	0.32	0.60				
	408	0.22	0.63				
	415	0.12	0.82				
	422	0.04	1.18				
	429	0.01	0.96	0.47	13.35	0.61	14.63
8	242	0.89	0.17				
	246	0.56	0.09				
	250	0.54	0.04				
	253	0.46	0.12				
	257	0.49	0.13				
	260	0.42	0.13				
	264	0.40	0.19				
	267	0.30	0.26				
	271	0.25	0.24				
	274	0.19	0.47				
	278	0.12	0.53				
	281	0.06	0.60				
	288	0.02	0.72	0.47	15.27	0.55	11.95
9	312	0.37	0.14				
	316	0.40	0.19				
	320	0.31	0.26				
	323	0.32	0.37				
	327	0.30	0.44				
	336	0.20	0.59				
	345	0.03	0.94	0.29	13.32	0.80	24.29
10	387	0.63	0.21				
	394	0.51	0.31				
	401	0.34	0.36				
	408	0.18	0.41				
	415	0.10	0.73				
	422	0.04	0.99	0.48	16.97	0.78	22.35
11	242	0.86	0.38				
	246	0.68	0.35				
	250	0.56	0.30				
	253	0.47	0.37				
	257	0.48	0.38				
	260	0.43	0.40				
	264	0.34	0.44				
	267	0.34	0.44				
	271	0.31	0.53				
	274	0.29	0.60				
	278	0.17	0.72				
	281	0.11	0.87				
	288	0.03	0.98	0.45	14.65	0.60	13.13
12	312	0.71	0.39				
	316	0.52	0.38				
	320	0.50	0.45				
	323	0.40	0.46				
	327	0.39	0.39				
	336	0.27	0.59				
	345	0.07	0.88				
	351	0.02	0.86	0.48	15.53	0.47	11.99

13	387	0.60	0.15				
	394	0.53	0.26				
	401	0.39	0.29				
	408	0.28	0.47				
	415	0.16	0.71				
	422	0.06	0.79	0.47	16.74	0.65	18.52
14	10	1.68	0.15				
	25	1.39	0.08				
	44	1.11	0.48				
	58	0.84	0.42				
	87	0.66	0.40				
	91	0.66	0.40				
	95	0.67	0.48				
	99	0.61	0.51				
	121	0.55	0.78				
	134	0.32	0.98				
	144	0.25	1.09				
	151	0.13	1.49	1.54	12.25	1.34	9.52
AVG					13.49		15.62
SD					2.407025		4.099

^{13}C-acetate-amended (mM)							
#	**d**	**benzene**	**sulfide**	**benzene degraded**	**rate**	**sulfide produced**	**rate**
1	0	0.58	0.61				
	4	0.38	0.48				
	8	0.36	0.87				
	12	0.36	0.92				
	34	0.12	1.26	0.47	13.70	0.65	19.06
2	43	0.57	0.84				
	47	0.25	1.05				
	57	0.18	1.26				
	64	0.16	1.15				
	71	0.14	1.12	0.43	15.43	0.42	20.23
3	34	0.73	0.77				
	47	0.64	0.82				
	57	0.47	0.96				
	64	0.46	0.93				
	71	0.39	1.02	0.34	9.22	0.25	10.80
AVG					12.78		16.70
SD					3.209789		5.13714

3.3. Starke et al., Soil Biology and Biochemistry (2016)

Bacteria dominate the short-term assimilation of plant-derived N in soil

Robert Starke[1,a,#], Rene Kermer[1,#], Lynn Ullmann-Zeunert[2], Ian T. Baldwin[2], Jana Seifert[1,a], Felipe Bastida[5], Martin von Bergen[1,3,4], Nico Jehmlich[1,*]

[1]Helmholtz-Centre for Environmental Research e UFZ, Department of Molecular Systems Biology, Permoserstr. 15, 04318, Leipzig, Germany

[2]Max Planck Institute for Chemical Ecology, Hans-Knoll-Str. 8, 07745, Jena, Germany

[3]Aalborg University, Center for Microbial Communities, Department of Chemistry and Bioscience, Fredrik Bajers Vej 7H, 9220, Aalborg, Denmark

[4]Institute of Biochemistry, Faculty of Biosciences, Pharmacy and Psychology, University of Leipzig, Germany

[5]CEBAS-CSIC, Department of Soil and Water Conservation, Centro de Edafología y Biología, Aplicada del Segura, Campus Universitario de Espinardo, Aptdo. De Correos 164, Espinardo, 30100, Murcia, Spain

[a]Present address: University of Hohenheim, Institute for Animal Science, Emil-Wolff-Str. 6-10, 70599, Stuttgart, Germany

[#]Authors contributed equally

[*]Corresponding author: Nico Jehmlich, nico.jehmlich@ufz.de

Received 16 June 2015

Accepted 18 January 2016

May 2016, Volume 96, pp 30-38

DOI: 10.1016/j.soilbio.2016.01.009

Keywords: Soil, Short-term leaf litter degradation, Microbial community, 16S and 18S rDNA, Metaproteomics, Protein-SIP

Abstract

In comparison to inorganic N cycling, only little is known regarding the assimilation of organic N in soil. Therefore, we used 16S and 18S rDNA gene profiling and functional metaproteomics to characterize the composition of a soil microbial community assimilating (15)N-labeled plant-derived organic matter (OM).

Genomic results showed an increase of the abundance of fungi and *Proteobacteria* related to the utilization of plant-derived OM within the first days of exposure. Similarly, metaproteomic analysis revealed *Proteobacteria* as the most abundant phylum followed by *Actinobacteria* and *Ascomycota*. Finally, protein stable isotope probing (protein-SIP) demonstrated copiotrophic behaviour for *Rhizobiales* belonging to *Proteobacteria*, *Actinomycetales* belonging to *Actinobacteria* and *Chroococcales* belonging to *Cyanobacteria* as these phylotypes immediately incorporated (15)N from the added plant tissue. Conversely, the fungal *Saccharomycetales* and the bacterial *Enterobacteriales, Pseudomonadales, Sphingomonadales* and *Xanthomonadales* displayed slower (15)N-assimilation.

We showed that, in contrast to the dominance of fungi in the degradation of complex carbon compounds, mostly bacteria were involved in the short-term assimilation of plant-derived N. The combined use of genomic and proteomic approaches allowed to track the flow of N within the soil microbial community.

Introduction

The viability of soil microbes depends on available energy and nutrient sources. Among them, N is a critical nutrient of OM which derives mainly from plants (240). The dominant form of N in plants is protein (ca. 2-5% of plant dry weight) whereas the concentration of free amino acids is typically 100-fold lower (241). Free amino acids can be taken up directly by soil microbes using various membrane transport systems (46) while proteins must be depolymerized by extracellular proteases as rate-limiting step of plant-derived OM decomposition (47-49). Resulting simple organic N compounds can be quickly utilized by microbes as energy and nutrient sources (50). However, despite the well-explored inorganic N cycling i.e. nitrification and denitrification (51, 52), the cycling of organic N in soil is not yet completely understood (47). Conversely, the decomposition and assimilation of organic C by soil microbes has been intensively studied (53-55). These studies have revealed a dominance of fungi in the degradation and assimilation of plant-derived polymeric organic C (54, 56). Moreover, the decomposition of carbon polymers by fungal activities releases low moleculer weight compounds that can be used for bacterial growth (242).

However, in comparison to C cycle, the knowledge about how plant-derived N is enteringthe microbial community and which microbial populations dominate the assimilation of N is still scarce. This is of fundamental interest to understand the N cycling and OM dynamics in soil. Therefore, the introduction of cultivation-independent approaches such as meta-OMICs allowed deeper insights into the structure and function of microbial communities and the exploration of biogeochemical cycles.

In the last years, genomics has offered a solution for describing the diversity and composition of soil microbial communities and the quantification of functional genes (243-247). Moreover, the combination of genomics and SIP studies using (15)N-labeled plants revealed the assimilation of organic N from plants by soil microbial populations (248, 249), but these studies do not allow to comparatively study the involvement of bacterial and fungal communities in the decomposition of plant inputs. However, a relationship between gene abundances and corresponding processes is not always observed (250).

Metaproteomics has become a central tool in microbial ecology (98, 101) and provided valuable insights to decipher functional-phylogenetic relationships in microbial communities (251-253).

However, since the mere protein abundance can not be directly linked to activity, stable isotope probing (SIP) is used to provide a direct link to the metabolic activity of an organism in a microbial community (86, 99, 100). In comparison to nucleic acid-SIP approaches which requires a minimal isotope incorporation of 25-30 atom% (100), (15)N can be used as a marker for the activity and assimilation capabilities of microbial populations with detection limits as low as 0.5 atom% (77). Despite its sensitivity and the potential information on the role of microbial populations involved in N-cycling, protein-SIP has not yet been applied to study the decomposition of plant-derived OM in soil.

We characterize the bacterial and fungal populations involved in the cycling of plant-derived OM using amplicon sequencing (16S and 18S rDNA), metaproteomics and 15(N)-protein-SIP. Considering that bacterial biomass has a lower C/N-ratio than fungi (254), we hypothesize that fast-growing bacterial populations dominate the short-term assimilation of N from plant-derived OM. The combination of meta-OMICs and SIP techniques may provide valuable information about the dynamics and functional role of individual populations in microbial communities.

Materials and methods

Studied soil and plant-material

Silty clay soil was collected from a long-term tobacco experimental field located in Mochkrena (51° 31 N, 12° 48' E, Saxony, Germany). Mean anual temperature and total precipitation in the area were 10ºC and 569 mm, respectively. The soil was classified as a Typic Ariudoll with a pH of 6.46, a total C of 11.60 g kg^{-1} and a total N of 1.6 g kg^{-1}. 10 kg of soil was collected from different spots of an area of 1,200 m² directly from below the surface to a maximum depth of 10 cm. Stones and roots were removed and the soil was sieved (<2 mm) and stored at 4°C.

Unlabeled and (15)N-labeled leaf litter was derived from tobacco plants which were grown as described (255). Briefly, 10 days after germination, the plants were transfered to round Teku pots (Pöppelmann GmbH & Co. KG, Lohne, Germany) and to single pots (1 L) with soil 10 days later. Labeled medium was prepared by substituting (14)NO_3^- to (15)NO_3^- at high concentrations without considering the natural abundance of (15)N. The plants were harvested 10 days after the transfer to 1 L single pots. Afterwards, plant leaves were separated from the stem and roots. All plant parts were dried at 100°C and subsequently stored at room temperature. Dried plant material was mechanically grounded to smaller pieces.

Soil mesocosm

In order to track the assimilation of N in the soil microbial community, (15)N and (14)N tobacco litter was added to the soil. Two replicated mesocosms were set up for each litter in sterilized 0.5 L flasks with 50 g of soil plus 0.5 g of the respective tobacco litter (1% (w/w)). Independent mesocosms were established for each incubation time: 0.1, 0.8, 1.9, 2.9, 5.0, 7.9 and 13.9 days. Four times (0.1, 0.8, 1.9 and 2.9 days) in the first three days and three times (5.0, 7.9 and 13.9 days) within the remaining 11 days and immediately subjected to multi-step protein and DNA extraction. Homogenized soil and shredded plant material were premixed in a glass beaker prior to the distribution to the mesocosms. As a control, mesocosms (n=2) without plant litter were set up in the same conditions than litter-amended treatments. Mesocosms were incubated at 20°C in an incubation chamber for 14 days in darkness. Soil moisture was kept constant during the experiment by adding water at 60% of the water holding capacity. To ensure aerobic conditions, a regular aeration every day was performed for each mesocosm.

Growth monitoring

For monitoring microbial growth during incubation, the biological oxygen demand (BOD) per h as respiration rate was measured using the OxiTop system (WTW Inc, Germany). Every mesocosm flask was supplemented with a 10 mL test tube containing 5 mL of a 5 M NaOH solution and equipped with an OxiTop cap for BOD measurement. The principle is the detection of a pressure decrease due to oxygen consumption by aerobic biological respiration processes. Carbon dioxide produced at the same time is precipitated as sodium carbonate in the test tube and therefore, does not affect the pressure measurement. Using BOD values, the respiration rates were determined according to BOD per h. As a proxy for the plant-litter decomposition, water-soluble carbon (WSC) was determined by soil extraction (2 h shaking with a soil/distilled water ratio of 1:5) followed by centrifugation, filtration, and analysis of the extract solution on a C analyzer for liquid samples (Analytik Jena TOC/TN multi N/C 3100).

Soil DNA extraction and sequencing

DNA extraction was accomplished using the PowerSoil® DNA Isolation Kit (MO BIO Laboratories, Inc., Carlsbad, USA). Genetic profiling was performed by IMGM Laboratories (Martinsried, Germany). For that, amplicons for different variable regions of 16S and 18S rRNA were generated for every sample using two primers each (**Table 1.3**).

Table 1.3: 16S and 18S rRNA primers used for amplicon sequencing.

rRNA	Primer name	Primer sequence (5' -> 3')	Primer Length (bp)	Amplicon size
16S	A519F	CAGCMGCCGCGGTAA	15	560 bp
	928R	CCCCGYCAATTCMTTTRAGT	20	
18S	F-1183	AATTTGACTCAACACGGG	18	590 bp
	R-1631	TACAAAGGGCAGGGACG	17	

One amplicon library was prepared from the PCR products of all samples. Sequencing was performed on the Illumina the Illumina MiSeq® next generation sequencing system (Illumina Inc., San Diego, USA). The resulting 2 x 250 bp reads were quality controlled and trimmed by

applying the CLC Genomics Workbench software (CLC Bio, Boston, USA). Further bioinformatics analysis including clustering, phylogenetic analysis and beta diversity was performed by Ribocon GmbH (Bremen, Germany). Both, the eukaryotic 18S and the prokaryotic 16S rDNA was analyzed regarding its phylogenetic distribution within the soil microbial community. Total number of reads of the input dataset were clustered at a 98% sequence identity treshold by OTU definition. As reference for classification, SILVA SSU Ref NR 115 dataset containing 479,726 classified sequence entries was used. The number of reads of the most abundant phylogenetic taxons was assembled for each of the six incubation points of (15)N exposition as well as for time point zero. The phylogenetic distribution was defined and plotted for the eukaryotic and the prokaryotic fraction of the community.

Soil protein extraction

The extraction step included the addition of an equal volume of extraction buffer (50 mM Tris-HCl pH 7.5, 1 mM PMSF, 0.1 mg/mL chloramphenicol) to the whole amount of soil (50 g) and shaking at room temperature for 2 h. Soil samples and supernatant were separated by centrifugation at 3,000 x g at room temperature for 10 min (Sorvall RC 6 plus, Thermo Electron Corporation, Waltham, MA, USA). Both fractions were stored at -20°C until further use. In the second extraction step, 2 g of the homogenized soil-litter pellet from the first step was mixed with 5.4 mL of extraction buffer. Further steps included three cycles of freeze and thaw (freeze in liquid nitrogen, thaw in 60°C water bath), the addition of 0.6 mL of 10% (w/v) SDS solution and two cycles of ultrasonic treatment using an ultrasonic disintegrator (4°C, 5 min / 70% amplitude / 70% power, break of 2.5 min between cycles; ultrasonic processor UP50H equipped with ultrasonic probe MS7, Hilscher Inc., Germany). For phenol extraction, equal volume of phenol solution (10 g mL^{-1} in ddH_2O) was added to 10 mL in case of the supernatant from the first extraction step and approximately 7 mL (entire volume) in case of the soil-litter-buffer-mixture from the second extraction step and incubated under shaking at 500 rpm and room temperature for 1 h. The mixture was centrifuged at 4°C and 12,000 x g for 10 min for phase separation (Sorvall RC 6 plus, Thermo Electron Corporation, Waltham, MA, USA). The lower phase was mixed with fivefold volume of ice cold 100 mM ammonium acetate in methanol. Precipitation was performed over night at -20°C followed by centrifugation at 12,000 x g as described above. The supernatant was removed and the pellet was air-dried. Protein extraction from pure tobacco plant material (unlabeled and ^{15}N labeled) was carried out by using a different protocol. It involved the initial grinding of the plant material in liquid nitrogen, followed by the

addition of 150 µL ex-strep buffer (100 mM Tris-HCl pH 8.0, 150 mM NaCl, 5 mM EGTA, 5 mM EDTA, 10 mM DTT, 0.5 mM PMSF and 0.5% (v/v) Triton-X 100) to 100 mg of ground plant material and strong mixing (vortex) and subsequent incubation on ice for 15 min. Afterwards, the pellet was separated from the supernatant by centrifugation (12,000 x g, 10 min and 4°C) with one repetition to clean the supernatant from remaining pellet particles. The clean supernatant was either directly processed or stored at -20°C until further use.

Metaproteomics

Complete protein pellets were used for one-dimensional (1D) gel electrophoresis without prior determination of protein amounts. Air-dried protein pellets were suspended in 30 µL 1x Laemmli buffer (229), dissolved via ultrasonication and incubated under shaking at 500 rpm and 60°C for 10 min. Samples were centrifuged at 12,000 x g (Sorvall RC 6 plus, Thermo Electron Corporation, Waltham, MA, USA) to remove precipitates before loading on sodium dodecyl sulfate gels (4% stacking gel and 12% separating gel). Electrophoresis was performed at 10 mA per gel. Polypeptides were stained by colloidal Coomassie Brilliant Blue G-250 (Roth, Kassel, Germany). Entire lanes were cut into gel pieces for each sample and an in-gel tryptic digestion was performed. Supernatants obtained from protein extraction of the pure plant material were subjected to in-solution trypsin cleavage. Finally, dried samples were resuspended in 0.1% formic acid, desalted and purified by ZipTip® treatment (EMD Millipore, Billerica, MA, USA). Mass spectrometric analysis of the peptide fractions was accomplished by UPLC-LTQ Orbitrap Velos MS/MS as described (90). Briefly, samples were injected by an autosampler and concentrated on a trapping column (nanoAcquity UPLC column, C18, 180 µm × 2 cm, 5 µm, Waters) with water containing 0.1% formic acid at flow rates of 15 µL min^{-1}. After 8 min, the peptides were eluted into a separation column (nanoAcquity UPLC column, C18, 75 µm × 15 cm, 1.75 µm, Waters). Chromatography was performed with 0.1% formic acid in solvent A (100% water) and B (100% acetonitrile). The LC gradient was set from 2 to 15% in the first 10 min and subsequently, from 15 to 40% in 67 min with a final switch to 85% for additional 10 min using a nano-high pressure LC system (nanoAcquity UPLC, Waters). Continuous scanning of eluted peptide ions was carried out between 400-2,000 *m/z*, automatically switching to MS/MS collision-induced dissociation (CID) mode on ions exceeding an intensity of 3,000.

Metaproteomic data analysis

Raw data obtained was processed using Proteome Discoverer (v1.4.0.288; Thermo Fisher Scientific, Waltham, MA, USA). Searches were performed using MASCOT algorithm with the following parameters: tryptic cleavage with maximal two missed cleavages, a peptide tolerance threshold of ±10 ppm and an MS/MS tolerance threshold of ±0.5 Da, and carbamidomethylation at cysteines as static and oxidation of methionines as variable modifications. As database, all annotated fungal, bacterial and archaea protein-coding sequences of the NCBInr database were downloaded. Proteins were considered as identified with at least one unique peptide with high confidence (false discovery rate, FDR<0.01). FDR's were determined using Percolator (256). The exported multireport was analyzed for phylogenetic classification and functional prediction (using the cluster of orthologous groups, COG) by Prophane (http://www.prophane.de/index.php).

Protein-SIP data analysis

The respective unlabeled peptides were measured as well to compare chromatographic retention time and MS/MS fragmentation patterns as described previously (73). For protein-SIP analysis, OpenMS and the new developed MetaProSIP node was used (233, 234, 257). MS raw data was converted into *.mzML files using MSConvert of ProteoWizard (235). Subsequently, the latter *.mzML files were converted to smaller *.mzML and *.featureXML files using a precursor mass tolerance of ±10 ppm and a fragment mass tolerance of ±0.5 Da as well as carbamidomethylation at cysteines as static and oxidation at methionines as variable modifications. The generated files were then used for the MetaProSIP searches with an m/z tolerance of ±10 ppm as well as an intensity threshold of 1,000 and a correlation threshold of 70%.

For the identification of (15)N peptides, phylogenetic taxa obtained by metaproteomics were used to create a combined database consisting of the most abundant orders. We dowloaded the reviewed protein-coding entries (Uniprot/Swiss-Prot 12/01/2014) of *Actinomycetales*, *Bacillales*, *Burkholderiales*, *Chroococcales*, *Enterobacteriales*, *Hypocreales*, *Pleosporales*, *Pseudomonadales*, *Rhizobiales*, *Saccharomycetales*, *Sphinomonadales* and *Xanthomonadales*.

In order to provide an ecological classification, microbial orders were sorted according to their genetic and metaproteomic abundances and to copiotrophic or oligotrophic behaviour regarding the utilization of plant-derived N (**Table 2.3**).

Table 2.3: Abundances of copiotrophs and oligototrophs assigned to microbial orders in genomic profiling, metaproteomics and protein-SIP sorted by fast (0-1 days) and slow (2-14 days) response to the amendment of ^{15}N-labeled tobacco plant leaves.

	Order	Time (days)	Genomic profile (mean ± SD %)	Metaproteome (mean ± SD %)	Protein-SIP (mean ± SD %)
Copiotrophs	*Rhizobiales*	0-1	6.6 ± 2.3	4.7 ± 3.3	34.6 ± 5.4
		2-14	4.8 ± 1.7	5.5 ± 2.0	41.0 ± 6.2
	Actinomycetales	0-1	8.4 ± 2.2	9.0 ± 2.6	23.1 ± 10.9
		2-14	3.8 ± 0.6	8.3 ± 2.0	8.3 ± 4.9
	Chroococcales	0-1	0.0	0.8 ± 0.7	15.4 ± 21.8
		2-14	0.0	0.2 ± 0.1	0.8 ± 1.7
Oligotrophs	*Saccharomycetales*	0-1	0.1 ± 0.0	0.6 ± 0.3	7.7 ± 0.0
		2-14	0.1 ± 0.0	0.2 ± 0.2	6.9 ± 3.2
	Enterobacteriales	0-1	1.2 ± 1.6	1.0 ± 0.3	7.7 ± 0.0
		2-14	3.1 ± 2.0	3.8 ± 1.8	16.5 ± 6.2
	Pseudomonadales	0-1	13.9 ± 19.0	9.0 ± 12.0	3.8 ± 5.5
		2-14	19.5 ± 3.0	13.2 ± 3.5	4.8 ± 4.3
	Sphingomonadales	0-1	7.6 ± 2.6	1.3 ± 0.0	0.0
		2-14	7.8 ± 0.3	1.5 ± 0.2	7.5 ± 4.5
	Xanthomonadales	0-1	7.3 ± 0.3	0.4 ± 0.2	3.8 ± 5.4
		2-14	12.2 ± 4.1	4.0 ± 1.1	5.7 ± 1.8

Results

Respiration rates and water-soluble carbon decreased over time

The general microbial activity during incubation was monitored by respiration rates (**Figure 1.3A**). For both the labeled and the unlabeled mesocosms, rates started at ~130 mg O_2 kg^{-1} h^{-1} after 2 hours reaching a local minimum of ~32 mg O_2 kg^{-1} h^{-1} after 18 hours. Afterwards, the respiration rates increased to ~43 mg O_2 kg^{-1} h^{-1} while subsequently decreasing steadily to 18 mg O_2 kg^{-1} h^{-1} after 14 days. As indicative for OM degradation, the water-soluble C (WSC) was analyzed (**Figure 1.3B**). A decay of WSC was observed within the first two days of incubation while WSC stabilized at around 100 mg C kg^{-1} $soil^{-1}$ after five days. WSC was always higher in the amended mesocosms than in the controls without litter.

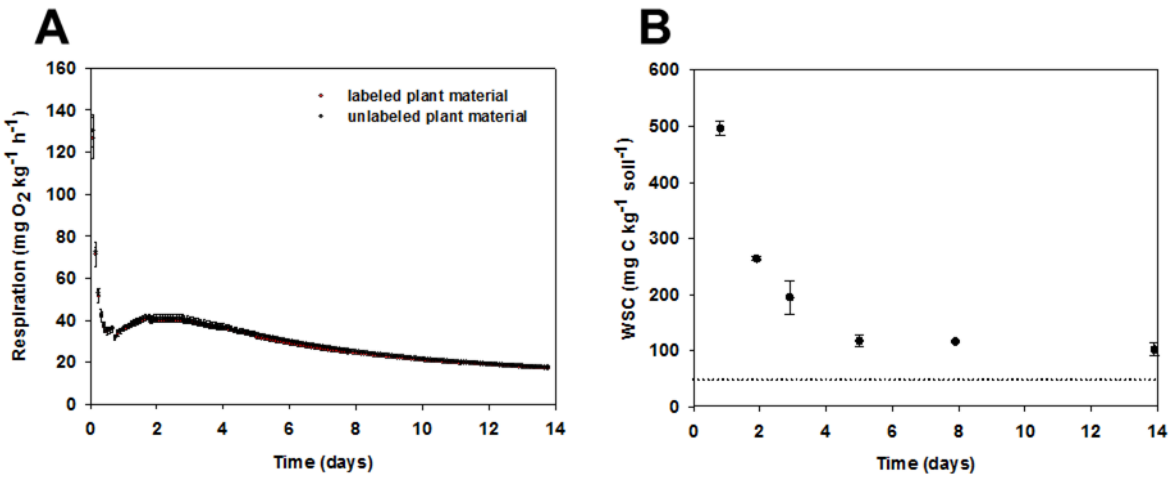

Figure 1.3: Microbial growth by the soil community during short-term decomposition of plant-derived material. Respiration rates (**A**) and water soluble carbon (WSC) (**B**) are shown.

Proteobacteria was the most abundant phylum in metagenomics and metaproteomics

In order to explore both the prokaryotic and the eukaryotic fraction of the microbial community, analysis considered 16S as well as 18S rDNA. For both 16S and 18S sequencing, ~150,000 reads per sample were assigned. As result, 16S rDNA featured *Acidobacteria*, *Actinobacteria*, *Bacteroidetes*, *Planctomycetes* and *Proteobacteria* as most abundant phyla comprising up to 75% (**Figure 2.3A**).

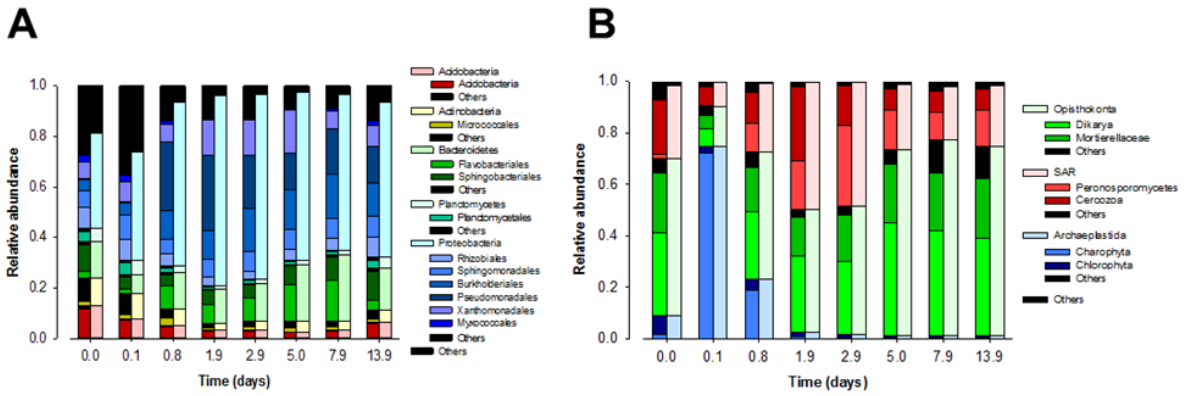

Figure 2.3: The phylogenetic distribution of the prokaryotic (**A**) and the eukaryotic (**B**) fraction of the soil microbial community obtained by genetic profiling.

Starting with 40% abundance at time point zero, *Proteobacteria* steadily increased as the most abundant phyla during incubation. Within the Proteobacteria, the microbial orders *Burkholderiales* (up to 18%), *Pseudomonadales* (up to 30%) and *Xanthomonadales* (up to 17%) were the most abundant ones. Further, *Flavobacteriales* and *Sphingobacteriales* (each up to 10%) were the most abundant orders affiliated to the *Bacteroidetes* being the second most abundant phyla within the microbial community reaching up to 26% abundance. However, the abundance of *Acidobacteria*, *Actinobacteria* and *Planctomycetes* decreased with prolonged incubation. *Proteobacteria* reached its maximum abundance after two days while *Bacteroidetes* featured significant increase in abundance just after day five. For 18S rDNA, the most abundant taxons were *Opisthokonta*, *SAR* and *Archaeplastida* (**Figure 2.3B**). Consisting of mostly *Charophyta* to which plants belong, the *Archaeplastida* featured an abundance of 75% at the first time point of sampling. After one day of incubation, the relative abundance of rDNA reads of *Archaeplastida* decreased to 23% and finally dropped below 1% during further incubation. The abundance of *Opisthokonta* to which fungi belong, on the other hand, increased from 15% at the start of incubation to 75% in the later stages of degradation. Thirdly, *SAR* belonging to *Bikonta* together with *Archaeplastida* constisted of *Cercozoa* and *Peronosporomycetes* and featured maximal relative rDNA read abundance of 50% at days two and three of incubation which was decreasing with prolonged leaf litter degradation.

Metaproteomics revealed that bacteria (up to 70%) and eukaryota (up to 10%) were the dominant kingdoms within the soil community whereas the abundance of archean proteins was about 1%. The dominant phylum was *Proteobacteria* featuring up to 50% abundance followed by *Actinobacteria* (up to 15%) and *Cyanobacteria* (10% after 0.1 days) while up to 35% of

detected protein groups remained unidentified (**Figure 3.3A**). With up to 60% unidentified protein groups at 0.1 days of exposure, the dominant eukaryotic orders were *Hypocreales* (up to 2%) and *Saccharomycetales* (up to 1%). On the other hand, *Actinomycetales* (up to 11%), *Bacillales* (up to 4%), *Burkholderiales* (up to 8%), *Chroococcales* (up to 2%), *Enterobacteriales* (up to 7%), *Pseudomonadales* (up to 20%), *Rhizobiales* (up to 9%), *Sphingomonadales* (up to 2%) and *Xanthomonadales* (up to 5%) were the most abundant orders within bacteria (**Figure 3.3B**).Increasing protein abundances immediately after the beginning of exposure were observed for *Actinomycetales*, *Chroococcales* and *Rhizobiales*.

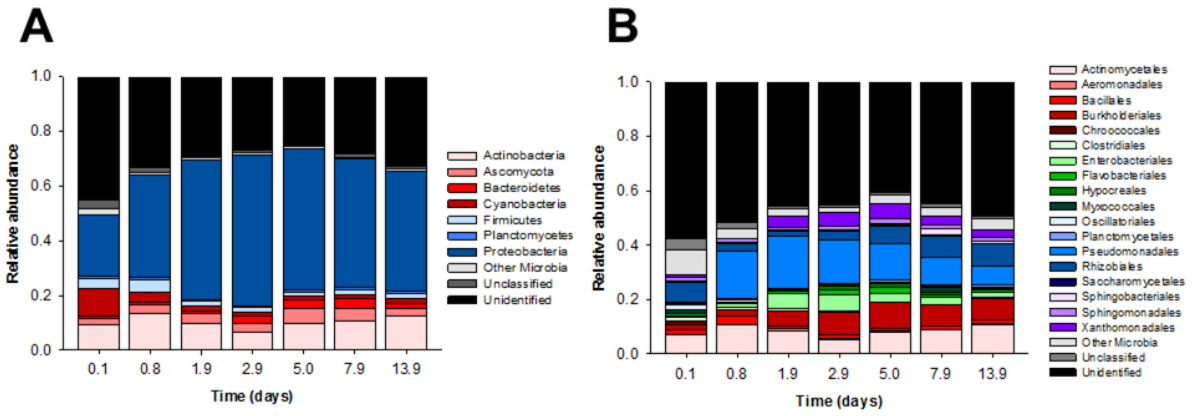

Figure 3.3: The phylogenetic distribution of the soil microbial community on the level of orders (**A**) and families (**B**) obtained by metaproteomic analysis.

Protein-stable isotope probing revealed a major role of bacteria over fungi in the assimilation of plant-derived N

The protein-SIP parameter relative isotope abundance (RIA) describes the number of (15)N-atoms in a peptide and gives information about the proportion of labeled substrate that was utilized by the organism. A second parameter, labeling ratio (lr) of a peptide, describes the ratio of labeled to unlabeled peptide and refers to protein turn over after the addition of the labeled substrate. Here, the relative isotope abundances (RIA) and the labeling ratio (LR) of all peptides were assigned to the corresponding time point (**Figure 4.3A**). The RIA values ranged between 40 and 98% (n=11-26 peptides per time point). A large amount of (15)N-incorporation is reflected by a RIA value of 71±8% (n=13 peptides) and a LR value of 0.59±0.29 (n=13 peptides) which started immediately with the beginning of the experiment. Remarkably, the RIA value at day 0.1 showed the highest value and a high abundance. Both RIA (55±10%, n=13) and LR (0.47±0.18, n=13) decreased after one day while subsequently increasing again

after two days (RIA=64±14%, LR=0.53±0.26, n=11) of exposure. A decrease of incorporation after three days (RIA=60±20%, LR=0.42±0.22, n=12) was followed by an increase until eight days (RIA=67±15%, LR=0.52±0.16, n=12) while decreasing after 14 days (RIA=62±14%, LR=0.57±0.16, n=26). Total (15)N-incorporation during labeled plant-derived material decomposition is performed by *Rhizobiales* (40%) as dominant utilizer within the soil microbial community followed by *Enterobacteriales* (14%) and *Actinomycetales* (13%) (**Figure 4.3B**).

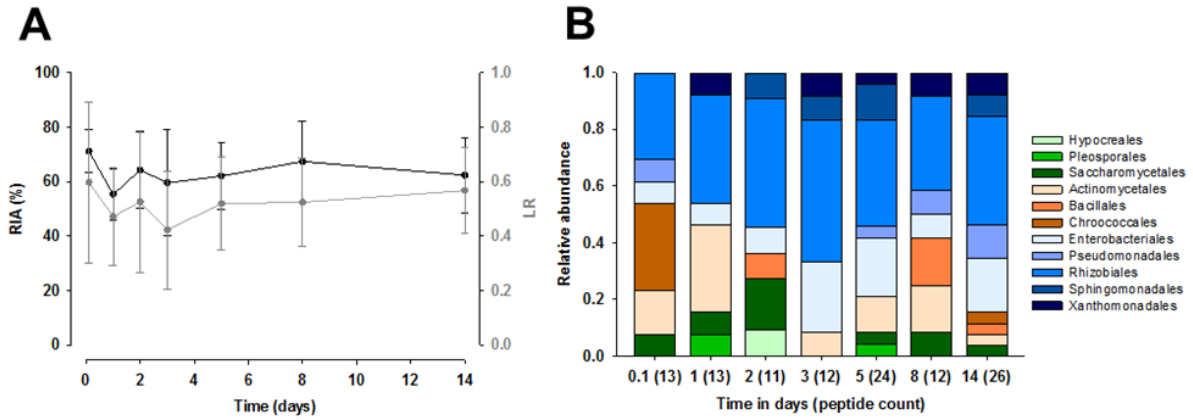

Figure 4.3: Outcome of the ^{15}N-labeled tobacco plant leaf protein-SIP. Peptides with incorporation were assigned to the mean relative isotope abundances (RIA, black) and labeling ratio (LR, grey) for each time point (**A**) and to the abundance of microbial orders (**B**).

Actinomycetales, *Chroococcales* and *Rhizobiales* showed (15)N-incorporation immediately at the beginning of exposure whereas the fungal *Hypocreales* and *Saccharomycetales* as well as *Enterobacteriales*, *Pseudomonadales*, *Sphingomonadales* and *Xanthomonadales* showed only a minor incorporation at the beginning of exposure which increased with prolonged incubation. The results from this multi-OMIC approach were reflected in ecological attributes of microbial populations. The ecological classification of microbial orders to copiotrophic or oligotrophic behaviour regarding the utilization of plant-derived N revealed that copiotrophic microbes showed a high isotope incorporation immediately at the beginning of exposure (20%, n=3 microbial orders) which decreased to about 14% after 14 days (**Table 2.3**). A 4D-plot summarized the data from sequencing, metaproteomics and protein-SIP with respect to the incubation times (**Figure 5.3**). Oligotrophs started with 5% abundance in protein-SIP (n=5 microbial orders) and increased to at maximum 9% whereas the copiotrophs behave complementary.

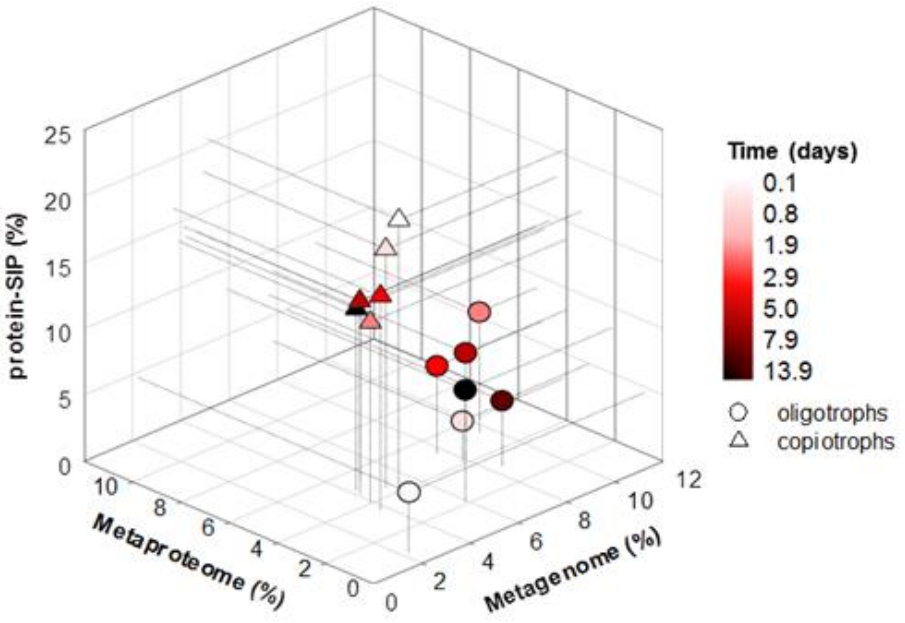

Figure 5.3: Four-dimensional distribution of soil microbes. Copiotrophs (△ = *Rhizobiales*, *Actinomycetales* and *Chroococcales*) and oligotrophs (○ = *Enterobacteriales*, *Pseudomonadales*, *Sphingomonadales*, *Saccharomycetales* and *Xanthomonadales*) were assigned to the abundance in the gene profile, the metaproteome and the protein-SIP during labeled leaf litter decomposition.

Discussion

Bacteria dominate the assimilation of plant-derived N

The assimilation of plant-derived N has been studied separately for bacterial and fungal populations (248, 258). Consequently, the overall contribution of bacterial and fungal populations in the cycle of plant-N has not been properly distinguised. Here, we used a multi-OMIC approach to decipher the key players involved in the plant-derived N assimilation within a whole soil microbial community.

Metaproteomics and SIP analyses revealed the dominance of bacteria over fungi in the short-term assimilation of N. Hence, our results support the hypothesis that, with respect to the lower C/N-ratio of bacteria compared to fungi (254), fast-growing bacterial populations would dominate the short-term assimilation of plant-derived N.

These results contrasts with the key role in the decomposition and assimilation of plant-derived C suggested for fungi (56). In compliance with the decreasing of WSC, fungi abundances increased which is in agreement with the plant decomposition model in which fungi feed on complex plant polymers (i.e. lignin, cellulose) while bacteria thrive on available energy sources (54). Metaproteomics revealed an impact of plant input on the abundance of the fungal populations *Saccharomycetales* and *Hypocreales*. Both fungal classes were active during later stages of short-term (15)N-leaf litter degradation. Similarly, España *et al*., (2011) found *Hypocreales* (i.e. *Fusarium* sp.) as fast-growing decomposers of plant tissues using DNA-SIP in soil microcosms with (15)N-plants. In addition, Hannula *et al*. (2012) found *Hypocreales* incolved in the decomposition of plants using a (13)C-RNA-SIP approach as well. Interestingly, we found (15)N incorporation into proteins of *Saccharomycetales*. This fact suggests a certain role of this fungal group in the decomposition and assimilation of plant-derived N that was not highlighted in the literature so far.

The involvement of bacterial populations in the assimilation of plant-derived N

Proteobacteria showed an increase abundance after one day of incubation with litter, both on 16S rDNA and metaproteome level. This is in agreement to a previous study accomplished by Fierer *et al*. (259) where they proposed that microbes affiliated to *Proteobacteria* may act as copiotrophic organisms and hence, they rapidly respond to nutrient improvements and condition

changes in the soil. Similar results have been observed by other authors using metagenomics (260) and metaproteomics (251).

In contrast, *Proteobacteria* members were not found to be involved in the assimilation ofplant-derived (15)Nin DNA-SIP and DGGE approaches (248). Probably, the lower resolution of DGGE in comparison to 16S rDNA genomics and metaproteomics compromises the identification of dominant populations involved in the decomposition of plant material and assimilation of nutrients. Multi-OMICs revealed that the composition of *Proteobacteria* was dominated by *Burkholderiales*, *Myxococcales*, *Pseudomonadales*, *Rhizobiales*, *Sphingomonadales* and *Xanthomonadales*. The highest (15)N-incorporation during the short-term utilization of labeled tobacco plant leaves was assigned to *Rhizobiales* comprising 40% of total peptides. Consistently, nucleic acid-SIP approaches have previously revealed that several *Rhizobiales* groups are commonly detected in the heavy DNA fractions after amendment of (13)C-labeled carbohydrates, cellulose or plants (261-264). In contrast, a low isotope incorporation while being abundant in genetic profiling and metaproteomics was observed for *Burkholderiales*, *Myxococcales*, *Pseudomonadales*, *Sphingomonadales* and *Xanthomonadales*. *Burkholderia* species were affiliated to utilize fungal-secreted metabolites and to overcome fungal defense mechanisms (265). In this study, *Burkholderiales* might have been outcompeted by copiotrophic microbes as the benefit of overcoming fungal defense mechanisms could be subsidiary during the short-term utilization of plant-derived OM. Moreover, *Myxococcales* were reported as micropredators in microbial soil communities playing a key role in the turnover of carbon in soil ecosystems (266, 267).

Genomic results pointed to an increased relative abundance of *Actinobacteria* after one day. Accompanied with high metaproteome abundances as well as a high (15)N-incorporation in the beginning of the experiment, an involvement of this taxa in the assimilation of plant-derived N is suggested. It was proposed that *Actinobacteria* are abundant in soil due to grazing of other intermediate bacteria (263). However, as regards of protein abundances *Actinobacteria* could not compete with the *Proteobacteria* but were certainly linked to immediate utilization of plant-derived N. España *et al*., (248) found different *Actinobacteria* such as *Arthrobacter* sp., *Nocardia* sp., *Streptomyces* sp. and *Saccharopolyspora* sp. as dominant soil microbes in the assimilation of (15)N from plants.

Bacteroidetes were found with increasing rDNA abundance during the later stages of plant-derived OM decomposition. Fierer *et al*., (259) proposed a copiotrophic behavior for *Bacteroidetes.* Recently, Bastida *et al.*, (268) suggested that *Bacteroidetes* are probably outcompeted by populations with an outstanding capacity of growing under improved conditions such as *Proteobacteria* (i.e. *Rhizobiales*) which was also observed in our study. While the information regarding the assimilation of N is limited, nucleic acid-SIP studies revealed constraining information about the involvement of *Bacteroidetes* in the assimilation of C from plants. Exemplary, Fan *et al.*, (261) did not find this clade in heavy DNA fractions of a SIP experiment while other authors did (262, 269). Further, a (13)C-DNA SIP study linked uncultured *Planctomycetes* with the degradation of complex heteropolysaccharides in soil (270). In our study, *Planctomycetes* were matched with a high 16S rDNA abundance level but only a low proteome abundance. Hence, *Planctomycetes* populations probably grow on complex compounds in our soil community as well.

We are aware that the utilized number of replicates (n=2) is limited and further studies will consider a higher number of replicates. In any case, this study establishes the basis for the application of protein-SIP approaches in soil as an state-of-the-art approach for understanding lifestyles of microbial populations. We propose that the copiotrophic lifestyle of *Rhizobiales* and *Actinomycetales* is linked to a high (15)N-incorporation and growth immediately at the beginning of plant-derived OM decomposition. Conversely, oligotrophs including *Saccharomycetales, Enterobacteriales, Pseudomonadales, Sphingomonadales* and *Xanthomonadales* were found with higher abundance in both genetic profiling and metaproteomics during prolonged incubation but less (15)N-assimilation at the beginning as indicated by protein-SIP. Ecological succession or competitive mechanisms might explain the different levels of (15)N into the proteins of differerent microbial groups.

Conclusions

The cascade of the assimilation of plant-derived N through soil microbial populations was tracked by genetic profiling and functional metaproteomics using (15)N-labeled tobacco plant material. In comparison to the dominant role of fungi in the metabolism of polymeric carbon, our multiOMIC approach indicated that bacterial populations assimilate plant-derived N faster than fungi as hypothesized.

We revealed that *Rhizobiales* played a pivotal role in the assimilation of plant-derived N. Copiotrophic behaviour was affiliated to*Actinomycetales*, *Chroococcales* and *Rhizobiales*. Conversely, the fungal *Saccharomycetales* and the bacterial *Enterobacteriales*, *Pseudomonadales*, *Sphingomonadales* and *Xanthomonadales* were identified as secondary N feeders during the decomposition of plant-derived OM. It is well-known that not the whole DNA is uniformly transcribed to RNA which is not equally translated into proteins that are not utterly active. Noteworthy, the use of protein-SIP simultaneously displays the metabolic activity of bacterial and fungal populations revealing not only a difference in genome and proteome abundances but also in the respective (15)N-assimilation capacity. Therefore, the future use of mulit-OMICs with SIP-techniques will enhance our knowledge on the ecological attributes of soil microbial communities. This information might be fundamental for understanding the dynamics of OM in response to climate change threats.

Acknowledgements

We acknowledge Kathleen Eismann for experimental processing. Felipe Bastida and Nico Jehmlich are grateful to the German Academic Exchange Service (DAAD) (PPP-Spain) for their funded project. Felipe Bastida is grateful to the Spanish Ministry for his "Ramón y Cajal" contract (RYC-2012-10666), FEDER fundings and the project AGL2014-54636-R.

4. Diskussion und Schlussfolgerung

4.1. Epsilonproteobakterien

Das Phylum der Epsilonproteobakterien kann grundsätzlich in Pathogene und Nichtpathogene eingeteilt werden (271). Pathogene Spezies, wie Helicobacter im Magen oder Campylobacter im Zwölffingerdarm, bewohnen den Verdauungstrakt von Menschen und Tieren, und können zu Entzündungen wie der Campylobacter-Enteritis führen (272). Dagegen kommt den nichtpathogenen Epsilonproteobakterien durch ihre metabolische Vielseitigkeit eine immer wachsendere, biologische Bedeutung zu (271). Eine chemoautotrophe Endosymbiose zwischen der Tiefwasserseeschnecke Provannidae und den in den großen Kiemen ansässigen *Alviniconcha hessleri* wurde bereits beschrieben (273). Viele nichtpathogene Epsilonproteobakterien werden beispielsweise in hydrothermalen Tiefseeöffnungen gefunden, die typischerweise chemolithotroph leben, in dem sie reduzierte Schwefelverbindungen, Formiat oder Wasserstoff, gekoppelt mit der Reduktion von Nitrat oder Sauerstoff, oxidieren (274). Gegensätzlich dazu nutzen autotrophe Epsilonproteobakterien, die im Mesoproterozoikum in sulfidischen Ozeanen mit geringen Sauerstoffkonzentrationen entstanden sein sollen, den sauerstoffempfindlichen, reversiblen Krebszyklus zur CO_2-Fixierung (36, 275). Der aus dem Aquifer in Zeitz angereicherte, epsilonproteobakterielle Phylotyp stellte bisher ein Enigma dar. Nukleinsäurebasierende Studien berichteten über die hohe Abundanz der Epsilonproteobakterien in dieser Gemeinschaft (32, 33), wohingegen dieser Phylotyp in der komplementären Proteomstudie komplett fehlte (35). Mit Hilfe der Verbindung von Metagenomik (**Artikel 3.1**) und funktionaler Metaproteomik (**Artikel 3.2**) konnte einerseits die Rolle der Epsilonproteobakterien in der Benzolfermentation bestätigt und andererseits mögliche, physiologische Modelle vorgeschlagen werden. Die DNA für das angereicherte Epsilonproteobakterienmetagenom stammte aus einer Kontrollkultur ohne organische Kohlenstoffquelle, die zuvor auf *m*-Xylen unter sulfatreduzierenden Bedingungen gewachsen ist (230, 276, 277). Das entsprechende Metagenom beinhaltete den kompletten rTCA Zyklus, der nur für wenige bakterielle Gruppen wie den grünen Schwefelbakterien und Deltaproteobakterien beschrieben, aber in Epsilonproteobakterien weit verbreitet ist (36, 278-280). Als Alternative zur anorganischen Kohlenstoffquelle wurde das Potenzial für die direkte Acetatassimilation aufgezeigt, welche die Gene *actP* als Importsystem und *acsA* zur Acetataktivierung umfasste (**Artikel 3.1**). Dementsprechend kann sich der Organismus mixotroph ernähren, was gleichermaßen für andere Epsilonproteobakterien berichtet wurde

(36) und diesen Organismen einen selektiven Wachstumsvorteil in Grundwasserhabitaten und Kohlenwasserstoff-kontaminierten Aquiferen verschafft (34). Weiterhin wurde das Potenzial für die Verwendung verschiedener Elektronenakzeptoren (Nitrat, Polysulfid und Fumarat) sowie Elektronendonoren (Wasserstoff, Formiat und Sulfid) aufgezeigt. Dabei ist die Nutzung von Sulfid am offensichtlichsten, da der Organismus aus einer sulfatreduzierenden Gemeinschaft angereichert wurde. Sulfid entsteht als Endprodukt der Sulfatreduktion, akkumuliert und hat in hohen Konzentrationen eine toxische Wirkung. Eine mögliche, vollständige Oxidation von Sulfid zu Sulfat ist unwahrscheinlich, da nicht alle Gene des Sox-Systems gefunden wurden. Stattdessen beinhaltete das Metagenom eine Sulfid Quinon Oxidoreduktase (SQR), die Sulfid zu Polysulfid oxidiert. Diese Oxidation könnte durch Menaquinon an die Polysulfidreduktase (PSR) gekoppelt sein, die die entsprechende Rückreaktion katalysiert. Diese Verknüpfung von Schwefelrespiration und Sulfidoxidation wurde für den nächsten Verwandten *Sulfurovum sp.* NBC37-1, der aus einer hydrothermalen Tiefseeöffnung isoliert wurde, bereits gezeigt (225-227). Da sie aber nur wenig Nettoenergie liefert (ΔE= -15 mV), erscheint eine Kopplung der PSR an die Oxidation von Wasserstoff (ΔE= -154 mV) oder Formiat (ΔE= -173 mV), die ebenfalls durch die Benzolfermentation entstehen, sinnvoller. Hierbei wurde nur das Gen der Untereinheit *fdhA* der Formiatdehydrogenase (FDH) gefunden, während alle Gene (*hydABC*) der Hydrogenase im Metagenom detektiert wurden. Allerdings wird angenommen, dass die hydrogenotrophen Deltaproteobakterien die Epsilonproteobakterien bezüglich Wasserstoff als Elektronendonor durch eine höhere Affinität auskonkurrieren (34), wodurch nur die Verwendung von Formiat und Sulfid kinetisch plausibel ist. Das Potenzial für die Acetatnutzung durch actP und acsA wurde durch den gepulsten $^{13}C_2$-Acetat Protein-SIP bestätigt (**Artikel 3.2**). Hierbei wurde die dominante C-Assimilation der epsilonproteobakteriellen Campylobacterales aus markiertem Acetat gezeigt, welche die Archaeoglobales sowie die deltaproteobakteriellen Syntrophobacterales im sekundären Benzolabbau auskonkurrieren. Zusammenfassend sind die epsilonproteobakteriellen Campylobacterales in der aus Zeitz angereichterten Gemeinschaft erstmals einer Funktion zugeordnet worden: Aus der Benzolfermentation stammendes Acetat, das in hohen Konzentrationen inhibierend auf den Benzolabbau der Clostridiales wirkt, wird von den Campylobacterales in hohen Stoffmengen metabolisiert. Weiterhin kann toxisches Sulfid durch die Oxidation zu Polysulfid mittels SQR umgewandelt werden, das anschließend durch die PSR gekoppelt an die Formiatoxidation weitergenutzt werden könnte. Eine Kopplung von PSR mit der Oxidation von Wasserstoff, wie es für Wolinella beschrieben wurde (122,

123), ist aufgrund der höheren Affinität der Deltaproteobakterien bezüglich Wasserstoff unwahrscheinlich. Bisher ist noch nicht demonstriert wurden, welche Prozesse tatsächlich an Sulfidoxidation sowie Polysulfidreduktion gekoppelt sind, aber es wurden mögliche Isolationsstrategien aufgezeigt, die die spezifische Physiologie der Epsilonproteobakterien in dieser Gemeinschaft aufdecken können und werden.

4.2. Benzolmineralisierende und sulfatreduzierende Grundwassergemeinschaft

Mikrobielle Gemeinschaften sind nicht nur in allen Umweltprozessen wie den Energie- und Nährstoffflüssen, aber auch für die Sanierung kontaminierter Gebiete bedeutsam (35). Der Großteil der persistenten und toxischen Kohlenwasserstoffe wird von anaerob lebenden Mikroorganismen in tieferen Gebieten wie dem Grundwasserleiter abgebaut, da der Sauerstoff von oberflächennahen, aeroben Mikroorganismen zur Oxidation einfacher Verbindungen verbraucht wird (24, 25). Das Verständnis der Interaktionen beim anaeroben Abbau persistenter Kohlenwasserstoffe wie den BTEX-Verbindungen (Benzol, Toluol, Ethylbenzol und *o*-, *m*- und *p*-Xylol) innerhalb einer mikrobiellen Gemeinschaft ist für die biologische Sanierung besonders wichtig (22, 23). Die hier untersuchte, anaerobe und benzolmineralisierende Grundwassergemeinschaft wurde bereits detailliert beschrieben (31-35), wobei die Stoffflüsse des sekundären Metabolismus des postulierten Schlüsselintermediats, Acetat, noch nicht bekannt sind. Mit Hilfe des gepulsten $^{13}C_2$-Acetat Protein-SIP Versuchs und früheren Studien wurde das bisher bestehende Verständnis der syntrophen, benzolmineralisierenden und in einem Aquifer in Zeitz angereichterten Gemeinschaft erweitert. Die Clostridiales fermentieren Benzol zu Acetat und Wasserstoff. Acetat wird von den Archaeoglobales, den Campylobacterales, den Syntrophobacterales, den Clostridiales sowie den Desulfobacterales verwendet. CO_2 wird von den Clostridiales und den Desulfobacterales über den Wood-Ljungdahl-Weg assimiliert. Letztlich wird die tote Biomasse und Metabolite von den Bacteroidetes, den Chlorobi und den Chloroflexi genutzt. Beim Austausch von Sulfat mit elementarem Schwefel als möglichen terminalen Elektronenakzeptor kollabierte die Benzolmineralisation während Sulfid rasch gebildet wurde (**Artikel 3.2**). Das Ausmaß der schnellen Sulfidbildung wurde auf die Polysulfiddisproportionierung (PSD) durch (andere) Deltaproteobakterien zurückgeführt, da zu wenig Benzol fermentiert wurde, um eine Polysulfidreduktion der Epsilonproteobakterien zu bestätigen (**Abbildung 7**).

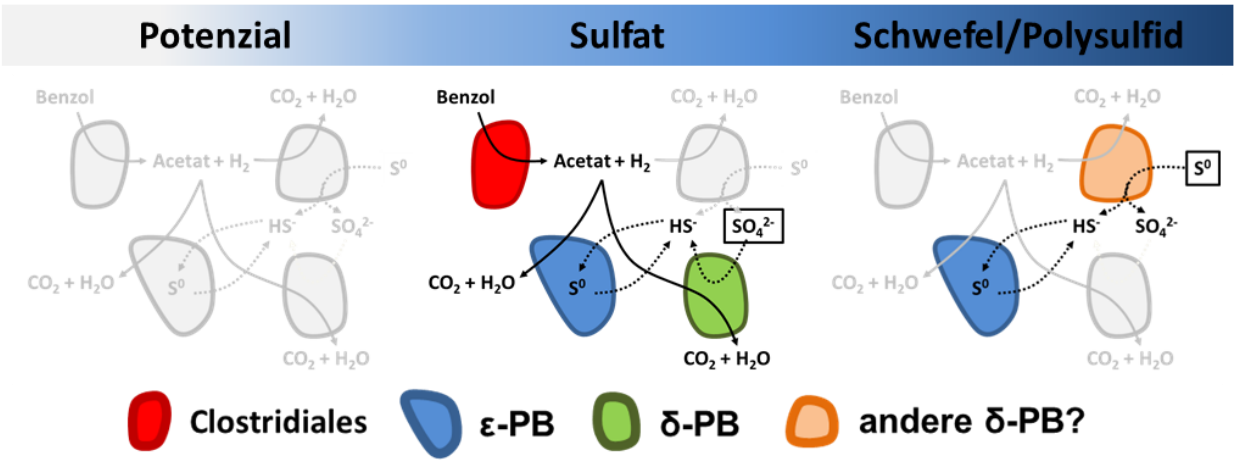

Abbildung 7: Das Potenzial der benzolmineralisierenden Grundwassergemeinschaft verschiedene terminale Elektronenakzeptoren zu verwenden. Dabei steht PB für Proteobakterien. Sulfat wird als Elektronenakzeptor des sekundären Metabolismus verwendet, um Acetat und Wasserstoff resuliertend aus der Benzolfermentation zu oxidieren. Bei Zugabe von elementaren Schwefel kollabiert die Benzolfermentation und Schwefel wird von (anderen) Deltaproteobakterien zu Sulfat und Sulfid disproportioniert.

Aus der von der PSD ausgehenden, schnellen Nutzung von extrazellulärem, elementarem Schwefel, das in sulfidischen Habitaten abiotisch und spontan zu Polysulfid reagiert, wird deutlich, dass entstandener Schwefel beziehungsweise Polysulfid durch Sulfidoxidation der Epsilonproteobakterien intrazellulär gehalten werden muss, um der Konkurrenz der schwefeldisproportionierenden Deltaproteobakterien zu entgehen und einen Wachstumsvorteil zu erhalten. Dieser intrazelluläre Schwefel kann beispielsweise durch Raman-Spektroskopie detektiert werden, um diese physiologischen Prozesse zu bestätigen. Weiterhin ist im Genom der Epsilonproteobakterien eine Untereinheit der Formiatdehydrogenase kodiert (281). Zusätzlich dazu wurde auch im Metaproteom eine Formiatdehydrogenase bei den Desulfobacterales gefunden, die eine mögliche Nutzung von Formiat verdeutlicht. Gleichermaßen lag die Konzentration an Acetat im Überstand stets unter der Detektionsgrenze von 6 µM, was geringer als die zuvor beschriebene Konzentration im Bereich von 17 µM war (34). Ebenfalls unter der Detektionsgrenze lagen Propionat (<8 µM) und Butyrat (<22 µM). Einzig Formiat konnte im Überstand quantifiziert werden (**Abbildung 8**).

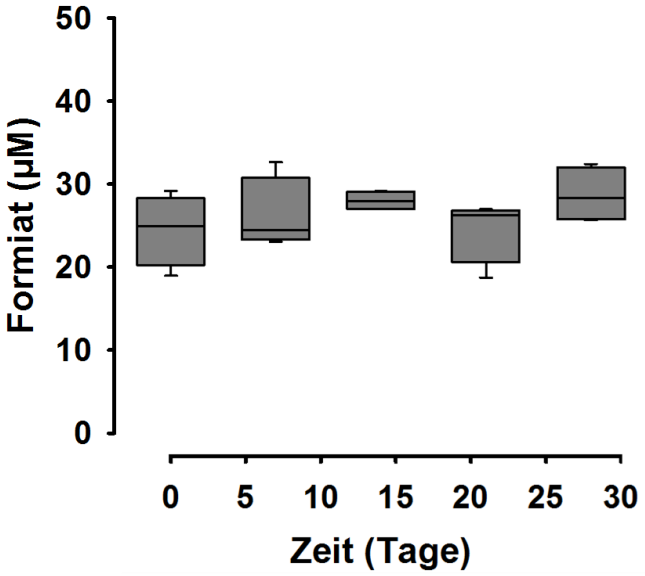

Abbildung 8: Formiatkonzentration im Überstand der anaeroben und benzolmineralisierenden Grundwassergemeinschaft. Andere kurzkettige freie Fettsäuren wie Acetat, Butyrat und Propionat konnten nicht quantifiziert werden.

Bei der Acetatsyntrophie beträgt die Energiebilanz ΔG= -102,0 kJ mol^{-1} (**Gleichung 1 und 2**), wobei die Bilanz bei der Benzolmineralisation über Formiat bei ΔG= +195,9 kJ mol^{-1} liegt (**Gleichung 3 und 4**).

[1] $C_6H_6 + 6\ H_2O \rightarrow 3\ CH_3COOH + 3\ H_2$ ΔG= +116,1 kJ mol^{-1}

[2] $CH_3COOH + SO_4^{2-} \rightarrow 2\ HCO_3^- + H_2S$ ΔG= -72,7 kJ mol^{-1}

[3] $C_6H_6 + 12\ H_2O \rightarrow 6\ HCOOH + 9\ H_2$ ΔG= +548,7 kJ mol^{-1}

[4] $4\ HCOOH + SO_4^{2-} \rightarrow 4\ HCO_3^- + H_2S + 2\ H^+$ ΔG= -235,2 kJ mol^{-1}

Anschließend kann Wasserstoff zu Methan (ΔG= -189,0 kJ mol^{-1}), zu Acetat (ΔG= -94,5 kJ mol^{-1}) oder gekoppelt an die Sulfatreduktion (ΔG= -160,0 kJ mol^{-1}) oxidiert werden. Dabei ist die Oxidation durch die sulfatreduzierenden Deltaproteobakterien durch ihre hohe Affinität zu Wasserstoff am wahrscheinlichsten und wird im folgenden als einziger wasserstoffnutzender Prozess angenommen. Daraus ergibt sich eine Nettoenergie von ΔG= -222,1 kJ mol^{-1} für die Acetatsyntrophie und für Formiat von ΔG= -164,3 kJ mol^{-1}. Die hohe Produktion an Wasserstoff ist dabei in der Lage, die Formiatsyntrophie anzutreiben. Ein gepulster SIP-Ansatz mit ^{13}C-Formiat parallel zur Benzolmineralisation könnte demonstrieren, ob auch Formiat als Intermediat durch die Clostridiales in den sekundären Abbau eingespeist wird. Zusammenfassend sind die Interaktionen der Schlüsselorganismen der in Zeitz angereicherten, mikrobiellen Gemeinschaft mittlerweile gut verstanden. Die Anwendungen von Protein- und DNA-SIP sowie metabolomischen Ansätzen konnten den Kohlenstofffluss detailliert darstellen.

Nichtsdestotrotz gibt es weiterhin unbeantwortete Fragen wie: Welche Organismen oxidieren Wasserstoff? Warum werden Enzyme zur dissimilatorischen Sulfatreduktion in den benzolfermentierenden Clostridiales gefunden? Welche Prozesse sind an die Sulfidoxidation und Polysulfidreduktion der Campylobacterales gekoppelt und wird parallel zur Acetatsyntrophie auch Formiat genutzt? Die Beantwortung dieser Fragen kann unter anderem durch die Isolation der Schlüsselorganismen und die Sequenzierung der jeweiligen Genome erreicht werden. Es bleibt jedoch zu beachten, dass Benzol nur eine der in Zeitz vorkommenden Kontaminationen darstellt und es angestrebt werden sollte, die mikrobiellen Netzwerke für den Abbau aller Kontaminanten aufzuzeigen.

4.3. Pflanzenabbau durch Bodenmikroorganismen

Die Verfügbarkeit von Stickstoff als notwendiger Nährstoff organischer Materie bestimmt die Lebensfähigkeit von Bodenmikroorganismen (44). Der Zyklus von anorganischem Stickstoff durch beispielsweise Nitrifikation und Denitrifikation wurde bereits detailliert beschrieben (51, 52), wobei der Kreislauf von organischem Stickstoff bisher nicht komplett verstanden wurde (47). Dagegen ist bekannt, dass Pilze die Assimilation von pflanzenabgeleitetem, polymerem, organischem Kohlenstoff dominieren (54, 56) und niedermolekulare Verbindungen abgeben, die anschließend von Bakterien genutzt werden (62). In dieser Arbeit wurde erstmals der Einbau aus ^{15}N-markiertem Pflanzenmaterial in Bodenmikroorganismen gezeigt (**Artikel 3.3**). Hierbei wurde demonstriert, dass, gegensätzlich zur bisherigen Annahme der Dominanz der Pilze im Abbau von Pflanzenmaterial, Bakterien die kurzzeitige Assimilation von pflanzenabgeleiteten Material im Boden dominieren. Daraus resultierend wurde ein neues Schema für die Pflanzenabbau durch Bodenorganismen entwickelt (**Abbildung 9**). Wahrscheinlich verlaufen diese Prozesse parallel, aber durch die schnellere Kinetik im bakteriellen Stoffwechsel niedermolekularer Verbindungen im Vergleich zum Abbau von Cellulose und Lignin durch Pilze erscheinen diese zeitlich getrennt. Weiterhin wurden im schnellen Abbau pflanzenabgeleiteter, niedermolekularer Verbindungen zwischen copiotrophen, die schnell auf veränderte Bedinungen und Stress reagieren sowie oligotrophen Mikroorganismen, die später im Abbau aktiv sind, unterschieden. Diese Gruppierung wurde durch die Verwendung von Amplikonsequenzierung, Metaproteomik und Protein-SIP erreicht, die eine multidimensionale Klassifizierung ermöglichte.

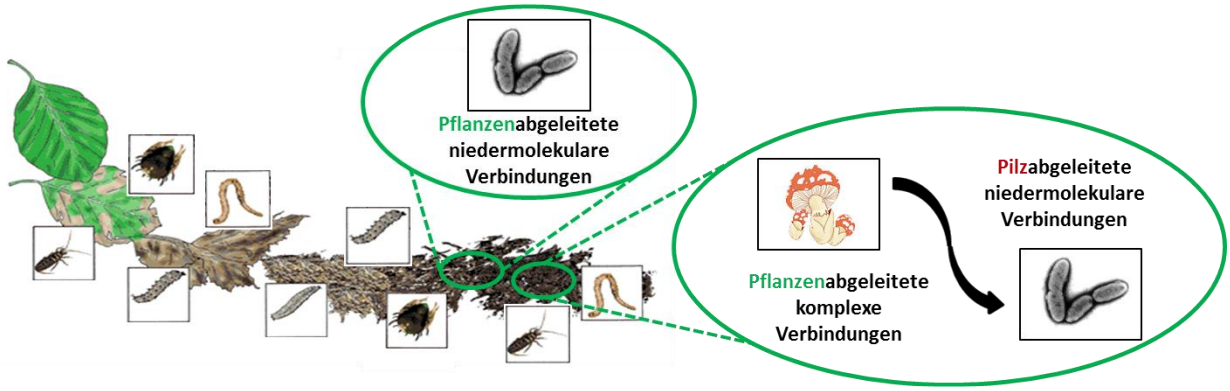

Abbildung 9: Überarbeitetes Modell der Dekomposition von Pflanzen durch Bodenmikroorganismen nach Schmidt, 1989. Die Pflanze wird von der Mikro-, Meso- und Makrofauna zerkleinert. Anschließend werden die pflanzenabgeleiteten einfachen Verbindungen von Bakterien metabolisiert. Gleichzeitig bauen die Pilze die pflanzenabgeleiteten komplexen Verbindungen wie Cellulose und Lignin zu einfachen Verbindungen ab, die letztlich von den Bakterien genutzt werden.

Die aus Artikel 3.3 ermittelten Abundanzen im 16S und 18S rDNA Genomprofil, im Metaproteom und im Protein-SIP verdeutlichen, dass sowohl die genomische als auch die proteomische Abundanz keinen Zusammenhang mit der Aktivität aufwiesen (siehe **Tabelle 2.3**). Generell wird der Phänotyp eines Organismus in absteigender Reihenfolge durch Protein-SIP, dem Proteom und dem Genom beschrieben. Hohe Aktivität bezüglich einer eingebrachten Energie- oder Nährstoffquelle resultiert in einer hohen Abundanz im Protein-SIP. Gegensätzlich zeigt eine niedrige Aktivität im Protein-SIP und eine hohe Aktivität im Proteom und Genom die präferierte Nutzung anderer Energie- und Nährstoffquellen. Chroococcales, Enterobacteriales und Saccharomycetales zeigten eine geringe Genom- und Proteomabundanz, aber eine hohe N-Einbauaktivität, dass auf eine hohe Affinität zu den Stickstoffverbindungen der eingebrachten Quelle hindeutet, aber gleichermaßen auch verdeutlicht, dass diese Phylotypen vermutlich nicht am routinemäßigen Stoffwechsel im Boden beteiligt sind. Andererseits wurde den Pseudomonadales eine hohe Genom- sowie Proteomabundanz und eine geringe Aktivität im Protein-SIP zugeordnet. Dieser Phylotyp ist prävalent im Boden, aber wurde durch copiotrophe Organismen wie den Rhizobiales, den Actinomycetales und den Chroococcales bezüglich der Stickstoffquellen aus dem Pflanzenmaterial auskonkurriert. Außerdem war die genomische und proteomische Abundanz für Sphingomonadales und Xanthomonadales nicht miteinander vergleichbar. Dabei wurde für beide Phylotypen jeweils eine höhere Abundanz im Genomprofil und nur eine geringe Abundanz im Metaproteom gefunden. Die genomische Abundanz spiegelt die generelle Beteiligung am Pflanzenabbau wieder, wobei diese Phylotypen im Phänotyp (Metaproteom,

Protein-SIP) durch die copiotrophen Organismen verdrängt wurden. Demnach könnten Sphingomonadales und Xanthomonadales komplexe Verbindungen im Boden abbauen. In dieser Studie wurden alle bisher annotierten Proteine von Bakterien und Pilzen als Datenbank genutzt. Dieser große Suchraum sollte und muss in weiteren Versuchen durch eine Sequenzierung verkleinert werden, um einerseits die Identifikationsrate zu erhöhen und andererseits die Annotationsgenauigkeit zu verbessern, wodurch die metaproteomischen Daten präziser werden. Durch die Verwendung von multiOMIK Techniken können methodenspezifische Probleme wie die teilweise schlechte Identifikationsrate in der Metaproteomik und des Protein-SIPs durch eine zuvorige Sequenzierung vermieden werden. Trotzdessen wurde gezeigt, dass zwischen Genom, Proteom und spezifischer Aktivität im Protein-SIP kein direkter Zusammenhang besteht, aber durch die Kombination aller Daten können verschiedene Mikroorganismen in einer Gemeinschaft anhand ihrer multidimensionalen Eigenschaften (copiotroph und oligotroph) gruppiert werden.

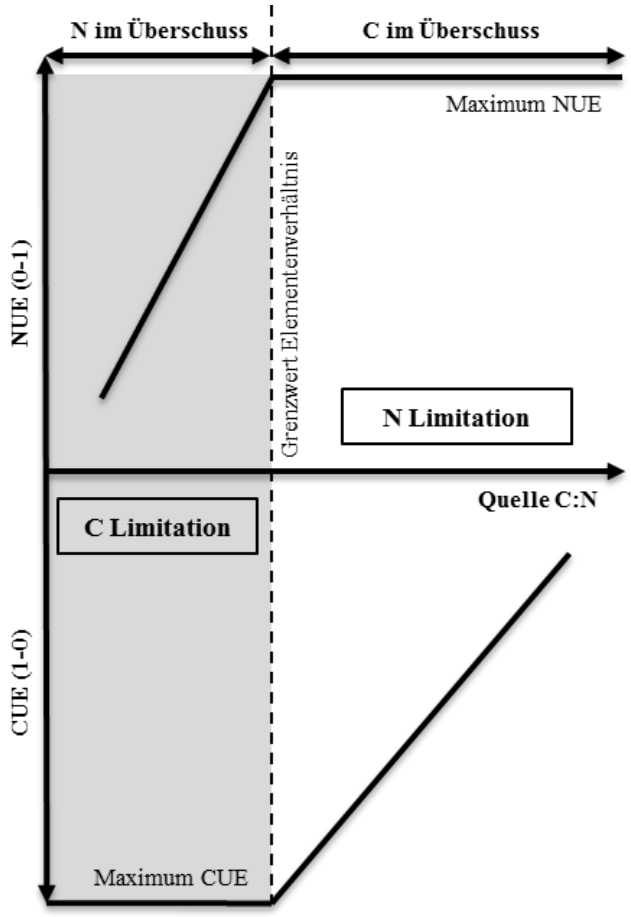

Abbildung 10: Der Zusammenhang von Energie- (C) und Nährstoff-stoffwechsel (N) nach Mooshammer, 2014 (50). NUE steht für die Nährstoffaufnahmeeffektivität und CUE für die Kohlenstoffaufnahmeeffektivität. Bei einer Kohlenstofflimitation wird der komplette Kohlenstoff in die Biomasse eingebaut, während Stickstoff im Überfluss vorhanden ist und auch oxidiert werden kann. Vice versa wird bei einer Stickstofflimitation der komplette Stickstoff in die Biomasse eingebaut, während der Kohlenstoff im Überfluss auch oxidiert werden kann.

Außerdem sollten in Zukunft multiatomare SIP-Ansätze verwendet werden, um beispielsweise das Zusammenspiel zwischen Energie- (C) und Nährstoffflüssen (N) aufzuzeigen. Es wurde durch Mooshammer und Kollegen postuliert, dass sich der Kohlenstoff- und Stickstoffkreislauf konträr verhalten (50). Daraus abgeleitet ergibt sich folgender theoretischer Zusammenhang zwischen Kohlenstoff und Stickstoff: Bei einer Limitation wird die komplette Ressource assimiliert, um Verluste zu vermeiden. Im Gegensatz dazu können überschüssige Ressourcen zur Energiegewinnung oxidiert werden (**Abbildung 10**). Ein konträres Verhältnis der Kohlenstoff- und Stickstoffassimilation könnte bedeuten, dass verschiedene Mikroorganismen an der Assimilation von Energie- (C) und Nährstoffquellen (N) beteiligt sind. Zudem müssten in einem multiatomaren Ansatz jegliche Limitationszustände vermieden werden, um eine vergleichbare Nährstoff- (NUE) und Kohlenstoffaufnahmeeffektivität (CUE) zu gewährleisten. Letztlich müsste die Assimilation einer Energie- oder Nährstoffquelle nicht als allgemeine, sondern als spezifische Aktivität angesehen werden. Eine generelle Aktivität könnte durch den Einsatz von nicht zu verstoffwechselndem, schweren Wasser beschrieben werden.

4.4. Abschließende Bemerkungen

Die funktionale Metaproteomik ist in der Lage, die primären, sekundären und tertiären Interaktionen von Schlüsselorganismen mikrobieller Gemeinschaften aufzudecken. Dabei können die in Proteinen vorkommenden Atome (C, N, S, O und H) als Isotope verwendet werden, wobei bevorzugt ^{13}C und ^{15}N genutzt werden. Es wurde gezeigt, dass die Energie- beziehungsweise Nährstoffquelle als einzelne Verbindungen wie Acetat (**Artikel 3.2**) aber auch als komplette Pflanzen (**Artikel 3.3**) vorgelegt werden können, um den Einbau der stabilen Isotope in metabolisch aktive Mikroorganismen zu zeigen. Weiterhin wurde demonstriert, dass sowohl die Mikroorganismen, die am Energiefluss (^{13}C) als auch die, die am Nährstoffffluss (^{15}N) beteiligt sind, spezifisch aus einer mikrobiellen Gemeinschaft identifiziert werden können. Fraglich bleibt, inwiefern sich verschiedene, stabile Isotope auf die Aktivität von Mikroorganismen in Gemeinschaften auswirken und gleichbedeutend, ob der Einbau verschiedener Isotope bezüglich des Ausmaßes und der aktiven Spezies vergleichbar ist. In früheren Studien wurde gezeigt, dass die *multi-isotope imaging mass spectometry* (MIMS) den Einbau verschiedener, stabiler Isotope wie ^{13}C, ^{15}N und ^{18}O in Proteinen von Stereozilien der Haarzellen und Dendriten nachverfolgen kann (282, 283). Inwieweit dieser Einbau mit der mikrobieller Aktivität vergleichbar ist, muss in weiteren Studien untersucht werden. Nichtsdestotrotz stellt vor allem die Verwendung von schwerem Wasser (D_2O oder $H_2{}^{18}O$) als

universeller Marker für eine generelle, mikrobielle Aktivität eine systemunabhängige Lösung dar. Bei der Anwendung von schwerem Wasser ist zu beachten, dass sich der Einbau von Wasserstoff und Sauerstoff grundlegend unterscheidet. ^{18}O wird biotisch über α-Ketoglutarat und Oxalacetat aus dem Citratzyklus in die Aminosäuren und folgend in die Proteine eingebaut (284), während D abiotisch über den durch Kaj Ulrik Linderstrøm-Lang bekannten HD-Austausch in die Proteine gelangt (285). Hinzu kommt, dass der Einbau von schweren Isotopen zu einem chromatographischen Änderung führt, der in einer früheren Elution des schweren Isotopomers resultiert (286). Die masseabhängige Änderung der Elutionszeit ist bei Wasserstoff aufgrund der doppelten Masse von D im Vergleich zu H besonders gravierend, wodurch bisher bevorzugt andere stabile Isotope in der Proteomik wurden (287). Die daraus resultierende, unterschiedliche Elutionszeit von markiertem und unmarkiertem Peptid führt dazu, dass die Zuordnung des Einbaumusters zu seiner monoisotopischen Spitze nicht im gleichen Chromatogramm erfolgen kann (siehe **Abbildung 5**) und demnach artifiziell zusammengefügt werden muss. Trotzallem zeichnet sich deuteriertes Wasser durch geringe Kosten aus (1:100 im Vergleich zu $H_2{}^{18}O$), was vor allem bei Versuchen im Bereich großer Volumina, wie beispielsweise Reaktoren, eine entscheidende Rolle spielen kann.

Allgemein beschreibt die funktionale Metaproteomik die Aktivität von Schlüsselorganismen aus komplexen, mikrobiellen Gemeinschaft. Dennoch wird lediglich ein aktiver Einbau einer vorgelegten, markierten Energie- oder Nährstoffquelle in das Proteom gezeigt. Ob ein identifiziertes und damit abundantes Protein auch enzymatisch aktiv ist, kann durch beispielsweise spektrometrische oder kalorimetrische Enzymassays nachgewiesen werden (288). Wechselnde Umweltbedingungen erfordern die Regulation und die Kontrolle der Enzymaktivität, um die Homöostase aufrecht zu erhalten. Die Aufrechterhaltung kann dabei durch verschiedene Anpassungsmechanismen erreicht werden. Eine schnelle Antwort ist beispielsweise die kompetetive Produkthemmung, wobei die Anhäufung des Reaktionsprodukts die Hinreaktion hemmt und die Rückreaktion fördert (289). Eine langfristige Anpassungsmaßnahme ist beispielsweise die genetische Regulation, während mittelfristige Maßnahmen kovalente Modifikationen wie beispielsweise Phosphorylierung (290-293) und Acetylierung (294, 295) darstellen. Die Acetylierung umfasst den Transfer einer Acetylgruppe an den N-Terminus des Proteins (N_α-Acetylierung) oder an den Seitenketten der Aminosäuren Lysin (N_ε-Acetylierung), Serin und Threonin (O-Acetylierung) (296). Bisher wurden nur wenige Proteomikstudieren zur N_α-Acetylierung publiziert (297, 298) und der O/N-Acyltransfer erschwert die Untersuchung der O-Acetylierung, weswegen der reversiblen und

dynamischen, posttranslationalen Modifikation der Nε-Acetylierung (LysAc) durch Lysinacetyltransferasen (KATs) und Lysindehydrogenasen (KDACs) eine besondere Bedeutung zukommt (299, 300). Die direkte Verbindung zwischen LysAc und dem Metabolismus wurde anhand der reversiblen Acetylierung als An-Aus-Schalter der Acetyl-CoA Synthetase (ACS) in *Salmonella enterica* gezeigt, wobei die Acetylierung oder Deacetylierung von Lys_{609} im aktiven Zentrum zur Inaktivierung oder Aktivierung führt (301). Zusammenfassend beschreibt das Proteom den Ist-Zustand der aktiven Zelle, in der Proteine aktiv umgebaut, abgebaut und synthetisiert werden müssen, um die Homöostase gegenüber wechselnder Umweltbedingungen aufrechtzuhalten und hebt sich dadurch entscheident von der Genomik und der Transkriptomik ab.

5. Literaturverzeichnis

1. **Glansdorff N, Xu Y, Labedan B.** 2008. The last universal common ancestor: emergence, constitution and genetic legacy of an elusive forerunner. Biology direct **3:**29.
2. **Mancini SA, Devine CE, Elsner M, Nandi ME, Ulrich AC, Edwards EA, Lollar BS.** 2008. Isotopic evidence suggests different initial reaction mechanisms for anaerobic benzene biodegradation. Environmental science & technology **42:**8290-8296.
3. **Woese C.** 1998. The universal ancestor. Proceedings of the National Academy of Sciences of the United States of America **95:**6854-6859.
4. **Goldblatt C, Lenton TM, Watson AJ.** 2006. Bistability of atmospheric oxygen and the Great Oxidation. Nature **443:**683-686.
5. **Dupraz C, Visscher PT.** 2005. Microbial lithification in marine stromatolites and hypersaline mats. Trends in microbiology **13:**429-438.
6. **Ehrlich HL.** 1998. Geomicrobiology: its significance for geology. Earth-Sci Rev **45:**45-60.
7. **Whitman WB, Coleman DC, Wiebe WJ.** 1998. Prokaryotes: The unseen majority. Proceedings of the National Academy of Sciences of the United States of America **95:**6578-6583.
8. **Madsen EL.** 2011. Microorganisms and their roles in fundamental biogeochemical cycles. Current Opinion Biotechnology **22:**456-464.
9. **Gadd GM.** 2010. Metals, minerals and microbes: geomicrobiology and bioremediation. Microbiology-Sgm **156:**609-643.
10. **Udwary DW, Gontang EA, Jones AC, Jones CS, Schultz AW, Winter JM, Yang JY, Beauchemin N, Capson TL, Clark BR, Esquenazi E, Eustaquio AS, Freel K, Gerwick L, Gerwick WH, Gonzalez D, Liu WT, Malloy KL, Maloney KN, Nett M, Nunnery JK, Penn K, Prieto-Davo A, Simmons TL, Weitz S, Wilson MC, Tisa LS, Dorrestein PC, Moore BS.** 2011. Significant natural product biosynthetic potential of actinorhizal symbionts of the genus frankia, as revealed by comparative genomic and proteomic analyses. Applied and environmental microbiology **77:**3617-3625.
11. **Yokota K, Hayashi M.** 2011. Function and evolution of nodulation genes in legumes. Cellular and molecular life sciences : CMLS **68:**1341-1351.
12. **Wong LJ, H'Ng P S, Wong SY, Lee SH, Lum WC, Chai EW, Wong WZ, Chin KL.** 2014. Termite digestomes as a potential source of symbiotic microbiota for lignocelluloses degradation: a review. Pakistan journal of biological sciences : PJBS **17:**956-963.
13. **Habe H, Omori T.** 2003. Genetics of polycyclic aromatic hydrocarbon metabolism in diverse aerobic bacteria. Bioscience, biotechnology, and biochemistry **67:**225-243.
14. **Scheffer FS, P. .** 2002. Lehrbuch der Bodenkunde. Spektrum Akademischer Verlag.
15. **Skidmore M, Anderson SP, Sharp M, Foght J, Lanoil BD.** 2005. Comparison of microbial community compositions of two subglacial environments reveals a possible role for microbes in chemical weathering processes. Applied and environmental microbiology **71:**6986-6997.
16. **Amend JP, Teske A.** 2005. Expanding frontiers in deep subsurface microbiology. Palaeogeography, Palaeoclimatology, Palaeoecology. **219:**131-155.
17. **Jorgensen BB.** 2011. Deep subseafloor microbial cells on physiological standby. Proceedings of the National Academy of Sciences of the United States of America **108:**18193-18194.
18. **Niemann H, Losekann T, de Beer D, Elvert M, Nadalig T, Knittel K, Amann R, Sauter EJ, Schluter M, Klages M, Foucher JP, Boetius A.** 2006. Novel microbial communities of the Haakon Mosby mud volcano and their role as a methane sink. Nature **443:**854-858.

19. **Rozanov AS, Bryanskaya AV, Malup TK, Meshcheryakova IA, Lazareva EV, Taran OP, Ivanisenko TV, Ivanisenko VA, Zhmodik SM, Kolchanov NA, Peltek SE.** 2014. Molecular analysis of the benthos microbial community in Zavarzin thermal spring (Uzon Caldera, Kamchatka, Russia). BMC genomics **15 Suppl 12:**S12.
20. **Ottow JCG.** 2012. Mikrobiologie von Böden. Biodiversität, Ökophysiologie und Metagenomik. Springer Verlag Berlin**:**56.
21. **Mancini SA, Ulrich AC, Lacrampe-Couloume G, Sleep B, Edwards EA, Lollar BS.** 2003. Carbon and hydrogen isotopic fractionation during anaerobic biodegradation of benzene. Applied and environmental microbiology **69:**191-198.
22. **Dean BJ.** 1985. Recent findings on the genetic toxicology of benzene, toluene, xylenes and phenols. Mutation research **154:**153-181.
23. **Snyder R.** 2000. Overview of the toxicology of benzene. Journal of toxicology and environmental health. Part A **61:**339-346.
24. **Christensen TH, Kjeldsen P, Albrechtsen HJ, Heron G, Nielsen PH, Bjerg PL, Holm PE.** 1994. Attenuation of Landfill Leachate Pollutants in Aquifers. Critical Reviews in Environmental Science and Technology. **24:**119-202.
25. **Christensen TH, Kjeldsen P, Bjerg PL, Jensen DL, Christensen JB, Baun A, Albrechtsen HJ, Heron C.** 2001. Biogeochemistry of landfill leachate plumes. Appl Geochem **16:**659-718.
26. **Grbic-Galic D, Vogel TM.** 1987. Transformation of toluene and benzene by mixed methanogenic cultures. Applied and environmental microbiology **53:**254-260.
27. **Harwood CS, Gibson J.** 1997. Shedding light on anaerobic benzene ring degradation: a process unique to prokaryotes? Journal of bacteriology **179:**301-309.
28. **Major DW, Mayfield CI, Barker JF.** 1988. Biotransformation of Benzene by Denitrification in Aquifer Sand. Ground Water **26:**8-14.
29. **Kunapuli U, Griebler C, Beller HR, Meckenstock RU.** 2008. Identification of intermediates formed during anaerobic benzene degradation by an iron-reducing enrichment culture. Environmental microbiology **10:**1703-1712.
30. **Ulrich AC, Beller HR, Edwards EA.** 2005. Metabolites detected during biodegradation of 13C6-benzene in nitrate-reducing and methanogenic enrichment cultures. Environmental science & technology **39:**6681-6691.
31. **Fischer A, Gehre M, Breitfeld J, Richnow HH, Vogt C.** 2009. Carbon and hydrogen isotope fractionation of benzene during biodegradation under sulfate-reducing conditions: a laboratory to field site approach. Rapid communications in mass spectrometry : RCM **23:**2439-2447.
32. **Herrmann S, Kleinsteuber S, Chatzinotas A, Kuppardt S, Lueders T, Richnow HH, Vogt C.** 2010. Functional characterization of an anaerobic benzene-degrading enrichment culture by DNA stable isotope probing. Environmental microbiology **12:**401-411.
33. **Kleinsteuber S, Schleinitz KM, Breitfeld J, Harms H, Richnow HH, Vogt C.** 2008. Molecular characterization of bacterial communities mineralizing benzene under sulfate-reducing conditions. FEMS microbiology ecology **66:**143-157.
34. **Rakoczy J, Schleinitz KM, Müller N, Richnow HH, Vogt C.** 2011. Effects of hydrogen and acetate on benzene mineralisation under sulphate-reducing conditions. FEMS microbiology ecology **77:**238-247.
35. **Taubert M, Vogt C, Wubet T, Kleinsteuber S, Tarkka MT, Harms H, Buscot F, Richnow HH, von Bergen M, Seifert J.** 2012. Protein-SIP enables time-resolved analysis of the carbon flux in a sulfate-reducing, benzene-degrading microbial consortium. Isme J **6:**2291-2301.
36. **Campbell BJ, Engel AS, Porter ML, Takai K.** 2006. The versatile epsilon-proteobacteria: key players in sulphidic habitats. Nature reviews Microbiology **4:**458-468.

37. **Nakagawa S, Takai K.** 2008. Deep-sea vent chemoautotrophs: diversity, biochemistry and ecological significance. FEMS microbiology ecology **65:**1-14.
38. **Takai K, Gamo T, Tsunogai U, Nakayama N, Hirayama H, Nealson KH, Horikoshi K.** 2004. Geochemical and microbiological evidence for a hydrogen-based, hyperthermophilic subsurface lithoautotrophic microbial ecosystem (HyperSLiME) beneath an active deep-sea hydrothermal field. Extremophiles : life under extreme conditions **8:**269-282.
39. **Hamilton TL, Jones DS, Schaperdoth I, Macalady JL.** 2014. Metagenomic insights into S(0) precipitation in a terrestrial subsurface lithoautotrophic ecosystem. Frontiers in microbiology **5:**756.
40. **Jones DS, Tobler DJ, Schaperdoth I, Mainiero M, Macalady JL.** 2010. Community structure of subsurface biofilms in the thermal sulfidic caves ofAcquasanta Terme, Italy. Applied and environmental microbiology **76:**5902-5910.
41. **Porter ML, Engel AS.** 2008. Diversity of uncultured Epsilonproteobacteria from terrestrial sulfidic caves and springs. Applied and environmental microbiology **74:**4973-4977.
42. **Handley KM, VerBerkmoes NC, Steefel CI, Williams KH, Sharon I, Miller CS, Frischkorn KR, Chourey K, Thomas BC, Shah MB, Long PE, Hettich RL, Banfield JF.** 2013. Biostimulation induces syntrophic interactions that impact C, S and N cycling in a sediment microbial community. The ISME journal **7:**800-816.
43. **Torsvik V, Ovreas L, Thingstad TF.** 2002. Prokaryotic diversity--magnitude, dynamics, and controlling factors. Science **296:**1064-1066.
44. **Zhang Q, Zak JC.** 1998. Potential physiological activities of fungi and bacteria in relation to plant litter decomposition along a gap size gradient in a natural subtropical forest. Microbial Ecology **35:**172-179.
45. **Jones DL, Healey JR, Willett VB, Farrar JF, Hodge A.** 2005. Dissolved organic nitrogen uptake by plants - an important N uptake pathway? Soil Biol Biochem **37:**413-423.
46. **Jones DL, Hodge A.** 1999. Biodegradation kinetics and sorption reactions of three differently charged amino acids in soil and their effects on plant organic nitrogen availability. Soil Biology & Biochemistry **31:**1331-1342.
47. **Jan MT, Roberts P, Tonheim SK, Jones DL.** 2009. Protein breakdown represents a major bottleneck in nitrogen cycling in grassland soils. Soil Biology & Biochemistry **41:**2272-2282.
48. **Mooshammer M, Wanek W, Schnecker J, Wild B, Leitner S, Hofhansl F, Blochl A, Hammerle I, Frank AH, Fuchslueger L, Keiblinger KM, Zechmeister-Boltenstern S, Richter A.** 2012. Stoichiometric controls of nitrogen and phosphorus cycling in decomposing beech leaf litter. Ecology **93:**770-782.
49. **Schimel JP, Bennett J.** 2004. Nitrogen mineralization: Challenges of a changing paradigm. Ecology **85:**591-602.
50. **Mooshammer M, Wanek W, Hammerle I, Fuchslueger L, Hofhansl F, Knoltsch A, Schnecker J, Takriti M, Watzka M, Wild B, Keiblinger KM, Zechmeister-Boltenstern S, Richter A.** 2014. Adjustment of microbial nitrogen use efficiency to carbon:nitrogen imbalances regulates soil nitrogen cycling. Nature communications **5:**3694.
51. **Bothe H, Jost G, Schloter M, Ward BB, Witzel K.** 2000. Molecular analysis of ammonia oxidation and denitrification in natural environments. FEMS microbiology reviews **24:**673-690.
52. **Leininger S, Urich T, Schloter M, Schwark L, Qi J, Nicol GW, Prosser JI, Schuster SC, Schleper C.** 2006. Archaea predominate among ammonia-oxidizing prokaryotes in soils. Nature **442:**806-809.
53. **Rinnan R, Baath E.** 2009. Differential utilization of carbon substrates by bacteria and fungi in tundra soil. Applied and environmental microbiology **75:**3611-3620.

54. **Torres IF, Bastida F, Hernandez T, Bombach P, Richnow HH, Garcia C.** 2014. The role of lignin and cellulose in the carbon-cycling of degraded soils under semiarid climate and their relation to microbial biomass. Soil Biology & Biochemistry **75:**152-160.
55. **Waldrop MP, Firestone MK.** 2004. Microbial community utilization of recalcitrant and simple carbon compounds: impact of oak-woodland plant communities. Oecologia **138:**275-284.
56. **Hannula SE, Boschker HT, de Boer W, van Veen JA.** 2012. 13C pulse-labeling assessment of the community structure of active fungi in the rhizosphere of a genetically starch-modified potato (Solanum tuberosum) cultivar and its parental isoline. The New phytologist **194:**784-799.
57. **Bengtsson G.** 1992. Interactions between Fungi, Bacteria and Beech Leaves in a Stream Microcosm. Oecologia **89:**542-549.
58. **Meidute S, Demoling F, Baath E.** 2008. Antagonistic and synergistic effects of fungal and bacterial growth in soil after adding different carbon and nitrogen sources. Soil Biology & Biochemistry **40:**2334-2343.
59. **Moller J, Miller M, Kjoller A.** 1999. Fungal-bacterial interaction on beech leaves: influence on decomposition and dissolved organic carbon quality. Soil Biology & Biochemistry **31:**367-374.
60. **Romani AM, Fischer H, Mille-Lindblom C, Tranvik LJ.** 2006. Interactions of bacteria and fungi on decomposing litter: Differential extracellular enzyme activities. Ecology **87:**2559-2569.
61. **Wohl DL, McArthur JV.** 2001. Aquatic actinomycete-fungal interactions and their effects on organic matter decomposition: A microcosm study. Microbial Ecology **42:**446-457.
62. **Velicer GJ.** 2003. Social strife in the microbial world. Trends in microbiology **11:**330-337.
63. **Espana M, Rasche F, Kandeler E, Brune T, Rodriguez B, Bending GD, Cadisch G.** 2011. Assessing the effect of organic residue quality on active decomposing fungi in a tropical Vertisol using N-15-DNA stable isotope probing. Fungal Ecology **4:**115-119.
64. **Espana M, Rasche F, Kandeler E, Brune T, Rodriguez B, Bending GD, Cadisch G.** 2011. Identification of active bacteria involved in decomposition of complex maize and soybean residues in a tropical Vertisol using N-15-DNA stable isotope probing. Pedobiologia **54:**187-193.
65. **Crick F.** 1970. Central Dogma of Molecular Biology. Nature **227:**561-&.
66. **Gygi SP, Rochon Y, Franza BR, Aebersold R.** 1999. Correlation between protein and mRNA abundance in yeast. Molecular and Cellular Biology **19:**1720-1730.
67. **Maier T, Guell M, Serrano L.** 2009. Correlation of mRNA and protein in complex biological samples. Febs Lett **583:**3966-3973.
68. **Vogel C, Marcotte EM.** 2012. Insights into the regulation of protein abundance from proteomic and transcriptomic analyses. Nature Reviews Genetics **13:**227-232.
69. **Boschker HTS, Nold SC, Wellsbury P, Bos D, de Graaf W, Pel R, Parkes RJ, Cappenberg TE.** 1998. Direct linking of microbial populations to specific biogeochemical processes by C-13-labelling of biomarkers. Nature **392:**801-805.
70. **Neufeld JD, Dumont MG, Vohra J, Murrell JC.** 2007. Methodological considerations for the use of stable isotope probing in microbial ecology. Microb Ecology **53:**435-442.
71. **Dumont MG, Murrell JC.** 2005. Stable isotope probing - linking microbial identity to function. Nature reviews. Microbiology **3:**499-504.
72. **Bastida F, Jechalke S, Bombach P, Franchini AG, Seifert J, von Bergen M, Vogt C, Richnow HH.** 2011. Assimilation of benzene carbon through multiple trophic levels traced by different stable isotope probing methodologies. FEMS microbiology ecology **77:**357-369.

73. **Jehmlich N, Schmidt F, Hartwich M, von Bergen M, Richnow HH, Vogt C.** 2008. Incorporation of carbon and nitrogen atoms into proteins measured by protein-based stable isotope probing (Protein-SIP). Rapid communications in mass spectrometry : RCM **22:**2889-2897.
74. **Bombach P, Richnow HH, Kastner M, Fischer A.** 2010. Current approaches for the assessment of in situ biodegradation. Applied microbiology and biotechnology **86:**839-852.
75. **Wang Y, Chen Y, Zhou Q, Huang S, Ning K, Xu J, Kalin RM, Rolfe S, Huang WE.** 2012. A culture-independent approach to unravel uncultured bacteria and functional genes in a complex microbial community. PloS one **7:**e47530.
76. **Radajewski S, Ineson P, Parekh NR, Murrell JC.** 2000. Stable-isotope probing as a tool in microbial ecology. Nature **403:**646-649.
77. **Taubert M, von Bergen M, Seifert J.** 2013. Limitations in detection of 15N incorporation by mass spectrometry in protein-based stable isotope probing (protein-SIP). Analytical and bioanalytical chemistry **405:**3989-3996.
78. **Taubert M, Baumann S, von Bergen M, Seifert J.** 2011. Exploring the limits of robust detection of incorporation of 13C by mass spectrometry in protein-based stable isotope probing (protein-SIP). Analytical and bioanalytical chemistry **401:**1975-1982.
79. **Seifert J, Taubert M, Jehmlich N, Schmidt F, Volker U, Vogt C, Richnow HH, von Bergen M.** 2012. Protein-based stable isotope probing (protein-SIP) in functional metaproteomics. Mass spectrometry reviews **31:**683-697.
80. **Bruice PY.** 2004. Organic Chemistry. Pearson Education Inc **4:**960-962.
81. **Jehmlich N, Vogt C, Lunsmann V, Richnow HH, von Bergen M.** 2016. Protein-SIP in environmental studies. Current opinion in biotechnology **41:**26-33.
82. **Bleck-Neuhaus J.** 2013. Elementare Teilchen. Springer.
83. **Clark I, Fritz P.** 1997. Environmental tracers in subsurface hydrology. Kluwer, Boston, MA.
84. **Chen Y, Dumont MG, McNamara NP, Chamberlain PM, Bodrossy L, Stralis-Pavese N, Murrell JC.** 2008. Diversity of the active methanotrophic community in acidic peatlands as assessed by mRNA and SIP-PLFA analyses. Environmental microbiology **10:**446-459.
85. **Eyice O, Namura M, Chen Y, Mead A, Samavedam S, Schafer H.** 2015. SIP metagenomics identifies uncultivated Methylophilaceae as dimethylsulphide degrading bacteria in soil and lake sediment. The ISME journal.
86. **Jehmlich N, Schmidt F, von Bergen M, Richnow HH, Vogt C.** 2008. Protein-based stable isotope probing (Protein-SIP) reveals active species within anoxic mixed cultures. Isme J **2:**1122-1133.
87. **Herbst FA, Bahr A, Duarte M, Pieper DH, Richnow HH, von Bergen M, Seifert J, Bombach P.** 2013. Elucidation of in situ polycyclic aromatic hydrocarbon degradation by functional metaproteomics (protein-SIP). Proteomics **13:**2910-2920.
88. **Rettedal EA, Brozel VS.** 2015. Characterizing the diversity of active bacteria in soil by comprehensive stable isotope probing of DNA and RNA with H O. MicrobiologyOpen.
89. **Frieden E.** 1972. The chemical elements of life. Scientific American **227:**52-60.
90. **Herbst FA, Taubert M, Jehmlich N, Behr T, Schmidt F, von Bergen M, Seifert J.** 2013. Sulfur-34S stable isotope labeling of amino acids for quantification (SULAQ34) of proteomic changes in Pseudomonas fluorescens during naphthalene degradation. Molecular & cellular proteomics : MCP **12:**2060-2069.
91. **Benjamin DR, Robinson CV, Hendrick JP, Hartl FU, Dobson CM.** 1998. Mass spectrometry of ribosomes and ribosomal subunits. Proceedings of the National Academy of Sciences of the United States of America **95:**7391-7395.

92. **Berry D, Mader E, Lee TK, Woebken D, Wang Y, Zhu D, Palatinszky M, Schintlmeister A, Schmid MC, Hanson BT, Shterzer N, Mizrahi I, Rauch I, Decker T, Bocklitz T, Popp J, Gibson CM, Fowler PW, Huang WE, Wagner M.** 2015. Tracking heavy water (D2O) incorporation for identifying and sorting active microbial cells. Proceedings of the National Academy of Sciences of the United States of America **112:**E194-203.
93. **Bensimon A, Heck AJ, Aebersold R.** 2012. Mass spectrometry-based proteomics and network biology. Annual review of biochemistry **81:**379-405.
94. **Blackstock WP, Weir MP.** 1999. Proteomics: quantitative and physical mapping of cellular proteins. Trends in biotechnology **17:**121-127.
95. **Lawrance IC, Klopcic B, Wasinger VC.** 2005. Proteomics: an overview. Inflammatory bowel diseases **11:**927-936.
96. **Li Z, Wang Y, Yao Q, Justice NB, Ahn TH, Xu D, Hettich RL, Banfield JF, Pan C.** 2014. Diverse and divergent protein post-translational modifications in two growth stages of a natural microbial community. Nature communications **5:**4405.
97. **Olsen JV, Mann M.** 2013. Status of Large-scale Analysis of Post-translational Modifications by Mass Spectrometry. Molecular & Cellular Proteomics **12:**3444-3452.
98. **Bastida F, Moreno JL, Nicolas C, Hernandez T, Garcia C.** 2009. Soil metaproteomics: a review of an emerging environmental science. Significance, methodology and perspectives. European Journal of Soil Science. **60:**845-859.
99. **Bastida F, Rosell M, Franchini AG, Seifert J, Finsterbusch S, Jehmlich N, Jechalke S, von Bergen M, Richnow HH.** 2010. Elucidating MTBE degradation in a mixed consortium using a multidisciplinary approach. FEMS microbiology ecology **73:**370-384.
100. **Jehmlich N, Schmidt F, Taubert M, Seifert J, Bastida F, von Bergen M, Richnow HH, Vogt C.** 2010. Protein-based stable isotope probing. Nature protocols **5:**1957-1966.
101. **von Bergen M, Jehmlich N, Taubert M, Vogt C, Bastida F, Herbst FA, Schmidt F, Richnow HH, Seifert J.** 2013. Insights from quantitative metaproteomics and protein-stable isotope probing into microbial ecology. The ISME Journal **7:**1877-1885.
102. **Boll M, Fuchs G.** 1995. Benzoyl-coenzyme A reductase (dearomatizing), a key enzyme of anaerobic aromatic metabolism. ATP dependence of the reaction, purification and some properties of the enzyme from Thauera aromatica strain K172. European journal of biochemistry **234:**921-933.
103. **Anders HJ, Kaetzke A, Kampfer P, Ludwig W, Fuchs G.** 1995. Taxonomic position of aromatic-degrading denitrifying pseudomonad strains K 172 and KB 740 and their description as new members of the genera Thauera, as Thauera aromatica sp. nov., and Azoarcus, as Azoarcus evansii sp. nov., respectively, members of the beta subclass of the Proteobacteria. International journal of systematic bacteriology **45:**327-333.
104. **Sachsenberg T, Herbst FA, Taubert M, Kermer R, Jehmlich N, von Bergen M, Seifert J, Kohlbacher O.** 2014. MetaProSIP: Automated Inference of Stable Isotope Incorporation Rates in Proteins for Functional Metaproteomics. Journal of proteome research.
105. **Wilson MH, Holman TJ, Sorensen I, Cancho-Sanchez E, Wells DM, Swarup R, Knox JP, Willats WG, Ubeda-Tomas S, Holdsworth M, Bennett MJ, Vissenberg K, Hodgman TC.** 2015. Multi-omics analysis identifies genes mediating the extension of cell walls in the Arabidopsis thaliana root elongation zone. Frontiers in cell and developmental biology **3:**10.
106. **Hultman J, Waldrop MP, Mackelprang R, David MM, McFarland J, Blazewicz SJ, Harden J, Turetsky MR, McGuire AD, Shah MB, VerBerkmoes NC, Lee LH, Mavrommatis K, Jansson JK.** 2015. Multi-omics of permafrost, active layer and thermokarst bog soil microbiomes. Nature **521:**208-212.

107. **Wu Z, Sahin O, Shen Z, Liu P, Miller WG, Zhang Q.** 2013. Multi-omics approaches to deciphering a hypervirulent strain of Campylobacter jejuni. Genome biology and evolution **5:**2217-2230.
108. **Yoon SH, Han MJ, Jeong H, Lee CH, Xia XX, Lee DH, Shim JH, Lee SY, Oh TK, Kim JF.** 2012. Comparative multi-omics systems analysis of Escherichia coli strains B and K-12. Genome biology **13:**R37.
109. **Engberg J, On SLW, Harrington CS, Gerner-Smidt P.** 2000. Prevalence of Campylobacter, Arcobacter, Helicobacter, and Sutterella spp. in human fecal samples as estimated by a reevaluation of isolation methods for Campylobacters. Journal of Clinical Microbiology **38:**286-291.
110. **Wolin MJ, Wolin EA, Jacobs NJ.** 1961. Cytochrome-Producing Anaerobic Vibrio, Vibrio Succinogenes, Sp N. Journal of bacteriology **81:**911-&.
111. **Brettar I, Labrenz M, Flavier S, Botel J, Kuosa H, Christen R, Hofle MG.** 2006. Identification of a Thiomicrospira denitrificans-like epsilonproteobacterium as a catalyst for autotrophic denitrification in the central Baltic Sea. Applied and environmental Microbiology **72:**1364-1372.
112. **Inagaki F, Takai K, Hideki KI, Nealson KH, Horikishi K.** 2003. Sulfurimonas autotrophica gen. nov., sp nov., a novel sulfur-oxidizing epsilon-proteobacterium isolated from hydrothermal sediments in the Mid-Okinawa Trough. International Journal of Systematic and Evolutionary Microbiology **53:**1801-1805.
113. **Gittel A, Kofoed MV, Sorensen KB, Ingvorsen K, Schramm A.** 2012. Succession of Deferribacteres and Epsilonproteobacteria through a nitrate-treated high-temperature oil production facility. Systematic and Applied Microbiology **35:**165-174.
114. **Handley KM, VerBerkmoes NC, Steefel CI, Williams KH, Sharon I, Miller CS, Frischkorn KR, Chourey K, Thomas BC, Shah MB, Long PE, Hettich RL, Banfield JF.** 2013. Biostimulation induces syntrophic interactions that impact C, S and N cycling in a sediment microbial community. The ISME Journal **7:**800-816.
115. **Hubert CRJ, Oldenburg TBP, Fustic M, Gray ND, Larter SR, Penn K, Rowan AK, Seshadri R, Sherry A, Swainsbury R, Voordouw G, Voordouw JK, Head IM.** 2012. Massive dominance of Epsilonproteobacteria in formation waters from a Canadian oil sands reservoir containing severely biodegraded oil. Environmental Microbiology **14:**387-404.
116. **Watanabe K, Watanabe K, Kodama Y, Syutsubo K, Harayama S.** 2000. Molecular characterization of bacterial populations in petroleum-contaminated groundwater discharged from underground crude oil storage cavities. Applied and environmental Microbiology **66:**4803-+.
117. **Sievert SM, Scott KA, Klotz MG, Chain PSG, Hauser LJ, Hemp J, Hugler M, Land M, Lapidus A, Larimer FW, Lucas S, Malfatti SA, Meyer F, Paulsen IT, Ren Q, Simon J, Class UG.** 2008. Genome of the epsilonproteobacterial chemolithoautotroph Sulfurimonas denitrificans. Applied and environmental Microbiology **74:**1145-1156.
118. **Takai K, Suzuki M, Nakagawa S, Miyazaki M, Suzuki Y, Inagaki F, Horikoshi K.** 2006. Sulfurimonas paralvinellae sp. nov., a novel mesophilic, hydrogen- and sulfur-oxidizing chemolithoautotroph within the Epsilonproteobacteria isolated from a deep-sea hydrothermal vent polychaete nest, reclassification of Thiomicrospira denitrificans as Sulfurimonas denitrificans comb. nov. and emended description of the genus Sulfurimonas. International Journal of Systematic and Evolutionary Microbiology **56:**1725-1733.

119. **Hugler M, Wirsen CO, Fuchs G, Taylor CD, Sievert SM.** 2005. Evidence for autotrophic CO2 fixation via the reductive tricarboxylic acid cycle by members of the epsilon subdivision of proteobacteria. Journal of bacteriology **187:**3020-3027.
120. **Campbell BJ, Engel AS, Porter ML, Takai K.** 2006. The versatile epsilon-proteobacteria: key players in sulphidic habitats. Nature Reviews Microbiology **4:**458-468.
121. **Miller WG, Parker CT, Rubenfield M, Mendz GL, Wosten MMSM, Ussery DW, Stolz JF, Binnewies TT, Hallin PF, Wang GL, Malek JA, Rogosin A, Stanker LH, Mandrell RE.** 2007. The Complete Genome Sequence and Analysis of the Epsilonproteobacterium Arcobacter butzleri. PloS one **2**.
122. **Kern M, Simon J.** 2009. Electron transport chains and bioenergetics of respiratory nitrogen metabolism in Wolinella succinogenes and other Epsilonproteobacteria. Biochimica et biophysica acta **1787:**646-656.
123. **Kroger A, Biel S, Simon J, Gross R, Unden G, Lancaster CR.** 2002. Fumarate respiration of Wolinella succinogenes: enzymology, energetics and coupling mechanism. Biochimica et biophysica acta **1553:**23-38.
124. **Miroshnichenko ML, L'Haridon S, Schumann P, Spring S, Bonch-Osmolovskaya EA, Jeanthon C, Stackebrandt E.** 2004. Caminibacter profundus sp nov., a novel thermophile of Nautiliales ord. nov within the class 'Epsilonproteobacteria', isolated from a deep-sea hydrothermal vent. International Journal of Systematic and Evolutionary Microbiology **54:**41-45.
125. **Nakagawa S, Takaki Y, Shimamura S, Reysenbach AL, Takai K, Horikoshi K.** 2007. Deep-sea vent epsilon-proteobacterial genomes provide insights into emergence of pathogens. P Natl Acad Sci USA **104:**12146-12150.
126. **Schauer R, Roy H, Augustin N, Gennerich HH, Peters M, Wenzhoefer F, Amann R, Meyerdierks A.** 2011. Bacterial sulfur cycling shapes microbial communities in surface sediments of an ultramafic hydrothermal vent field. Environmental Microbiology **13:**2633-2648.
127. **Stokke R, Dahle H, Roalkvam I, Wissuwa J, Daae FL, Tooming-Klunderud A, Thorseth IH, Pedersen RB, Steen IH.** 2015. Functional interactions among filamentous Epsilonproteobacteria and Bacteroidetes in a deep-sea hydrothermal vent biofilm. Environmental Microbiology **17:**4063-4077.
128. **Grote J, Schott T, Bruckner CG, Glockner FO, Jost G, Teeling H, Labrenz M, Jurgens K.** 2012. Genome and physiology of a model Epsilonproteobacterium responsible for sulfide detoxification in marine oxygen depletion zones. PNAS **109:**506-510.
129. **Engel AS, Porter ML, Stern LA, Quinlan S, Bennett PC.** 2004. Bacterial diversity and ecosystem function of filamentous microbial mats from aphotic (cave) sulfidic springs dominated by chemolithoautotrophic "Epsilonproteobacteria". FEMS microbiology ecology **51:**31-53.
130. **Hamilton TL, Jones DS, Schaperdoth I, Macalady JL.** 2015. Metagenomic insights into S(0) precipitation in a terrestrial subsurface lithoautotrophic ecosystem. Frontiers in microbiology **5**.
131. **Jones DS, Tobler DJ, Schaperdoth I, Mainiero M, Macalady JL.** 2010. Community Structure of Subsurface Biofilms in the Thermal Sulfidic Caves of Acquasanta Terme, Italy. Applied and environmental Microbiology **76:**5902-5910.
132. **Porter ML, Engel AS.** 2008. Diversity of uncultured Epsilonproteobacteria from terrestrial sulfidic caves and springs. Applied and environmental Microbiology **74:**4973-4977.

133. **Rossmassler K, Engel AS, Twing KI, Hanson TE, Campbell BJ.** 2012. Drivers of epsilonproteobacterial community composition in sulfidic caves and springs. FEMS microbiology ecology **79:**421-432.
134. **Green-Saxena A, Feyzullayev A, Hubert CR, Kallmeyer J, Krueger M, Sauer P, Schulz HM, Orphan VJ.** 2012. Active sulfur cycling by diverse mesophilic and thermophilic microorganisms in terrestrial mud volcanoes of Azerbaijan. Environmental Microbiology **14:**3271-3286.
135. **Zhang T, Ke SZ, Liu Y, Fang HP.** 2005. Microbial characteristics of a methanogenic phenol-degrading sludge. Water Science and Technology **52:**73-78.
136. **Kasai Y, Takahata Y, Hoaki T, Watanabe K.** 2005. Physiological and molecular characterization of a microbial community established in unsaturated, petroleum-contaminated soil. Environmental Microbiology **7:**806-818.
137. **Bozinovski D, Herrmann S, Richnow HH, von Bergen M, Seifert J, Vogt C.** 2012. Functional analysis of an anaerobic m-xylene-degrading enrichment culture using protein-based stable isotope probing. FEMS microbiology ecology **81:**134-144.
138. **Jehmlich N, Kleinsteuber S, Vogt C, Benndorf D, Harms H, Schmidt F, von Bergen M, Seifert J.** 2010. Phylogenetic and proteomic analysis of an anaerobic toluene-degrading community. Journal of Applied Microbiology **109:**1937-1945.
139. **Kleinsteuber S, Schleinitz KM, Breitfeld J, Harms H, Richnow HH, Vogt C.** 2008. Molecular characterization of bacterial communities mineralizing benzene under sulfate-reducing conditions. FEMS microbiology ecology **66:**143-157.
140. **Kuppardt A, Kleinsteuber S, Vogt C, Luders T, Harms H, Chatzinotas A.** 2014. Phylogenetic and Functional Diversity Within Toluene-Degrading, Sulphate-Reducing Consortia Enriched from a Contaminated Aquifer. Microbial ecology **68:**222-234.
141. **Muller S, Vogt C, Laube M, Harms H, Kleinsteuber S.** 2009. Community dynamics within a bacterial consortium during growth on toluene under sulfate-reducing conditions. FEMS microbiology ecology **70:**586-596.
142. **Pilloni G, von Netzer F, Engel M, Lueders T.** 2011. Electron acceptor-dependent identification of key anaerobic toluene degraders at a tar-oil-contaminated aquifer by Pyro-SIP. FEMS microbiology ecology **78:**165-175.
143. **Webster G, Rinna J, Roussel EG, Fry JC, Weightman AJ, Parkes RJ.** 2010. Prokaryotic functional diversity in different biogeochemical depth zones in tidal sediments of the Severn Estuary, UK, revealed by stable-isotope probing. FEMS microbiology ecology **72:**179-197.
144. **Herrmann S, Kleinsteuber S, Neu TR, Richnow HH, Vogt C.** 2008. Enrichment of anaerobic benzene-degrading microorganisms by in situ microcosms. FEMS microbiology ecology **63:**94-106.
145. **Schirmer M, Dahmke A, Dietrich P, Dietze M, Godeke S, Richnow HH, Schirmer K, Weiss H, Teutsch G.** 2006. Natural attenuation research at the contaminated megasite Zeitz. Journal of Hydrology **328:**393-407.
146. **Vogt C, Godeke S, Treutler HC, Weiss H, Schirmer M, Richnow HH.** 2007. Benzene oxidation under sulfate-reducing conditions in columns simulating in situ conditions. Biodegradation **18:**625-636.
147. **Herrmann S, Kleinsteuber S, Chatzinotas A, Kuppardt S, Lueders T, Richnow HH, Vogt C.** 2010. Functional characterization of an anaerobic benzene-degrading enrichment culture by DNA stable isotope probing. Environ Microbiol **12:**401-411.
148. **Bozinovski D, Taubert M, Kleinsteuber S, Richnow HH, von Bergen M, Vogt C, Seifert J.** 2014. Metaproteogenomic analysis of a sulfate-reducing enrichment culture reveals genomic

organization of key enzymes in the m-xylene degradation pathway and metabolic activity of proteobacteria. Systematic and Applied Microbiology **37:**488-501.

149. **Herrmann S, Vogt C, Fischer A, Kuppardt A, Richnow HH.** 2009. Characterization of anaerobic xylene biodegradation by two-dimensional isotope fractionation analysis. Environmental Microbiology Reports **1:**535-544.
150. **Ziganshin AM, Schmidt T, Scholwin F, Il'inskaya ON, Harms H, Kleinsteuber S.** 2011. Bacteria and archaea involved in anaerobic digestion of distillers grains with solubles. Applied Microbiology and Biotechnology **89:**2039-2052.
151. **Patil KR, Roune L, McHardy AC.** 2012. The PhyloPythiaS Web Server for Taxonomic Assignment of Metagenome Sequences. PloS one **7**.
152. **Lagesen K, Hallin P, Rodland EA, Staerfeldt HH, Rognes T, Ussery DW.** 2007. RNAmmer: consistent and rapid annotation of ribosomal RNA genes. Nucleic acids research **35:**3100-3108.
153. **Wang Q, Garrity GM, Tiedje JM, Cole JR.** 2007. Naive Bayesian classifier for rapid assignment of rRNA sequences into the new bacterial taxonomy. Applied and environmental Microbiology **73:**5261-5267.
154. **Rissman AI, Mau B, Biehl BS, Darling AE, Glasner JD, Perna NT.** 2009. Reordering contigs of draft genomes using the Mauve Aligner. Bioinformatics **25:**2071-2073.
155. **Vallenet D, Belda E, Calteau A, Cruveiller S, Engelen S, Lajus A, Le Fevre F, Longin C, Mornico D, Roche D, Rouy Z, Salvignol G, Scarpelli C, Smith AAT, Weiman M, Medigue C.** 2013. MicroScope-an integrated microbial resource for the curation and comparative analysis of genomic and metabolic data. Nucleic acids research **41:**E636-E647.
156. **Vallenet D, Labarre L, Rouy Z, Barbe V, Bocs S, Cruveiller S, Lajus A, Pascal G, Scarpelli C, Medigue C.** 2006. MaGe: a microbial genome annotation system supported by synteny results. Nucleic acids research **34:**53-65.
157. **Gil R, Silva FJ, Pereto J, Moya A.** 2004. Determination of the core of a minimal bacterial gene set. Microbiology and molecular biology reviews : MMBR **68:**518-537, table of contents.
158. **Rinke C, Schwientek P, Sczyrba A, Ivanova NN, Anderson IJ, Cheng JF, Darling A, Malfatti S, Swan BK, Gies EA, Dodsworth JA, Hedlund BP, Tsiamis G, Sievert SM, Liu WT, Eisen JA, Hallam SJ, Kyrpides NC, Stepanauskas R, Rubin EM, Hugenholtz P, Woyke T.** 2013. Insights into the phylogeny and coding potential of microbial dark matter. Nature **499:**431-437.
159. **Gross R, Simon J, Theis F, Kroger A.** 1998. Two membrane anchors of Wolinella succinogenes hydrogenase and their function in fumarate and polysulfide respiration. Archives of Microbiology **170:**50-58.
160. **Yates MG.** 1988. The role of oxygen and hydrogen in nitrogen fixation, p. 386–416. *In* Cole IA, Ferguson SI (ed.), The nitrogen and sulphur cycles, vol. 42. University Press Cambridge.
161. **Tsygankov AA.** 2007. Nitrogen-fixing cyanobacteria: A review. Applied Biochemistry and Microbiology **43:**250-259.
162. **Griesbeck C, Schutz M, Schodl T, Bathe S, Nausch L, Mederer N, Vielreicher M, Hauska G.** 2002. Mechanism of sulfide-quinone reductase investigated using site-directed mutagenesis and sulfur analysis. Biochemistry **41:**11552-11565.
163. **Schutz M, Maldener I, Griesbeck C, Hauska G.** 1999. Sulfide-quinone reductase from Rhodobacter capsulatus: Requirement for growth, periplasmic localization, and extension of gene sequence analysis. Journal of bacteriology **181:**6516-6523.
164. **Bokranz M, Gutmann M, Kortner C, Kojro E, Fahrenholz F, Lauterbach F, Kroger A.** 1991. Cloning and Nucleotide-Sequence of the Structural Genes Encoding the Formate Dehydrogenase of Wolinella-Succinogenes. Archives of Microbiology **156:**119-128.

165. **Bertero MG, Rothery RA, Palak M, Hou C, Lim D, Blasco F, Weiner JH, Strynadka NCJ.** 2003. Insights into the respiratory electron transfer pathway from the structure of nitrate reductase A. Nature Structural & Molecular Biology **10:**681-687.
166. **Jormakka M, Yokoyama K, Yano T, Tamakoshi M, Akimoto S, Shimamura T, Curmi P, Iwata S.** 2008. Molecular mechanism of energy conservation in polysulfide respiration. Nature Structural & Molecular Biology **15:**730-737.
167. **Raymond J, Siefert JL, Staples CR, Blankenship RE.** 2004. The natural history of nitrogen fixation. Molecular Biology and Evolution **21:**541-554.
168. **Bohme H.** 1998. Regulation of nitrogen fixation in heterocyst-forming cyanobacteria. Trends in Plant Science **3:**346-351.
169. **Dixon R, Eady RR, Espin G, Hill S, Iaccarino M, Kahn D, Merrick M.** 1980. Analysis of Regulation of Klebsiella-Pneumoniae Nitrogen-Fixation (Nif) Gene-Cluster with Gene Fusions. Nature **286:**128-132.
170. **Fu W, Jack RF, Morgan TV, Dean DR, Johnson MK.** 1994. nifU gene product from Azotobacter vinelandii is a homodimer that contains two identical [2Fe-2S] clusters. Biochemistry **33:**13455-13463.
171. **Gosink MM, Franklin NM, Roberts GP.** 1990. The Product of the Klebsiella-Pneumoniae Nifx-Gene Is a Negative Regulator of the Nitrogen-Fixation (Nif) Regulon. Journal of bacteriology **172:**1441-1447.
172. **Baar C, Eppinger M, Raddatz G, Simon J, Lanz C, Klimmek O, Nandakumar R, Gross R, Rosinus A, Keller H, Jagtap P, Linke B, Meyer F, Lederer H, Schuster SC.** 2003. Complete genome sequence and analysis of Wolinella succinogenes. PNAS **100:**11690-11695.
173. **Handley KM, Bartels D, O'Loughlin EJ, Williams KH, Trimble WL, Skinner K, Gilbert JA, Desai N, Glass EM, Paczian T, Wilke A, Antonopoulos D, Kemner KM, Meyer F.** 2014. The complete genome sequence for putative H-2- and S-oxidizer Candidatus Sulfuricurvum sp., assembled de novo from an aquifer-derived metagenome. Environmental Microbiology **16:**3443-3462.
174. **Berg IA.** 2011. Ecological aspects of the distribution of different autotrophic CO2 fixation pathways. Applied and Environmental Microbiology **77:**1925-1936.
175. **Evans MCW, Buchanan BB, Arnon DI.** 1966. A New Ferredoxin-Dependent Carbon Reduction Cycle in a Photosynthetic Bacterium. P Natl Acad Sci USA **55:**928-&.
176. **Berg P.** 1956. Acy adenylates: An enzymatic mechanism of acetate activation. Journal of Biological Chemistry **222:**991 - 1013.
177. **Gimenez R, Nunez MF, Badia J, Aguilar J, Baldoma L.** 2003. The gene yjcG, cotranscribed with the gene acs, encodes an acetate permease in Escherichia coli. Journal of bacteriology **185:**6448-6455.
178. **Starke R, Keller A, Jehmlich N, Vogt C, Richnow H, Kleinsteuber S, von Bergen M, Seifert J.** 2016. Pulsed C-13(2)-Acetate Protein-SIP Unveils Epsilonproteobacteria as Dominant Acetate Utilizers in a Sulfate-Reducing Microbial Community Mineralizing Benzene. Microbial ecology **71:**901-911.
179. **Rakoczy J, Schleinitz KM, Muller N, Richnow HH, Vogt C.** 2011. Effects of hydrogen and acetate on benzene mineralisation under sulphate-reducing conditions. FEMS microbiology ecology **77:**238-247.
180. **Beller HR, Chain PS, Letain TE, Chakicherla A, Larimer FW, Richardson PM, Coleman MA, Wood AP, Kelly DP.** 2006. The genome sequence of the obligately chemolithoautotrophic, facultatively anaerobic bacterium Thiobacillus denitrificans. Journal of bacteriology **188:**1473-1488.

181. **Beller HR, Letain TE, Chakicherla A, Kane SR, Legler TC, Coleman MA.** 2006. Whole-genome transcriptional analysis of chemolithoautotrophic thiosulfate oxidation by Thiobacillus denitrificans under aerobic versus denitrifying conditions. Journal of bacteriology **188:**7005-7015.
182. **Yamamoto M, Nakagawa S, Shimamura S, Takai K, Horikoshi K.** 2010. Molecular characterization of inorganic sulfur-compound metabolism in the deep-sea epsilonproteobacterium Sulfurovum sp NBC37-1. Environmental Microbiology **12:**1144-1152.
183. **Hedderich R, Klimmek O, Kroger A, Dirmeier R, Keller M, Stetter KO.** 1998. Anaerobic respiration with elemental sulfur and with disulfides. FEMS Microbioly Reviews **22:**353-381.
184. **Takai K, Hirayama H, Nakagawa T, Suzuki Y, Nealson KH, Horikoshi K.** 2005. Lebetimonas acidiphila gen. nov., sp nov., a novel thermophilic, acidophilic, hydrogen-oxidizing chemolithoautotroph within the Epsilonproteobacteria', isolated from a deep-sea hydrothermal fumarole in the Mariana Arc. International Journal of Systematic and Evolutionary Microbiology **55:**183-189.
185. **Kroger A, Geisler V, Lemma E, Theis F, Lenger R.** 1992. Bacterial Fumarate Respiration. Archives of Microbiology **158:**311-314.
186. **Ullmann R, Gross R, Simon J, Unden G, Kroger A.** 2000. Transport of C-4-dicarboxylates in Wolinella succinogenes. Journal of bacteriology **182:**5757-5764.
187. **Wang SN, Huang HY, Kahnt J, Thauer RK.** 2013. A Reversible Electron-Bifurcating Ferredoxin- and NAD-Dependent [FeFe]-Hydrogenase (HydABC) in Moorella thermoacetica. Journal of bacteriology **195:**1267-1275.
188. **Kodama Y, Watanabe K.** 2004. Sulfuricurvum kujiense gen. nov., sp nov., a facultatively anaerobic, chemolithoautotrophic, sulfur-oxidizing bacterium isolated from an underground crude-oil storage cavity. International Journal of Systematic and Evolutionary Microbiology **54:**2297-2300.
189. **Yamamoto M, Takai K.** 2011. Sulfur metabolisms in epsilon- and gamma-Proteobacteria in deep-sea hydrothermal fields. Frontiers in microbiology **2**.
190. **Kreddich NM.** 1996. Biosynthesis of cystein. Washington DC: ASM Press.
191. **Khademi S, O'Connell J, 3rd, Remis J, Robles-Colmenares Y, Miercke LJ, Stroud RM.** 2004. Mechanism of ammonia transport by Amt/MEP/Rh: structure of AmtB at 1.35 A. Science **305:**1587-1594.
192. **Zheng L, Kostrewa D, Berneche S, Winkler FK, Li XD.** 2004. The mechanism of ammonia transport based on the crystal structure of AmtB of Escherichia coli. PNAS **101:**17090-17095.
193. **Mcclung CR, Patriquin DG, Davis RE.** 1983. Campylobacter-Nitrofigilis Sp-Nov, a Nitrogen-Fixing Bacterium Associated with Roots of Spartina-Alterniflora Loisel. International journal of systematic bacteriology **33:**605-612.
194. **Schutz K, Happe T, Troshina O, Lindblad P, Leitao E, Oliveira P, Tamagnini P.** 2004. Cyanobacterial H-2 production - a comparative analysis. Planta **218:**350-359.
195. **Tamagnini P, Costa JL, Almeida L, Oliveira MJ, Salema R, Lindblad P.** 2000. Diversity of cyanobacterial hydrogenases, a molecular approach. Current microbiology **40:**356-361.
196. **Weissgerber T, Zigann R, Bruce D, Chang YJ, Detter JC, Han C, Hauser L, Jeffries CD, Land M, Munk AC, Tapia R, Dahl C.** 2011. Complete genome sequence of Allochromatium vinosum DSM 180(T). Standards in Genomic Sciences **5:**311-330.
197. **Kern M, Klipp W, Klemme JH.** 1994. Increased Nitrogenase-Dependent H(2) Photoproduction by hup Mutants of Rhodospirillum rubrum. Applied and Environmental Microbiology **60:**1768-1774.

198. **Bruschi M, Guerlesquin F.** 1988. Structure, Function and Evolution of Bacterial Ferredoxins. FEMS Microbiology Letters **54:**155-175.
199. **Fay P.** 1992. Oxygen Relations of Nitrogen-Fixation in Cyanobacteria. Microbiological reviews **56:**340-373.
200. **Bronowski C, James CE, Winstanley C.** 2014. Role of environmental survival in transmission of Campylobacter jejuni. FEMS Microbiology Letters **356:**8-19.
201. **Storz G, Tartaglia LA, Farr SB, Ames BN.** 1990. Bacterial Defenses against Oxidative Stress. Trends in Genetics **6:**363-368.
202. **Cosgrove K, Coutts G, Jonsson IM, Tarkowski A, Kokai-Kun JF, Mond JJ, Foster SJ.** 2007. Catalase (KatA) and alkyl hydroperoxide reductase (AhpC) have comensatory roles in peroxide stress resistance and are required for survival, persistence, and nasal colonization in Staphylococcus aureus. Journal of bacteriology **189:**1025-1035.
203. **Seaver LC, Imlay JA.** 2001. Alkyl hydroperoxide reductase is the primary scavenger of endogenous hydrogen peroxide in Escherichia coli. Journal of bacteriology **183:**7173-7181.
204. **Allen RM, Chatterjee R, Madden MS, Ludden PW, Shah VK.** 1994. Biosynthesis of the iron-molybdenum cofactor of nitrogenase. Critical reviews in biotechnology **14:**225-249.
205. **Chan MK, Kim JS, Rees DC.** 1993. The Nitrogenase Femo-Cofactor and P-Cluster Pair - 2.2-Angstrom Resolution Structures. Science **260:**792-794.
206. **Ames GF.** 1986. Bacterial periplasmic transport systems: structure, mechanism, and evolution. Annual review of biochemistry **55:**397-425.
207. **Steed PM, Wanner BL.** 1993. Use of the Rep Technique for Allele Replacement to Construct Mutants with Deletions of the Pstscab-Phou Operon - Evidence of a New Role for the Phou Protein in the Phosphate Regulon. Journal of bacteriology **175:**6797-6809.
208. **Wanner BL, Jiang W, Kim S-K, Yamagata S, Haldimann A, Daniels LL.** 1996. Are the multiple signal transduction pathways of the Pho regulon due to cross talk or cross regulation?, p. 297-315, Regulation of Gene Expression in Escherichia coli. Springer US.
209. **Gardner SG, Johns KD, Tanner R, McCleary WR.** 2014. The PhoU protein from Escherichia coli interacts with PhoR, PstB, and metals to form a phosphate-signaling complex at the membrane. Journal of bacteriology **196:**1741-1752.
210. **Holtmann G, Bakker EP, Uozumi N, Bremer E.** 2003. KtrAB and KtrCD: Two K+ uptake systems in Bacillus subtilis and their role in adaptation to hypertonicity. Journal of bacteriology **185:**1289-1298.
211. **Patzer SI, Hantke K.** 1998. The ZnuABC high-affinity zinc uptake system and its regulator zur in Escherichia coli. Molecular Microbiology **28:**1199-1210.
212. **Moeck GS, Coulton JW.** 1998. TonB-dependent iron acquisition: mechanisms of siderophore-mediated active transport. Molecular Microbiology **28:**675-681.
213. **Kammler M, Schon C, Hantke K.** 1993. Characterization of the Ferrous Iron Uptake System of Escherichia-Coli. Journal of bacteriology **175:**6212-6219.
214. **Kim H, Lee H, Shin D.** 2012. The FeoA protein is necessary for the FeoB transporter to import ferrous iron. Biochemical and Biophysical Research Communications **423:**733-738.
215. **Korotkov KV, Sandkvist M, Hol WGJ.** 2012. The type II secretion system: biogenesis, molecular architecture and mechanism. Nature Reviews Microbiology **10:**336-351.
216. **Voulhoux R, Ball G, Ize B, Vasil ML, Lazdunski A, Wu LF, Filloux A.** 2001. Involvement of the twin-arginine translocation system in protein secretion via the type II pathway. Embo Journal **20:**6735-6741.
217. **Takai K, Inagaki F, Nakagawa S, Hirayama H, Nunoura T, Sako Y, Nealson KH, Horikoshi K.** 2003. Isolation and phylogenetic diversity of members of previously uncultivated

epsilon-proteobacteria in deep-sea hydrothermal fields. FEMS Microbiology Letters **218:**167-174.

218. **Kodama Y, Ha LT, Watanabe K.** 2007. Sulfurospirillum cavolei sp nov, a facultatively anaerobic sulfur-reducing bacterium isolated from an underground crude oil storage cavity. International Journal of Systematic and Evolutionary Microbiology **57:**827-831.
219. **Cordruwisch R, Seitz HJ, Conrad R.** 1988. The Capacity of Hydrogenotrophic Anaerobic-Bacteria to Compete for Traces of Hydrogen Depends on the Redox Potential of the Terminal Electron-Acceptor. Archives of Microbiology **149:**350-357.
220. **Poser A, Vogt C, Knoller K, Ahlheim J, Weiss H, Kleinsteuber S, Richnow HH.** 2014. Stable Sulfur and Oxygen Isotope Fractionation of Anoxic Sulfide Oxidation by Two Different Enzymatic Pathways. Environmental science & technology **48:**9094-9102.
221. **Gevertz D, Telang AJ, Voordouw G, Jenneman GE.** 2000. Isolation and characterization of strains CVO and FWKO B, two novel nitrate-reducing, sulfide-oxidizing bacteria isolated from oil field brine. Applied and Environmental Microbiology **66:**2491-2501.
222. **Steudel R.** 1996. Mechanism for the formation of elemental sulfur from aqueous sulfide in chemical and microbiological desulfurization processes. Industrial & Engineering Chemistry Research **35:**1417-1423.
223. **Zhang T, Tremblay PL, Chaurasia AK, Smith JA, Bain TS, Lovley DR.** 2013. Anaerobic benzene oxidation via phenol in Geobacter metallireducens. Applied and environmental microbiology **79:**7800-7806.
224. **Abu Laban N, Selesi D, Rattei T, Tischler P, Meckenstock RU.** 2010. Identification of enzymes involved in anaerobic benzene degradation by a strictly anaerobic iron-reducing enrichment culture. Environmental microbiology **12:**2783-2796.
225. **Yamamoto M, Takai K.** 2011. Sulfur metabolisms in epsilon- and gamma-proteobacteria in deep-sea hydrothermal fields. Frontiers in microbiology **2:**192.
226. **Nakagawa S, Takaki Y, Shimamura S, Reysenbach AL, Takai K, Horikoshi K.** 2007. Deep-sea vent epsilon-proteobacterial genomes provide insights into emergence of pathogens. PNAS **104:**12146-12150.
227. **Nakagawa S, Takai K, Inagaki F, Hirayama H, Nunoura T, Horikoshi K, Sako Y.** 2005. Distribution, phylogenetic diversity and physiological characteristics of epsilon-Proteobacteria in a deep-sea hydrothermal field. Environmental microbiology **7:**1619-1632.
228. **Benndorf D, Vogt C, Jehmlich N, Schmidt Y, Thomas H, Woffendin G, Shevchenko A, Richnow HH, von Bergen M.** 2009. Improving protein extraction and separation methods for investigating the metaproteome of anaerobic benzene communities within sediments. Biodegradation **20:**737-750.
229. **Laemmli UK.** 1970. Cleavage of structural proteins during the assembly of the head of bacteriophage T4. Nature **227:**680-685.
230. **Bozinovski D, Taubert M, Kleinsteuber S, Richnow HH, von Bergen M, Vogt C, Seifert J.** 2014. Metaproteogenomic analysis of a sulfate-reducing enrichment culture reveals genomic organization of key enzymes in the m-xylene degradation pathway and metabolic activity of proteobacteria. Systematic and applied microbiology **37:**488-501.
231. **Vallenet D, Belda E, Calteau A, Cruveiller S, Engelen S, Lajus A, Le Fevre F, Longin C, Mornico D, Roche D, Rouy Z, Salvignol G, Scarpelli C, Thil Smith AA, Weiman M, Medigue C.** 2013. MicroScope--an integrated microbial resource for the curation and comparative analysis of genomic and metabolic data. Nucleic Acids Res **41:**D636-647.

232. **Vallenet D, Labarre L, Rouy Z, Barbe V, Bocs S, Cruveiller S, Lajus A, Pascal G, Scarpelli C, Medigue C.** 2006. MaGe: a microbial genome annotation system supported by synteny results. Nucleic acids research **34:**53-65.
233. **Kohlbacher O, Reinert K, Gropl C, Lange E, Pfeifer N, Schulz-Trieglaff O, Sturm M.** 2007. TOPP--the OpenMS proteomics pipeline. Bioinformatics **23:**e191-197.
234. **Sturm M, Bertsch A, Gropl C, Hildebrandt A, Hussong R, Lange E, Pfeifer N, Schulz-Trieglaff O, Zerck A, Reinert K, Kohlbacher O.** 2008. OpenMS - an open-source software framework for mass spectrometry. BMC bioinformatics **9:**163.
235. **Chambers MC, Maclean B, Burke R, Amodei D, Ruderman DL, Neumann S, Gatto L, Fischer B, Pratt B, Egertson J, Hoff K, Kessner D, Tasman N, Shulman N, Frewen B, Baker TA, Brusniak MY, Paulse C, Creasy D, Flashner L, Kani K, Moulding C, Seymour SL, Nuwaysir LM, Lefebvre B, Kuhlmann F, Roark J, Rainer P, Detlev S, Hemenway T, Huhmer A, Langridge J, Connolly B, Chadick T, Holly K, Eckels J, Deutsch EW, Moritz RL, Katz JE, Agus DB, MacCoss M, Tabb DL, Mallick P.** 2012. A cross-platform toolkit for mass spectrometry and proteomics. Nature biotechnology **30:**918-920.
236. **Herrmann S, Kleinsteuber S, Neu TR, Richnow HH, Vogt C.** 2008. Enrichment of anaerobic benzene-degrading microorganisms by in situ microcosms. FEMS microbiology ecology **63:**94-106.
237. **Klenk HP, Clayton RA, Tomb JF, White O, Nelson KE, Ketchum KA, Dodson RJ, Gwinn M, Hickey EK, Peterson JD, Richardson DL, Kerlavage AR, Graham DE, Kyrpides NC, Fleischmann RD, Quackenbush J, Lee NH, Sutton GG, Gill S, Kirkness EF, Dougherty BA, McKenney K, Adams MD, Loftus B, Peterson S, Reich CI, McNeil LK, Badger JH, Glodek A, Zhou LX, Overbeek R, Gocayne JD, Weidman JF, McDonald L, Utterback T, Cotton MD, Spriggs T, Artiach P, Kaine BP, Sykes SM, Sadow PW, DAndrea KP, Bowman C, Fujii C, Garland SA, Mason TM, Olsen GJ, Fraser CM, Smith HO, Woese CR, Venter JC.** 1997. The complete genome sequence of the hyperthermophilic, sulphate-reducing archaeon Archaeoglobus fulgidus. Nature **390:**364-&.
238. **Frigaard NU, Dahl C.** 2009. Sulfur metabolism in phototrophic sulfur bacteria. Advances in microbial physiology **54:**103-200.
239. **Wood HG.** 1991. Life with CO or CO2 and H2 as a source of carbon and energy. FASEB journal : official publication of the Federation of American Societies for Experimental Biology **5:**156-163.
240. **Zhang Q, Zak JC.** 1998. Potential Physiological Activities of Fungi and Bacteria in Relation to Plant Litter Decomposition along a Gap Size Gradient in a Natural Subtropical Forest. Microbial ecology **35:**172-179.
241. **Jones DL, Healey JR, Willett VB, Farrar JF, Hodge A.** 2005. Dissolved organic nitrogen uptake by plants—an important N uptake pathway? Soil Biology & Biochemistry **37:**413-423.
242. **Velicer GJ.** 2003. Social strife in the microbial world. Trends in microbiology **11:**330-337.
243. **Fierer N, Lauber CL, Ramirez KS, Zaneveld J, Bradford MA, Knight R.** 2012. Comparative metagenomic, phylogenetic and physiological analyses of soil microbial communities across nitrogen gradients. The ISME journal **6:**1007-1017.
244. **Fierer N, Leff JW, Adams BJ, Nielsen UN, Bates ST, Lauber CL, Owens S, Gilbert JA, Wall DH, Caporaso JG.** 2012. Cross-biome metagenomic analyses of soil microbial communities and their functional attributes. PNAS **109:**21390-21395.
245. **Mendes LW, Kuramae EE, Navarrete AA, van Veen JA, Tsai SM.** 2014. Taxonomical and functional microbial community selection in soybean rhizosphere. The ISME journal **8:**1577-1587.

246. **Rondon MR, Goodman RM, Handelsman J.** 1999. The Earth's bounty: assessing and accessing soil microbial diversity. Trends in biotechnology **17:**403-409.
247. **Vos M, Wolf AB, Jennings SJ, Kowalchuk GA.** 2013. Micro-scale determinants of bacterial diversity in soil. FEMS microbiology reviews **37:**936-954.
248. **España M, Rasche F, Kandeler E, Brune T, Rodriguez B, Bending GD, Cadisch G.** 2011. Identification of active bacteria involved in decomposition of complex maize and soybean residues in a tropical Vertisol using N-15-DNA stable isotope probing. Pedobiologia **54:**187-193.
249. **Pratscher J, Dumont MG, Conrad R.** 2011. Ammonia oxidation coupled to CO2 fixation by archaea and bacteria in an agricultural soil. PNAS **108:**4170-4175.
250. **Rocca JD, Hall EK, Lennon JT, Evans SE, Waldrop MP, Cotner JB, Nemergut DR, Graham EB, Wallenstein MD.** 2015. Relationships between protein-encoding gene abundance and corresponding process are commonly assumed yet rarely observed. The ISME journal **9:**1693-1699.
251. **Bastida F, Hernandez T, Garcia C.** 2014. Metaproteomics of soils from semiarid environment: functional and phylogenetic information obtained with different protein extraction methods. Journal of proteomics **101:**31-42.
252. **Chourey K, Jansson J, VerBerkmoes N, Shah M, Chavarria KL, Tom LM, Brodie EL, Hettich RL.** 2010. Direct cellular lysis/protein extraction protocol for soil metaproteomics. Journal of proteome research **9:**6615-6622.
253. **Keiblinger KM, Wilhartitz IC, Schneider T, Roschitzki B, Schmid E, Eberl L, Riedel K, Zechmeister-Boltenstern S.** 2012. Soil metaproteomics - Comparative evaluation of protein extraction protocols. Soil Biology & Biochemistry **54:**14-24.
254. **de Vries FT, Hoffland E, van Eekeren N, Brussaard L, Bloem J.** 2006. Fungal/bacterial ratios in grasslands with contrasting nitrogen management. Soil Biology & Biochemistry **38:**2092-2103.
255. **Ullmann-Zeunert L, Muck A, Wielsch N, Hufsky F, Stanton MA, Bartram S, Bocker S, Baldwin IT, Groten K, Svatos A.** 2012. Determination of (15)N-Incorporation into Plant Proteins and their Absolute Quantitation: A New Tool to Study Nitrogen Flux Dynamics and Protein Pool Sizes Elicited by Plant-Herbivore Interactions. Journal of proteome research **11:**4947-4960.
256. **Käll L, Canterbury JD, Weston J, Noble WS, MacCoss MJ.** 2007. Semi-supervised learning for peptide identification from shotgun proteomics datasets. Nature methods **4:**923-925.
257. **Sachsenberg T, Herbst FA, Taubert M, Kermer R, Jehmlich N, von Bergen M, Seifert J, Kohlbacher O.** 2015. MetaProSIP: automated inference of stable isotope incorporation rates in proteins for functional metaproteomics. Journal of proteome research **14:**619-627.
258. **España M, Rasche F, Kandeler E, Brune T, Rodriguez B, Bending GD, Cadisch G.** 2011. Assessing the effect of organic residue quality on active decomposing fungi in a tropical Vertisol using N-15-DNA stable isotope probing. Fungal Ecology **4:**115-119.
259. **Fierer N, Bradford MA, Jackson RB.** 2007. Toward an ecological classification of soil bacteria. Ecology **88:**1354-1364.
260. **Cleveland CC, Nemergut DR, Schmidt SK, Townsend AR.** 2007. Increases in soil respiration following labile carbon additions linked to rapid shifts in soil microbial community composition. Biogeochemistry **82:**229-240.
261. **Fan FL, Yin C, Tang YJ, Li ZJ, Song A, Wakelin SA, Zou J, Liang YC.** 2014. Probing potential microbial coupling of carbon and nitrogen cycling during decomposition of maize residue by C-13-DNA-SIP. Soil Biology & Biochemistry **70:**12-21.

262. **Lee CG, Watanabe T, Sato Y, Murase J, Asakawa S, Kimura M.** 2011. Bacterial populations assimilating carbon from C-13-labeled plant residue in soil: Analysis by a DNA-SIP approach. Soil Biology & Biochemistry **43:**814-822.
263. **Semenov AV, Silva MCPE, Szturc-Koestsier AE, Schmitt H, Salles JF, van Elsas JD.** 2012. Impact of incorporated fresh C-13 potato tissues on the bacterial and fungal community composition of soil. Soil Biology & Biochemistry **49:**88-95.
264. **Voriskova J, Baldrian P.** 2013. Fungal community on decomposing leaf litter undergoes rapid successional changes. The ISME journal **7:**477-486.
265. **Stopnisek N, Zuhlke D, Carlier A, Barberan A, Fierer N, Becher D, Riedel K, Eberl L, Weisskopf L.** 2015. Molecular mechanisms underlying the close association between soil Burkholderia and fungi. The ISME journal.
266. **Lueders T, Kindler R, Miltner A, Friedrich MW, Kaestner M.** 2006. Identification of bacterial micropredators distinctively active in a soil microbial food web. Applied and environmental microbiology **72:**5342-5348.
267. **Reichenbach H.** 1999. The ecology of the myxobacteria. Environmental microbiology **1:**15-21.
268. **Bastida F, Garcia C, von Bergen M, Moreno JL, Richnow HH, Jehmlich N.** 2015. Deforestation fosters bacterial diversity and the cyanobacterial community responsible for carbon fixation processes under semiarid climate: a metaproteomics study. Applied Soil Ecology **93:**65-67.
269. **Eichorst SA, Joshua C, Sathitsuksanoh N, Singh S, Simmons BA, Singer SW.** 2014. Substrate-Specific Development of Thermophilic Bacterial Consortia by Using Chemically Pretreated Switchgrass. Applied and environmental microbiology **80:**7423-7432.
270. **Wang X, Sharp CE, Jones GM, Grasby SE, Brady AL, Dunfield PF.** 2015. Stable-Isotope Probing Identifies Uncultured Planctomycetes as Primary Degraders of a Complex Heteropolysaccharide in Soil. Applied and environmental microbiology **81:**4607-4615.
271. **Nakagawa ST, Y.** 2009. Nonpathogenic Epsilonproteobacteria. eLS.
272. **Baenkler H-WC, U.** 2001. Duale Reihe Innere Medizin. Georg Thieme, Stuttgart.
273. **Suzuki Y, Sasaki T, Suzuki M, Nogi Y, Miwa T, Takai K, Nealson KH, Horikoshi K.** 2005. Novel chemoautotrophic endosymbiosis between a member of the Epsilonproteobacteria and the hydrothermal-vent gastropod Alviniconcha aff. hessleri (Gastropoda: Provannidae) from the Indian Ocean. Applied and environmental microbiology **71:**5440-5450.
274. **Takai K, Campbell BJ, Cary SC, Suzuki M, Oida H, Nunoura T, Hirayama H, Nakagawa S, Suzuki Y, Inagaki F, Horikoshi K.** 2005. Enzymatic and genetic characterization of carbon and energy metabolisms by deep-sea hydrothermal chemolithoautotrophic isolates of Epsilonproteobacteria. Applied and environmental microbiology **71:**7310-7320.
275. **Anbar AD, Knoll AH.** 2002. Proterozoic ocean chemistry and evolution: a bioinorganic bridge? Science **297:**1137-1142.
276. **Herrmann S, Vogt C, Fischer A, Kuppardt A, Richnow HH.** 2009. Characterization of anaerobic xylene biodegradation by two-dimensional isotope fractionation analysis. Environmental microbiology reports **1:**535-544.
277. **Bozinovski D, Herrmann S, Richnow HH, von Bergen M, Seifert J, Vogt C.** 2012. Functional analysis of an anaerobic m-xylene-degrading enrichment culture using protein-based stable isotope probing. FEMS microbiology ecology **81:**134-144.
278. **Hugler M, Wirsen CO, Fuchs G, Taylor CD, Sievert SM.** 2005. Evidence for autotrophic CO2 fixation via the reductive tricarboxylic acid cycle by members of the epsilon subdivision of proteobacteria. Journal of bacteriology **187:**3020-3027.

279. **Handley KM, Bartels D, O'Loughlin EJ, Williams KH, Trimble WL, Skinner K, Gilbert JA, Desai N, Glass EM, Paczian T, Wilke A, Antonopoulos D, Kemner KM, Meyer F.** 2014. The complete genome sequence for putative H(2)- and S-oxidizer Candidatus Sulfuricurvum sp., assembled de novo from an aquifer-derived metagenome. Environmental microbiology **16:**3443-3462.
280. **Sievert SM, Scott KM, Klotz MG, Chain PS, Hauser LJ, Hemp J, Hugler M, Land M, Lapidus A, Larimer FW, Lucas S, Malfatti SA, Meyer F, Paulsen IT, Ren Q, Simon J, Class USFG.** 2008. Genome of the epsilonproteobacterial chemolithoautotroph Sulfurimonas denitrificans. Applied and environmental microbiology **74:**1145-1156.
281. **Keller AH, Schleinitz KM, Starke R, Bertilsson S, Vogt C, Kleinsteuber S.** 2015. Metagenome-Based Metabolic Reconstruction Reveals the Ecophysiological Function of Epsilonproteobacteria in a Hydrocarbon-Contaminated Sulfidic Aquifer. Frontiers in microbiology **6:**1396.
282. **Brismar H, Aperia A, Westin L, Moy J, Wang M, Guillermier C, Poczatek C, Lechene C.** 2014. Study of protein and RNA in dendritic spines using multi-isotope imaging mass spectrometry (MIMS). Surface and interface analysis : SIA **46:**158-160.
283. **Zhang DS, Piazza V, Perrin BJ, Rzadzinska AK, Poczatek JC, Wang M, Prosser HM, Ervasti JM, Corey DP, Lechene CP.** 2012. Multi-isotope imaging mass spectrometry reveals slow protein turnover in hair-cell stereocilia. Nature **481:**520-524.
284. **Krebs HA, Johnson WA.** 1937. The role of citric acid in intermediate metabolism in animal tissues. Enzymologia **4:**148–156.
285. **Linderstrøm-Lang KU.** 1952. Proteins and Enzymes. Stanford University Press **6**.
286. **Filer CN.** 1999. Isotopic fractionation of organic compounds in chromatography. Journal of Labelled Compounds and Radiopharmaceuticals **42:**169-197.
287. **Ong SE, Mann M.** 2005. Mass spectrometry-based proteomics turns quantitative. Nature Chemical Biology **1:**252-262.
288. **Bergmeyer HU.** 1974. Methods of Enzymatic Analysis, vol. 4. New York: Academic Press.
289. **Bisswanger H.** 2000. Enzymkinetik. Theorie und Methoden. Wiley-VCH.
290. **Barford D, Das AK, Egloff MP.** 1998. The structure and mechanism of protein phosphatases: insights into catalysis and regulation. Annual review of biophysics and biomolecular structure **27:**133-164.
291. **Chang C, Stewart RC.** 1998. The two-component system. Regulation of diverse signaling pathways in prokaryotes and eukaryotes. Plant physiology **117:**723-731.
292. **Cozzone AJ.** 1988. Protein phosphorylation in prokaryotes. Annual review of microbiology **42:**97-125.
293. **Stock JB, Ninfa AJ, Stock AM.** 1989. Protein phosphorylation and regulation of adaptive responses in bacteria. Microbiological reviews **53:**450-490.
294. **Wang Q, Zhang Y, Yang C, Xiong H, Lin Y, Yao J, Li H, Xie L, Zhao W, Yao Y, Ning ZB, Zeng R, Xiong Y, Guan KL, Zhao S, Zhao GP.** 2010. Acetylation of metabolic enzymes coordinates carbon source utilization and metabolic flux. Science **327:**1004-1007.
295. **Zhao S, Xu W, Jiang W, Yu W, Lin Y, Zhang T, Yao J, Zhou L, Zeng Y, Li H, Li Y, Shi J, An W, Hancock SM, He F, Qin L, Chin J, Yang P, Chen X, Lei Q, Xiong Y, Guan KL.** 2010. Regulation of cellular metabolism by protein lysine acetylation. Science **327:**1000-1004.
296. **Cain JA, Solis N, Cordwell SJ.** 2014. Beyond gene expression: the impact of protein post-translational modifications in bacteria. Journal of proteomics **97:**265-286.

297. **Bonissone S, Gupta N, Romine M, Bradshaw RA, Pevzner PA.** 2013. N-terminal protein processing: a comparative proteogenomic analysis. Molecular & cellular proteomics : MCP **12:**14-28.
298. **Ouidir T, Jarnier F, Cosette P, Jouenne T, Hardouin J.** 2015. Characterization of N-terminal protein modifications in Pseudomonas aeruginosa PA14. Journal of proteomics **114:**214-225.
299. **Hu LI, Lima BP, Wolfe AJ.** 2010. Bacterial protein acetylation: the dawning of a new age. Mol Microbiol **77:**15-21.
300. **Jones JD, O'Connor CD.** 2011. Protein acetylation in prokaryotes. Proteomics **11:**3012-3022.
301. **Starai VJ, Escalante-Semerena JC.** 2004. Identification of the protein acetyltransferase (Pat) enzyme that acetylates acetyl-CoA synthetase in Salmonella enterica. Journal of molecular biology **340:**1005-1012.

6. Lebenslauf

Persönliche Details

Name	Robert Starke
Adresse	Südblick 30
	04329 Leipzig
	Deutschland
Mobil	(+49) 1638214504
Email	robstarke@web.de
Geburtstag und –ort	23.09.1988 in Leipzig

Ausbildung

01/08/1995 – 31/07/1999	Brüder-Grimm Grundschule, Leipzig
01/08/1999 – 02/07/2007	Gustav-Hertz Gymnasium, Leipzig (Abitur 1.8)

Grundwehrdienst

01/10/2007 – 30/07/2008	13. Panzergrenadierdivsion, Leipzig

Studium

01/10/2008 – 30/09/2011	Bachelor of Science Biochemie (2.1)
	Universität Leipzig, Institut für Biochemie
	Brüderstraße 34, 04103 Leipzig
01/10/2011 – 30/09/2013	Master of Science Biochemie (1.8)
	Universität Leipzig, Institut für Biochemie
	Brüderstraße 34, 04103 Leipzig
01/10/2013 – 03/31/2017	Promotion
	Universität Hohenheim, Institut für Tierernährung
	Emil-Wolff-Straße 6-10, 70599 Stuttgart

Praktika

01/04/2011 – 30/09/2011	AG Prof. Dr. Matthias Boll, Universität Leipzig *"Investigation of the Metabolism of Fluorinated Benzoic Acids in Facultative Anaerobic Bacteria"* Methods: Anaerobe Kultivierung & enzymatische Assays, HPLC
01/10/2012 – 28/02/2013	AG Dr. Roland Müller, Helmholtz-Zentrum für Umweltforschung, UFZ Leipzig *"Biotechnological Production of 2-HIBA for the Manufacturing of Plastics"* Methods: Substratsynthese, anaerobe Proteinaufreinigung anaerobe Enzymassays, HPLC
01/04/2013 – 30/09/2013	AG Dr. Carsten Vogt, Helmholtz-Zentrum für Umweltforschung, UFZ Leipzig *"Investigations of the Aerobic and the Anaerobic Microbial Degradation of Polycyclic Aromatic Hydrocarbons (PAH) with Isotope Specific Methods"* Methods: Aerobe und Anaerobe Kultivierung, 2D-komponentenspezifische Isotopenanalyse (2D-CSIA), GC-IRMS
01/10/2013 – 03/31/2017	AG Prof. Dr. Jana Seifert, Universität Hohenheim *"Elucidation of anaerobic benzene and alkylated aromatic compound degradation pathways and associated proteins by proteomic and metabolomic analyses"* Methods: Aerobe und Anaerobe Kultivierung, Proteinextraktion, LC-MS/MS, functionale Metaproteomik
01/08/2015 – 30/11/2015	AG Prof. Dr. Joseph Suflita, Universität Oklahoma, USA *"Investigation of anaerobic PAH degradation by a 2-methylnaphthalene-degrading consortium"* Methods: Anaerobe Kultivierung, IC-MS, HPLC-QTOF, NMR

Konferenzen – Präsentationen

05/10/2014 – 08/10/2014	VAAM Dresden
	"Elucidation of anaerobic benzene and alkylated aromatic compound degradation pathways and associated proteins by proteomic and metabolomic analyses"
08/02/2016 – 09/02/2016	Symposium Metaproteomics Magdeburg
	"Bacteria dominate the short-term assimilation of plant-derived N in soil"
13/03/2016 – 16/03/2016	VAAM Jena
	"Bacteria dominate the short-term assimilation of plant-derived N in soil"

Konferenzen – Poster

20/09/2015 – 25/09/2015	ICCE Leipzig
	"Pulsed $^{13}C_2$-acetate protein-SIP unveils Epsilonproteobacteria as dominant acetate utilizers in a sulfate-reducing microbial community mineralizing benzene"

Publikationen

2015 (**3**)

N. Hoth, C. Gniese, J. Rakoczy, A. Weber, S. Kümmel, S. Reichel, C. Freese, M. Hache, A. Kassahun, A. Schulz, H. Fischer, M. Mühling, **R. Starke**, R. Kahnt, C. Vogt, H. Richnow, M. Krüger, A. Schippers, M. Schlömann, CO2BioPerm – influence of bio-geochemical CO2-transformation processes on the long-term permeabilityIn: A. Liebscher, U. Münch, (eds.) Geological Storage of CO2 – Long Term Security Aspects. GEOTECHNOLOGIEN Science Report No. 22. Advanced Technologies in Earth Sciences Springer, Berlin, Heidelberg, p. 73 – 96 (2015).

N. Kurteva-Yaneva, M. Zahn, M. T. Weichler, **R. Starke**, H. Harms, R. H. Muller, N. Strater, T. Rohwerder, Structural basis of the stereospecificity of bacterial B12-dependent 2-hydroxyisobutyryl-CoA mutase. The Journal of biological chemistry 290, 9727-9737 (2015); published online EpubApr 10 (10.1074/jbc.M115.645689).

A. H. Keller, K. M. Schleinitz, **R. Starke**, S. Bertilsson, C. Vogt, S. Kleinsteuber, Metagenome-Based Metabolic Reconstruction Reveals the Ecophysiological Function of Epsilonproteobacteria in a Hydrocarbon-Contaminated Sulfidic Aquifer. Frontiers in microbiology 6, 1396 (2015) 10.3389/fmicb.2015.01396).

2016 (**5**)

S. Kummel, **R. Starke**, G. Chen, F. Musat, H. H. Richnow, C. Vogt, Hydrogen Isotope Fractionation As a Tool to Identify Aerobic and Anaerobic PAH Biodegradation. Environmental science & technology 50, 3091-3100 (2016); published online EpubMar 15 (10.1021/acs.est.5b04819).

R. Starke, A. Keller, N. Jehmlich, C. Vogt, H. H. Richnow, S. Kleinsteuber, M. von Bergen, J. Seifert, Pulsed (13)C2-Acetate Protein-SIP Unveils Epsilonproteobacteria as Dominant Acetate Utilizers in a Sulfate-Reducing Microbial Community Mineralizing Benzene. Microbial Ecology 71, 901-911 (2016); published online EpubMay (10.1007/s00248-016-0731-y).

R. Starke, R. Kermer, L. Ullmann-Zeunert, I. T. Baldwin, J. Seifert, F. Bastida, M. von Bergen, N. Jehmlich, Bacteria dominate the short-term assimilation of plant-derived N in soil. Soil Biology and Biochemistry 96, 30-38 (2016); published online EpubMay (10.1016/j.soilbio.2016.01.009).

F. Bastida, I. F. Torres, J. L. Moreno, P. Baldrian, S. Ondono, A. Ruiz-Navarro, T. Hernandez, H. H. Richnow, **R. Starke**, C. Garcia, N. Jehmlich, The active microbial diversity drives ecosystem multifunctionality and is physiologically related to carbon-availability in Mediterranean semiarid soils. Molecular Ecology, (2016); published online EpubAug 2 (10.1111/mec.13783).

R. Starke, M. Müller, M. Gaspar, M. Marz, K. Küsel, K. U. Totsche, M. von Bergen, N. Jehmlich, Candidate Brocadiales dominates C, N and S cycling in anoxic groundwater of a pristine limestone-fracture aquifer. Journal of Proteomics **152**, 30 January 2017, Pages 153–160 (2016); published online EpubNov 14 http://dx.doi.org/10.1016/j.jprot.2016.11.003.

Sprachen

Englisch (fließend)

Spanisch (Grundkenntnisse)

Aktivitäten

Handball	1st Beachhandball Sachsen, 2013
	1st Universität Dresden, 2012 & 2014; 2nd 2013 & 2015
	1st Schwabencup, 2016

Leipzig, den 13.04.2017

7. Eidesstattliche Versicherung

Eidesstattliche Versicherung gemäß § 7 Absatz 7 der Promotionsordnung der Universität Hohenheim zum Dr. rer. nat.

1. Bei der eingereichten Dissertation zum Thema „Untersuchung der Energie- und Nährstoffflüsse mikrobieller Gemeinschaften“ handelt es sich um meine eigenständig erbrachte Leistung.
2. Ich habe nur die angegebenen Quellen und Hilfsmittel benutzt und mich keiner unzulässigen Hilfe Dritter bedient. Insbesondere habe ich wörtlich und sinngemäß aus anderen Werken übernommene Inhalte als solche kenntlich gemacht.
3. Ich habe nicht die Hilfe einer kommerziellen Promotionsvermittlung oder –beratung in Anspruch genommen.
4. Die Bedeutung der eidesstattlichen Versicherung und der strafrechtlichen Folgen einer unrichtigen oder unvollständigen eidesstattlichen Versicherung sind mir bekannt.

Die Richtigkeit der vorstehenden Erklärung bestätige ich: Ich versichere an Eides Statt, dass ich nach bestem Wissen die reine Wahrheit erklärt und nichts verschwiegen habe.

_____ _____

Ort und Datum Unterschrift

8. Danksagung

Ich bedanke mich bei Jun.-Prof. Dr. Jana Seifert und bei Prof. Dr. Martin von Bergen für die Bereitstellung des Themas und ihre Betreuung.

Bei der Deutschen Forschungsgemeinschaft (DFG) im Rahmen der Projekte SPP 1319 und CRC 1076 „AquaDiva“ sowie dem Deutschen Akademischen Austausch Dienst (DAAD) bedanke ich mich für die Finanzierung der Projekte.

Weiterhin bedanke ich mich bei Prof. Dr. Julia Fritz-Steuber und Jun.-Prof. Dr. Jana Seifert für die Bereitschaft, bei dieser Arbeit als Gutachter zu fungieren.

Besonderer Dank gilt meinen Kollegen Dr. Nico Jehmlich, Dr. Sabine Kleinsteuber, Dr. Carsten Vogt und Dr. Felipe Bastida, die mich jederzeit rat- und tatkrätig unterstützten.

Außerdem möchte ich mich bei meinen Kollegen im Department Molekulare Systembiologie bedanken, die eine lebhafte, wissenschaftliche Diskussion ermöglichten.

Abschließend möchte ich mich bei meiner Familie, insbesondere meinen Eltern, Bettina und Thomas Starke, bedanken, weil ihr bei meinen Entscheidungen stets hinter mir standet und mich immer und bei allem unterstützt habt.